



# UNIVERSITÀ DEGLI STUDI DI MILANO

DIPARTIMENTO DI BIOTECNOLOGIE MEDICHE E MEDICINA TRASLAZIONALE

DOTTORATO IN SCIENZE BIOCHIMICHE

CICLO XXX – BIO/10

## **Enzymes from marine microorganisms for the preparation of biologically active molecules**

Docente guida: Prof. Patrizia Ferraboschi

Direttore del corso di dottorato: Prof. Sandro Sonnino

Tesi di Dottorato di:  
**BENEDETTA GUIDI**  
Matricola n. R10868

Anno Accademico 2016/2017



*A tutte le famiglie che ho avuto in questi tre anni,*

*« If the doors of perception were cleansed, everything would appear to man as it is, infinite. »*

W. Blake

*“In dreams begins responsibility.”*

W. B. Yeats

*“Quando la tempesta sarà finita, probabilmente non saprai neanche tu come hai fatto ad attraversarla e a uscirne vivo. Anzi, non sarai neanche sicuro se sia finita per davvero. Ma su un punto non c'è dubbio...Ed è che tu, uscito da quel vento, non sarai lo stesso che vi è entrato.”*

H. Murakami

## ABSTRACT

This PhD project focuses on the identification, isolation and characterization of new biocatalysts able to generate biologically active molecules with significant enantioselectivity. Through screening, we identified marine strains, from MaCuMBA (Marine Culturable Microorganism for Biotechnological Applications) and BIODEEP (Biotechnologies from the deep) European project collections, which show a marked enantioselectivity on intermediates of molecules of biological interest. Biotransformation substrate range included pramipexole, as main target, but it also embraces other common building blocks for synthetic industrial preparation.

The stereoselective reduction of structurally different ketones using halotolerant marine yeasts (*Meyerozyma guilliermondii* and *Rhodotorula mucilaginosa*) was studied using cells grown and bio-converted in seawater. The preparation of valuable chemicals through water-saving (bio)processes based on the direct exploitation of seawater is a significant step towards sustainable biocatalysis. By choosing a suitable strain, high yields and stereoselectivity could be achieved in most cases. Notably, high chemoselectivity and enantioselectivity were observed using *R. mucilaginosa* in the reduction of aromatic  $\beta$ -ketonitriles, which allowed the recovery of the optically pure corresponding alcohols; notably, reduction with whole cells of yeasts generally gives a mixture of undesired products, as observed with *M. guilliermondii*.

Keto-reduction potential of thirty-three marine bacterium species was checked and afterwards the possibility to convert this substrate directly into the optically pure amine was investigated: marine bacteria were screened to identify transaminase activity. Based on the previous results in terms of halotolerance and transaminase activity, the marine bacterium strain *Virgibacillus pantothenicus* 21D was selected for the genome sequencing in order to clone and express an  $\omega$ -transaminase enzyme.

A recombinant non-marine ketoreductase from *Pichia glucozyma* (KRED1-Pglu) was used for the enantioselective reduction of various cyclic ketones including pramipexole ketone intermediate. Thanks to co-factor recycling system, the purified enzyme showed very promising results.

The soluble expression of a novel  $\omega$ -transaminase from a newly isolated halotolerant marine bacterium *Virgibacillus pantothenicus* was attained. Despite of several standard methodologies applied, the marine wild-type enzyme was total insoluble in *E. coli* host and it was satisfactorily solubilized by one single-point mutation, allowing the characterization of the new omega transaminase. The enzyme shows an interesting salt and solvent tolerance, in accordance to its origin and it results particularly active on some interesting building block molecules.

## INDEX

ABSTRACT .....	5
INTRODUCTION.....	9
BLUE FOR GREEN.....	10
BIOCATALYSIS .....	13
BIOCATALYTIC APPLICATIONS .....	16
ENZYMES .....	21
CLASSIFICATION.....	21
KINETIC PARAMETERS .....	22
SPECIFICITY AND SELECTIVITY .....	24
STABILITY.....	24
ENZYME ENGINEERING.....	25
KETO-REDUCTASES.....	26
TRANSAMINASES.....	26
TARGET MOLECULES.....	27
PRAMIPEXOLE .....	27
REFERENCES .....	29
AIM OF THE WORK .....	33
WHOLE CELL SCREENING .....	35
MARINE YEASTS ACTIVITY.....	35
MARINE BACTERIA ACTIVITY.....	35
RECOMBINANT ENZYME SCREENING .....	35
KETO-REDUCTASE ACTIVITY .....	35
ESTERASE AND LIPASE ACTIVITY.....	35
MARINE $\omega$ -TRANSAMINASE ACTIVITY.....	36
VIRGIBACILLUS PANTOTHENTICUS $\omega$ -TRANSAMINASE .....	36
WHOLE CELL SCREENING - MARINE YEASTS .....	36
BACKGROUND.....	37
MARINE YEASTS .....	37
KETO-REDUCTASE.....	38
PROJECT AIM.....	41
RESULTS AND DISCUSSION.....	42

KETO-REDUCTASE SCREENING .....	42
HALOTOLERANCE SCREENING .....	48
MATERIALS AND METHODS .....	52
MATERIALS .....	52
CHARACTERISATION .....	53
MICROORGANISMS.....	53
GROWING MEDIUM .....	55
HALOTOLERANCE SCREENING .....	55
BIOTRANSFORMATIONS .....	57
PURIFICATION AND CHEMICAL CHARACTERISATION .....	58
REFERENCES .....	60
WHOLE CELL SCREENING – MARINE BACTERIA .....	62
BACKGROUND .....	63
MARINE BACTERIA.....	63
MARINE BACTERIA BIOCATALYSIS.....	65
$\omega$ -TRANSAMINASE .....	66
PROJECT AIM.....	68
RESULTS AND DISCUSSION.....	68
KETO-REDUCTASE.....	68
$\omega$ -TRANSAMINASE .....	69
VIRGIBACILLUS PANTOTHENTICUS .....	69
MATERIALS AND METHODS .....	70
MATERIALS .....	70
CHARACTERISATION .....	71
MICROORGANISMS.....	71
MEDIA AND GROWING CONDITIONS .....	72
BIOTRANSFORMATION.....	73
PURIFICATION AND CHEMICAL CHARACTERISATION .....	73
REFERENCES .....	74
RECOMBINANT ENZYMES .....	76
BACKGROUND .....	77
KETO-REDUCTASE.....	77
ESTERASE AND LIPASE .....	78
$\omega$ -TRANSAMINASE .....	79

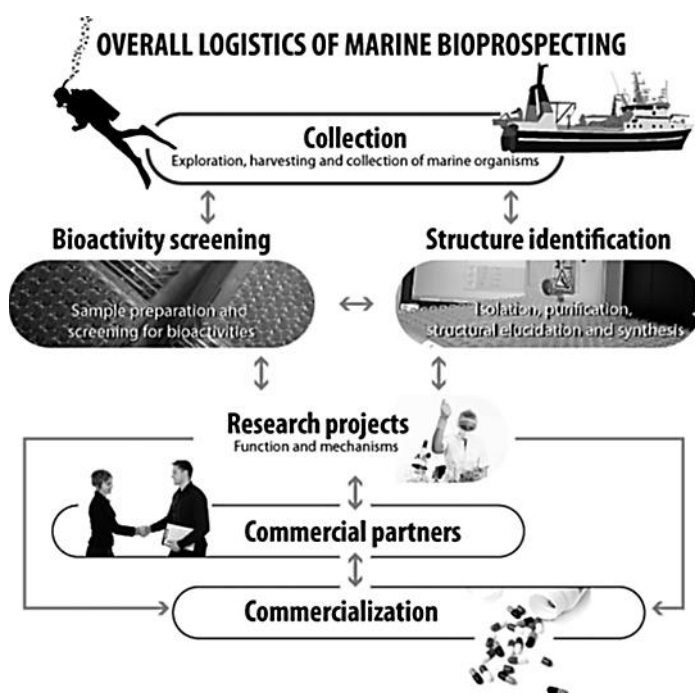
PROJECT AIM.....	80
RESULTS.....	80
KETO-REDUCTASE.....	80
ESTERASE AND LIPASE .....	81
$\omega$ -TRANSAMINASE .....	82
MATERIALS AND METHODS .....	82
MATERIALS .....	82
CHARACTERISATION .....	82
KETO-REDUCTASE.....	83
ESTERASE AND LIPASE .....	83
$\omega$ -TRANSAMINASE .....	84
PURIFICATION AND CHEMICAL CHARACTERISATION .....	84
REFERENCES .....	85
VPTA - <i>Virgibacillus pantothenicus</i> $\omega$ -transaminase.....	86
BACKGROUND.....	87
$\omega$ -TRANSAMINASE .....	87
SOLUBILITY ISSUE.....	88
MUTAGENESIS .....	89
PROJECT AIM.....	89
RESULTS AND DISCUSSIONS.....	90
WILD-TYPE VPTA AND SOLUBILISATION STRATEGIES .....	90
MUTAGENESIS .....	92
b.....	<b>Errore. Il segnalibro non è definito.</b>
c.....	<b>Errore. Il segnalibro non è definito.</b>
d.....	<b>Errore. Il segnalibro non è definito.</b>
a.....	<b>Errore. Il segnalibro non è definito.</b>
VPTA T16F.....	94
EFFECT OF pH AND TEMPERATURE .....	95
EFFECT OF CO-SOLVENTS AND SALTS.....	96
AMINO DONORS .....	97
AMINO ACCEPTORS.....	98
ENZYME KINETICS .....	100
MATERIALS AND METHODS .....	100
MARINE MICROORGANISM, GENE IDENTIFICATION AND CLONING .....	100

EXPRESSION OF WILD-TYPE VPTA .....	101
MUTAGENESIS ON VPTA .....	101
EXPRESSION OF VPTA T16F .....	101
PURIFICATION .....	102
SDS-PAGE ANALYSIS .....	102
SPECTROPHOTOMETRIC ENZYMATIC ASSAY .....	102
ENZYMATIC REACTION.....	103
ANALYTICAL METHODS .....	104
REFERENCES .....	104
CONCLUSIONS .....	108
WHOLE CELL SCREENING – MARINE YEASTS.....	109
WHOLE CELL SCREENING – MARINE BACTERIA.....	109
RECOMBINANT ENZYME .....	109
VPTA.....	110
LIST OF PUBLICATIONS & CONFERENCE PROCEEDINGS .....	111

## INTRODUCTION

## BLUE FOR GREEN

The marine ecosystem is the largest habitat on Earth, representing 70% of the surface of our planet and thus it is a critical driver of hydrologic cycle and climate system, important for commerce, transport, and tourism, a source of economically important resources, as well as new therapeutic



compounds. Seas and oceans include the greatest extremes of temperature, light and pressure and habitats that still remain largely unexplored, understudied and underexploited in comparison with terrestrial ecosystems and organisms. Marine organisms are sources of natural bioactive substances with potential therapeutic activity, and they should also be valued as a source of genetic material to be explored by the bioprospecting industry<sup>1</sup> (fig. 1.1).

**Fig. 1.1.** A new term for an ancient process: bioprospecting refers to discovery and commercialization of new products starting from biological resources<sup>1</sup>.

Only recently, indeed, the sea has been rediscovered as untapped source of novel biocatalysts and its extraordinary micro-biodiversity can offer new possibilities for conducting highly selective, enzyme-catalysed reactions in industrial processing, laboratory analyses, and medical therapy<sup>1</sup> (fig. 1.2).

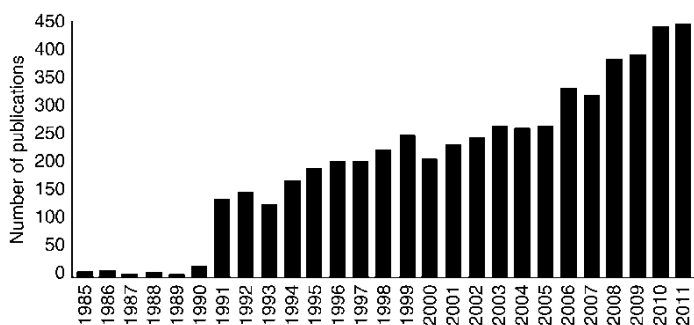


**Fig. 1.2.** Web of Knowledge Scientific hits containing “marine enzymes” (5528 total hits).

Biocatalysts produced by marine microorganisms are naturally endowed with an excellent stability towards high salinity, as a consequence of different structural adjustments adopted to cope with high ionic strength conditions. Interestingly, adaptation to high salinity corresponds to an increased tolerance towards organic solvents, a requisite for many enzymes to be used as biocatalysts in organic chemistry<sup>2</sup>. From this point of view, marine habitats containing high salt concentrations, such a salt lake, the Dead Sea and deep hypersaline anoxic basins (DHABs), provide ideal locations to source novel marine biocatalysts<sup>3</sup> (figure 1.3).

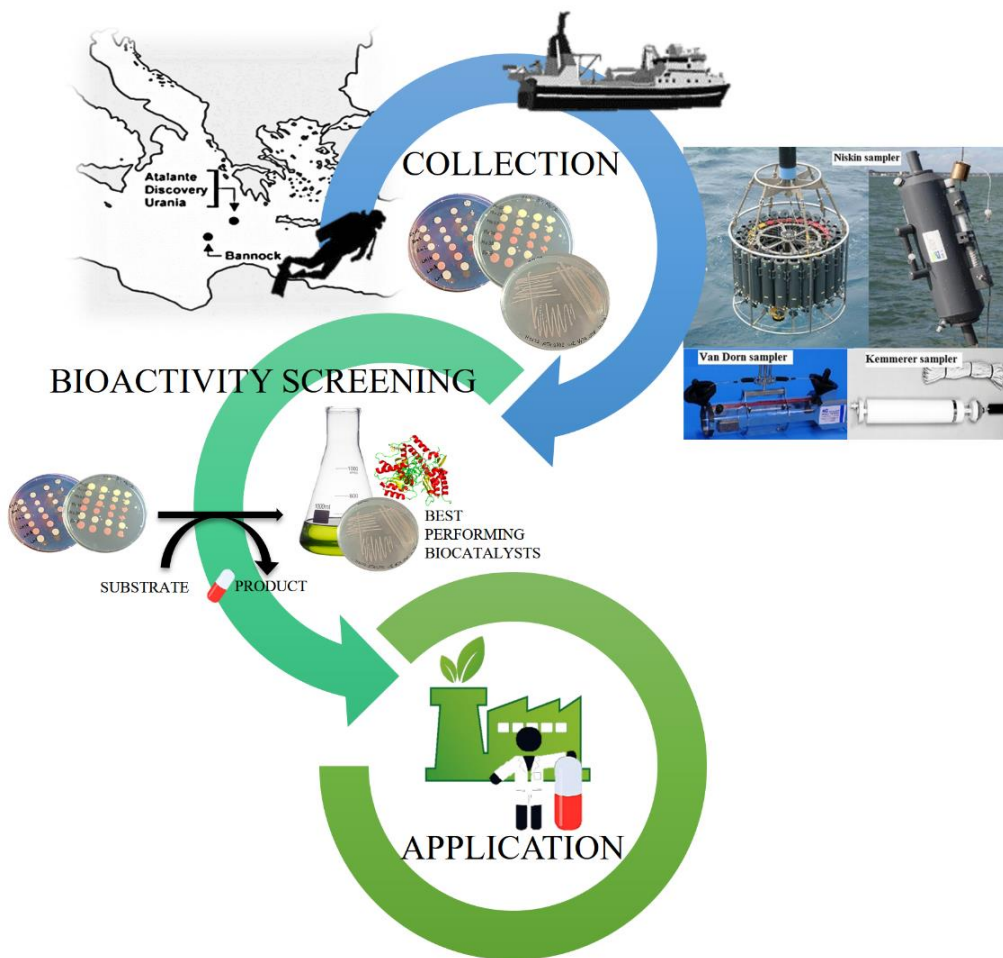


**Fig. 1.3.** Biodiversity still represents an incredible resource and source of new and naturally high performing biocatalysts, thanks to a unique evolutionary pathway.

The ability to tolerate high NaCl concentrations was investigated, since these extreme environments are usually characterised by high concentrations of this salt. In this condition, the cell is exposed to two different stimuli from the environment: osmotic and ionic stress. Typically, hyperosmotic stress causes immediate water outflow from the cell, reduces turgor pressure and consequently dehydrates the cytosol<sup>4</sup>. Ionic stress, on the other hand, results in an intake of ions (e.g. Na<sup>+</sup>) by the cell that increases intracellular ionic concentration leading damages to membranes and water discharge from the cell. One of the strategies adopted by marine microorganisms to counteract changes in turgor pressure is to lower the absorption of water and compensate with a build of compatible solutes that do not interfere with cell metabolism and maintaining internal concentration of Na<sup>+</sup> at non-toxic levels<sup>5</sup>. Those microorganisms that can grow at high NaCl concentrations preferring to other conditions are defined as halophiles. Differently, the category of halotolerants is representative of those microorganisms that survive at different concentrations of NaCl and outweigh osmotic and saline stress but are not, however, in their optimal growth condition. Non-halophiles are all those

microorganisms that do not overcome the stress due to the presence of salt at high concentrations and therefore are not able to perform their vital functions in this particular condition.

Taking into account what deals with molecular adaptation of proteins that are stable and function at high salt concentration, understanding how these enzymes maintain their fold stable and avoid aggregation under harsh conditions is of great interest for biotechnological applications. Comparisons between the sequences of halophilic/non-halophilic homologous protein pairs indicated that Asp and Glu are significantly more frequent, while Lys, Ile and Leu are less frequent in halophilic proteins. Homologous halophilic and non-halophilic proteins have similar overall structure, secondary structure content, and number of residues involved in the formation of H-bonds. On the other hand, on the halophilic protein surface, a decrease of nonpolar residues and an increase of charged residues are observed. Particularly, halophilic adaptation correlates with an increase of Asp and Glu, compensated by a decrease of basic residues, mainly Lys, on protein surface<sup>6</sup>. Future studies will give further insights into the adaptation strategies to high salinity environment and will indicate strategies for rational protein engineering in order to improve enzyme industrial performance.

## BIOCATALYSIS

Biocatalysis, assumed as applications of enzymes or whole cells for chemical synthesis, is an appealing technology for fine chemical, food and pharmaceutical industry for several reasons.

The employment of biologic systems, such as whole cells or isolated enzymes, offers important advantages:

- High efficiency – high turnover numbers; rates ( $10^8 - 10^{10}$ ).
- Selectivity/specificity – chemo-, regio- and stereoselectivity.
- Mild conditions – mild temperature and pH; atmospheric pressure.
- Low energy consumption.
- Not bound to their natural role (substrate tolerance).
- Highly selective in complex mixtures (no side reactions).
- Fewer by-products.
- Biodegradable (natural bioproducts).
- Can be overproduced.

The excellent regio- and stereoselectivity of enzyme catalysts along with their ability to work under mild reaction conditions (thus protecting existing functionality within a molecule) enables transformations without the need for multiple protection and deprotection steps within a synthesis. Additionally, biocatalysis offers both economic and environmental advantages over chemocatalytic

methods<sup>7,8</sup>.

Enzymes are produced from inexpensive renewable resources and are themselves biodegradable, fulfilling the central tenants of Green Chemistry<sup>9</sup> and sustainable development (fig. 1.4).



**Fig. 1.4.** The Twelve Principles of Green Chemistry by Anastas and Warner (1998)<sup>9</sup>.

Image from Compound of Interest<sup>®</sup>  
(<http://www.compoundchem.com/2015/09/24/green-chemistry/>).

Besides the above-mentioned advantages, some drawbacks coming from the application of biocatalysis in chemistry must be recognized, such as:

- Biocatalysts often show lower stability than conventional catalysts.
- Development of industrial biocatalytic processes is usually much longer to establish.
- Low number of commercially available biocatalysts.
- Necessity of microbiological facilities if the biocatalyst is not a commercial enzyme.

Most of these disadvantages might be overcome by modern techniques (screening, molecular biology, protein engineering, immobilization) able to furnish a much higher number of biocatalysts with improved performances.

The whole process that sees the industrial application of a new enzyme usually begins with *in vivo* or *in silico* screening. The dominant strategy to discover new biocatalysts has varied from straightforward experimental assays for certain functions (experimental assays for functions) to deduction of protein functions from bioinformatics data-bases (from sequence to function, from structure to function). After a biocatalyst characterization, process design has to fit with enzyme specifications and *vice versa* (fig.1. 5).

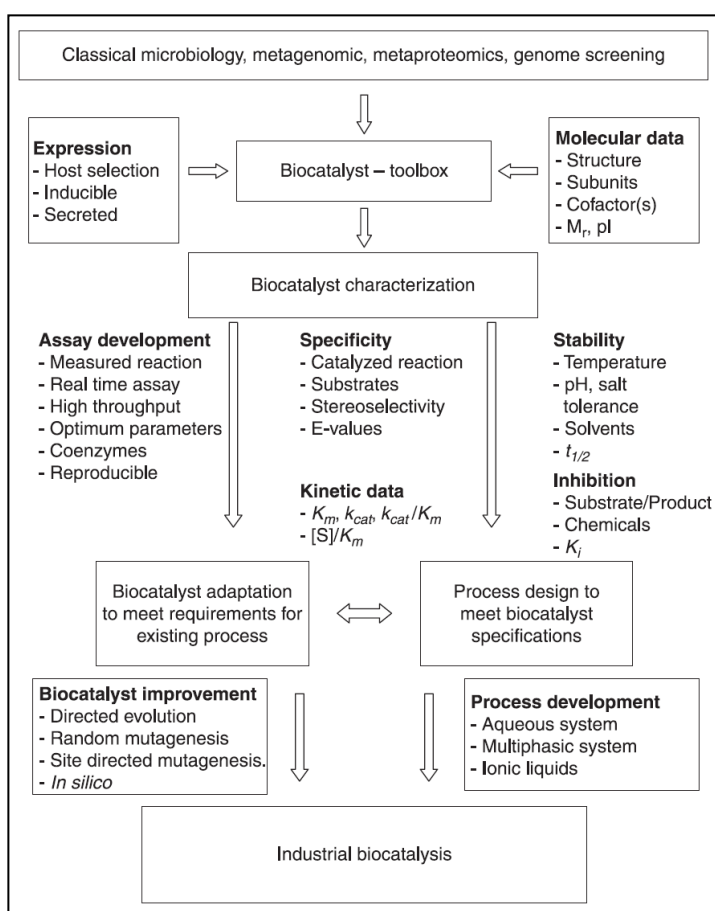


**Fig. 1.5.** Flowchart of essential elements of biocatalyst discovery, characterization and improvement by protein engineering<sup>1</sup>.

As Bornscheuer et al. described<sup>10</sup>, we are living the third wave of biocatalysis progress. During the first wave of biocatalysis (fig. 1.6), which started more than a century ago, scientists recognized that components of living cells could be applied to useful chemical transformations (in contrast to the fermentation processes, which had been commonplace for millennia already). The main challenge for these applications is the limited stability of the biocatalyst, and such shortcomings were primarily overcome by immobilization of the enzyme, which also facilitated the reuse of the enzyme. During the second wave of biocatalysis, in the 1980s and 1990s, initial protein engineering technologies,

typically structure based, extended the substrate range of enzymes to allow the synthesis of unusual synthetic intermediates. This change expanded biocatalysis to the manufacture of pharmaceutical intermediates and fine chemicals. Apart from stabilization, the challenges now included optimizing the biocatalyst for the non-natural substrates. The third, and present, wave of biocatalysis started with the work of Pim Stemmer and Frances Arnold in the mid and late 1990s. They pioneered molecular biology methods that rapidly and extensively modify biocatalysts via an *in vitro* version of Darwinian evolution. The methods are now commonly called directed evolution (see “Enzyme engineering” paragraph).

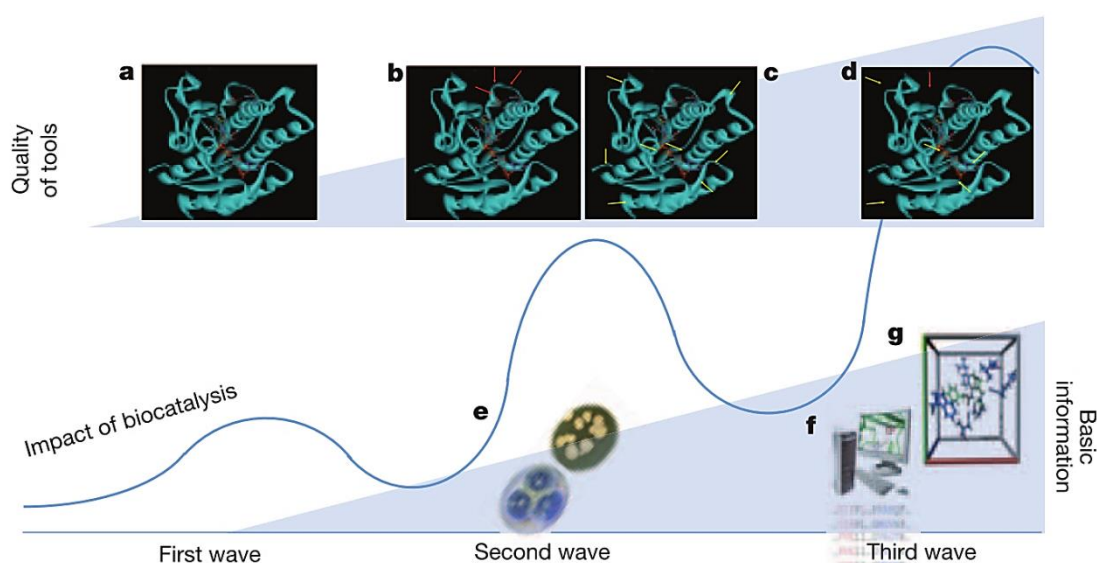


**Fig. 1.6.** Based on protein structures (a) or homology models, rational design (b) approach is able to identify distinct point mutations, whereas for directed evolution experiments random mutagenesis (c) combined with screening is the starting point. Combining these methods makes it possible to create smaller, but smarter, libraries (d). The classical screening of enzymes by enrichment cultures (e) is now replaced by key motif database searches (f) to guide identification of novel enzymes or those with desired properties. Still in its infancy is the computational de novo design of enzymes (g)<sup>10</sup>.

## BIOCATALYTIC APPLICATIONS

Despite the clear benefits of biocatalytic processes, the historical number of industrial applications has been modest, with a dramatic increase in the use of biocatalysis only occurring within the last two decades (fig. 1.7).

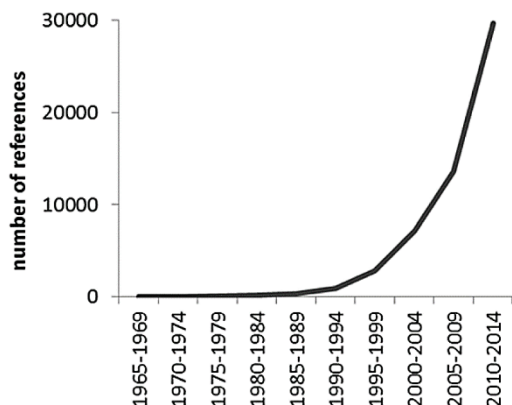
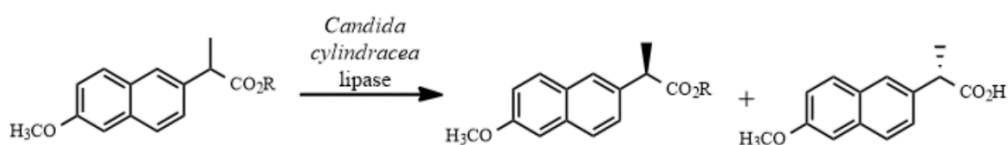


**Fig. 1.7.** Number of publications and patents discussing “pharmaceutical biocatalysis” for each 5-year period of the last 50 years. Metrics from Google Scholar

The use of biocatalyst has acquired importance as a complement to conventional chemical techniques in various application fields. In particular, biocatalyst selectivity is important for obtaining biologically active molecules, whose stereochemistry affect their *in vivo* behaviour. The specific reactions that can be replaced with biocatalysis have been identified in the synthesis of biologically active molecules, including chiral amine preparation, stereo and regiospecific hydroxylation of complex molecules, and other redox reactions<sup>10,11</sup>.

One of the first enzymatic applications in biologically active molecule synthesis was lipase resolution for the preparation of Naproxen in 1987 by Gu and co-workers<sup>12</sup> (scheme 1.1). (+)-2-(6-Methoxy-2-naphthyl) propionic acid has been prepared *via* enzymatic enantiospecific hydrolysis of ( $\pm$ )-chloroethyl-2-(6-methoxy-2-naphthyl) propionate, catalyzed by the lipase of *Candida cylindracea* with E > 100 (39% conversion; 98% e.e.).

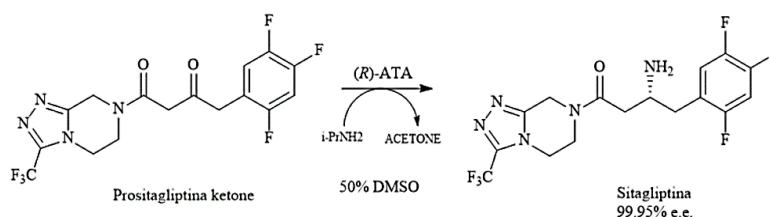


**Scheme 1.1.** Biocatalytic resolution of Naproxen intermediate by *Candida cylindracea*.

Other examples of smart commercial enzyme applications are described for the antitumoral Capecitabine<sup>13</sup> and anti-thrombotic Clopidogrel<sup>14</sup> synthesis, both exploiting a serine protease catalysis. Alcalase CLEA enzyme is able to catalyse alcoholysis allowing the selective deprotection of primary acetyl ester of the N<sup>1</sup>-(2', 3', 5'-tri-O-acetyl-β-D-ribofuranosyl)-5-fluoro-N<sup>4</sup>-(n-pentyloxycarbonyl) cytosine and thus affording the corresponding 5'-hydroxyderivative, an advanced intermediate of capecitabine synthesis with a good yield (80% after purification). The (*S*)-2-chlorophenylglycine moiety is well recognized in the structure of (*S*)-clopidogrel. The enantiomerically pure chiral

building block synthesis was performed via an enzyme-catalyzed resolution of (*RS*)-*N*-Boc-2-chlorophenylglycine methylester. The high enantiomeric excess of the synthon was obtained by immobilized subtilisin (Alcalase CLEA). The simplicity of the process makes this pathway suitable for large-scale preparation.

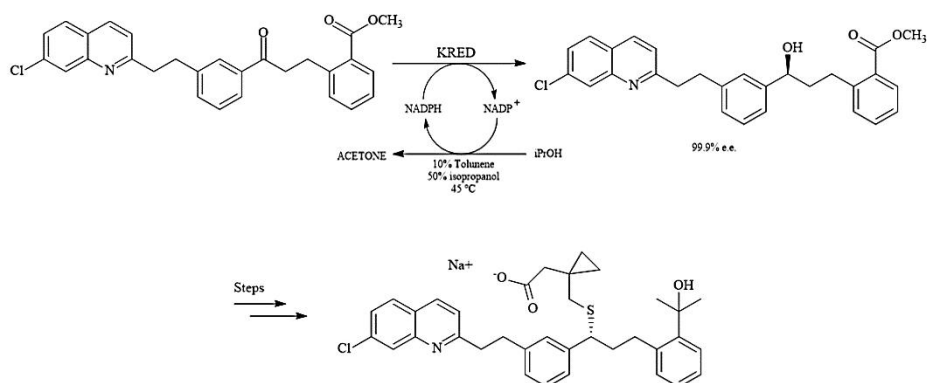
One of the most successful examples in the practical application of enzymes in the pharmaceutical industry is the anti-diabetic compound, sitagliptin<sup>15,16</sup>. Sitagliptin is a drug for type II diabetes that has been marketed under the trade name *Januvia* by Merck<sup>15</sup>. Researchers at Codexis and Merck engineered *R*-selective transaminase (*R*-ATA, ATA-117) from *Arthrobacter* sp. for the asymmetric amination of pro-sitagliptin ketone. By applying a substrate walking, modeling, and mutation approach, they were able to overcome the limitation of the substrate's size for the enzyme. A combination of the further directed enzyme evolution and process engineering yielded a variant that converts 200 g/L of pro-sitagliptin ketone into sitagliptin with enantio-purity higher than 99.95% even in the presence of 1 M *i*-PrNH<sub>2</sub>, 50% DMSO and 40 °C<sup>16</sup> (scheme 1.2). Immobilization of engineered (*R*) selective-ATA enables the maintenance of the enzyme activity and stability in an organic solvent, simplifying the workup and allowing a repetitive use of the enzyme<sup>17</sup>.



**Scheme 1.2.** Synthesis of sitagliptin from pro-sitagliptin ketone using engineered (*R*)-selective ATA.

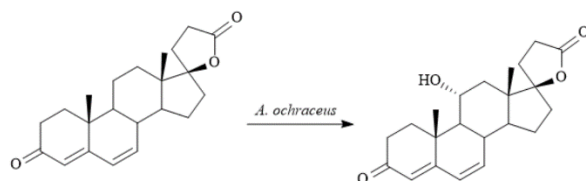
Codexis recently developed a biocatalytic process for producing intermediates for blockbuster drugs such as atorvastatin, montelukast, duloxetine, phenylephrine, ezetimibe, and crizotinib based on stereo and regio-specific hydroxylation using keto-reductase (KRED) from *Lactobacillus*<sup>18,19</sup>. The anti-asthmatic drug, montelukast, was developed and marketed under the trade name *Singulair* by Merck<sup>20</sup>. Combined with a directed evolution and process optimization, the engineered KRED exhibits a high enantio-selectivity (> 99.9%) and stability even in the presence of ~ 70% organic solvents at 45 °C (scheme 1.3). The biocatalytic process is currently operated on a > 200 kg scale substrate. The most intriguing point in KRED engineering is the increase of the enzyme stability even at a high organic solvent concentration and temperature. Because of the low solubility of the substrate in water, the high organic solvent concentration and temperature are necessary. Based on the correlation between the thermostability and solvent tolerance<sup>19</sup>, researchers at Codexis primarily

screened enzyme mutants with increased thermal stability followed by a screening for solvent tolerant mutants<sup>19</sup>.



**Scheme 1.3.** Regio-specific hydroxylation of key intermediate in synthesis of montelukast using engineered KRED<sup>20</sup>.

In regards to whole cell biocatalysis, a high yielding bioprocess for 11- $\alpha$  hydroxylation of canrenone using *Aspergillus ochraceus* ATCC 18500 was described<sup>21</sup>. The optimization of the bioprocess involved both fermentation (for achieving highly active mycelium of *A. ochraceus*) and biotransformation with the aim to obtain 11- $\alpha$  hydroxylation with high selectivity and yield. A medium based on sucrose as C-source resulted particularly suitable for conversion of canrenone into the corresponding 11-hydroxy derivative, whereas the use of O<sub>2</sub>-enriched air and DMSO as a co-solvent for increasing substrate solubility played a crucial role for obtaining high yields (>95%) of the desired product in high chemical purity starting from 30 mM (10.2 g/L) of substrate (scheme 1.4).



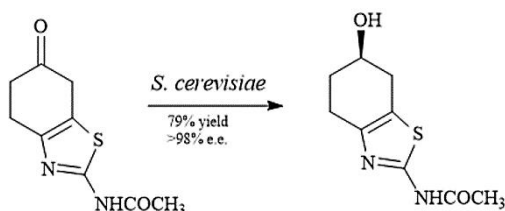
**Scheme 1.4.** Conversion of canrenone into the corresponding 11-hydroxy derivative by *Aspergillus ochraceus*<sup>21</sup>.

Another successful whole cell bioconversion led to the achievement of the enantiomerically pure advanced intermediate of the synthesis of (*S*)-pramipexole, a anti-Parkinson drug, showing the Baker's yeast efficiency (figure 1.5). The use of readily available and inexpensive *Saccharomyces cerevisiae*, the easy preparation of the biotransformation substrate, and the simple steps required to accomplish the synthesis, make the method applicable to a preparative scale.

This synthon, not yet described in the literature, was transformed through very simple steps into the desired dihydrochloride monohydrate derivative of (*S*)-pramipexole in 21% overall yield. A complete

inversion of the configuration realized under the Mitsunobu<sup>22</sup> conditions allowed the (*S*)-alcohol achievement.

The (*S*)-alcohol obtained is a suitable substrate for dexpramipexole, the (*R*)-isomer of pramipexole, which is currently under investigation in the treatment of ALS (amyotrophic lateral sclerosis)<sup>23</sup>.



**Scheme 1.5.** Enantioselective reduction of the keto-intermediate in pramipexole synthesis by *Saccharomyces cerevisiae*.

## BIOCATALYST FORM

Biocatalysis can be performed by both whole cells and isolated enzymes. The type of bioconversion and enzyme features address the choice. Whole cells allow the production of compounds also ensuring cofactor regeneration, with high regio- and stereoselectivity, under mild operational and environment-friendly conditions. A limit of employing whole cells is sterile initial conditions and prevention of biological contamination. However, they are quite effective in multi-step reactions, they provide a protective environment to enzymes (e.g. in non-conventional media) and are significantly cheaper to produce than free enzymes which require several isolation and purification steps<sup>24,25</sup>. In one-step reactions, isolated enzymes should provide significant benefit when compared to whole cells as no side-reactions should occur and substrates do not have to be transported across membranes. The enzymes are able to catalyse more efficient reactions and under mild conditions, within a narrow range of pH and temperature. Furthermore, enzymes are able to maintain their activity under *in vitro* conditions and can catalyse reactions in conditions not suitable for cell growth. The use of pure enzymes in biocatalysis has several advantages such as the specificity for selected reactions, simple apparatus and procedures and better tolerance to co-solvents used to solubilise low-water soluble substrates<sup>26</sup>. However, enzyme isolation and purification can be quite expensive and time consuming, the addition of co-factors or their recycling may be required and, in general, it is more difficult to carry out reactions requiring more than one enzyme, contrarily to the use of whole microbial cells (table 1.1).

BIOCATALYST	FORM	PROS	CONS
ISOLATED ENZYME	any	<ul style="list-style-type: none"> <li>→ simple apparatus,</li> <li>→ simple work-up,</li> <li>→ better productivity due to higher concentration tolerance</li> </ul>	<ul style="list-style-type: none"> <li>→ cofactor recycling necessary</li> </ul>

	dissolved in water	→ high enzyme activities	→ side reaction possible, → lipophilic substrates insoluble, → work-up requires extraction
	suspended in organic solvents	→ easy to perform, → easy work-up, → lipophilic substrates soluble, → enzyme recovery easy	→ low activities
	immobilised	→ enzyme recovery easy	→ loss of activity during immobilisation
WHOLE CELLS	any	→ no cofactor recycling necessary	→ expensive equipment, → tedious work-up due to large volumes, → low productivity due to lower concentration tolerance, → low tolerant of organic solvents, → side reactions likely due to uncontrolled metabolism
	growing culture	→ higher activities	→ large biomass, → more by-products, → process control difficult
	resting cells	→ work-up easier, → fewer by-products	→ lower activities
	immobilised cells	→ cell re-use possible	→ lower activities

**Table 1.1.** Pros and cons of using isolated enzymes and whole cell systems<sup>27</sup>.

An important issue related to employing isolated enzyme is stability under relatively harsh conditions, such as high temperatures, pH and in the presence of solvents<sup>28</sup>. Limitations of biocatalysts can be overcome by integrating different techniques, such as genetic engineering, that allows the production of large quantities of enzymes at relatively low costs, biocatalyst immobilization, and suited reactor technology. Numerous molecular techniques have been developed to improve the activity or substrate specificity of an enzyme with a particular industrial application in mind. This includes random mutagenesis of a target gene followed by screening and rational protein engineering<sup>28,29</sup> and directed evolution<sup>30,31</sup>.

## ENZYMES

### CLASSIFICATION

The identity of the biocatalyst must be specified as per name of reaction type: EC number; strain deposit, GenBank sequence accession number.

In according to International Union of Biochemistry and Molecular Biology, Enzyme commission (IUBMB EC) classification:

→ EC 1 oxidoreductases: oxygenation of C-H, C-C, C = C bonds; transfer of electrons.

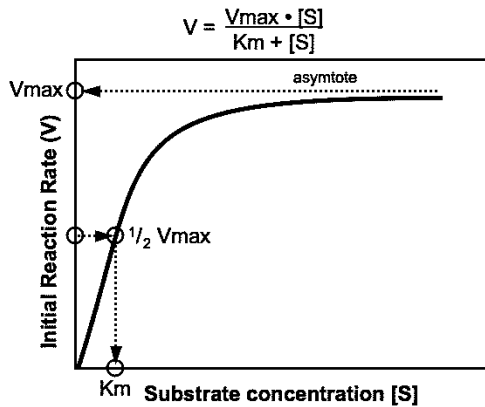
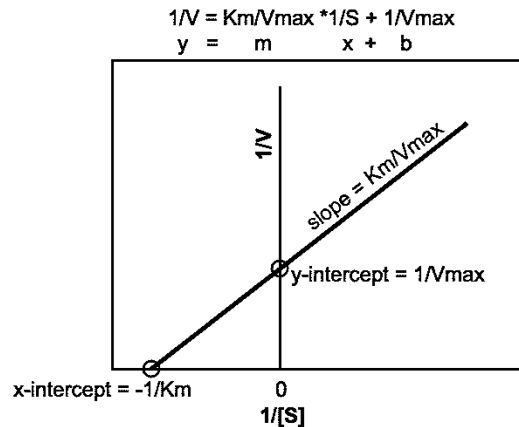
- EC 2 transferases: transfer of functional groups: aldehyde, ketone, acyl, phosphoryl, or methyl.
- EC 3 hydrolases: formation/breakdown of esters, amides, lactones, lactams, epoxides, nitriles, anhydrides, glucosides, etc.
- EC 4 lyases: removal or addition on C = C, C = N, C = O bonds.
- EC 5 isomerases: racemization and epimerization.
- EC 6 ligases: formation- cleavage of C-O, C-S, C-N, C-C bonds requiring ATP cleavage.

## KINETIC PARAMETERS

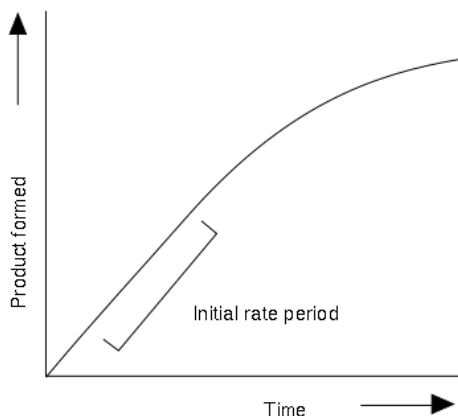
The core kinetic parameters of an enzyme are  $K_m$  and  $V_{max}$  values, described by the Henry-Michaelis-Menten equation<sup>32</sup> that correlates the dependence of the reaction velocity ( $v$ ) on the free substrate concentration (S). Briggs and Haldane (1925) provided a derivation of this equation introducing the steady-state approximation<sup>33</sup> which assumes that the enzyme-substrate complex (ES) after initial formation reaches its climax and remains unchanged over the time the reaction is monitored.

$K_m$  and  $V_{max}$  are determined by directly plotting  $v$  over S (Michaelis- Menten plot) or more favourably by one of the linear transformations such as Lineweaver-Burk ( $1/v$  vs.  $1/S$ ), Hanes ( $S/v$  vs. S) or Eadie-Hofstee ( $v/S$  vs.  $v$ ).

Transformation of the Michaelis-Menten equation<sup>32</sup> shows that  $K_m$  specifies the substrate concentration where the reaction proceeds at half of  $V_{max}$ .  $k_{cat}$ , often referred to as the turnover number, can be calculated directly as the quotient of  $V_{max}$  and the total enzyme concentration. Turnover numbers are normally reported as molecules product produced per molecules of enzyme per time (e.g. mol/mol s). Thus, if the same units are used for product and enzyme they eventually cancel each other and the unit for reporting  $k_{cat}$  will be reciprocal time (e.g.  $s^{-1}$ ). The  $k_{cat}/K_m$  ratio, originally referred to as “specificity<sup>34</sup>” or “performance<sup>35</sup>” constant and representing a second-order rate constant ( $M^{-1} s^{-1}$ ) is used as a measure for catalytic efficiency of an enzyme. In general, the higher  $k_{cat}/K_m$  the better is the enzymatic performance which can be used to compare enzymes or different substrates of one enzyme.

**Michaelis Menten Plot****The Lineweaver-Burk Transformation****Fig. 1.7.** Michaelis Menten Plot versus Lineweaver-Burk linear kinetic representation<sup>32</sup>.

In a simple enzyme reaction over time one substrate is converted to yield one single product. This of course is not totally true since it often requires coenzymes (e.g. NAD(P)H for oxidoreductases) or co-substrates (e.g. water for hydrolases) or, in the case of lyases (synthases), yields, technically speaking, two products or converts two products into one substrate. To kinetically describe these kinds of reactions it is important to define one speed-limiting factor which could be substrate, co-substrate, etc., at a time and supply the respective others in excess. During the enzymatic assay, substrate concentration is much higher than enzyme concentration remaining virtually unchanged, and product accumulation is linear and there is no back reaction into substrate. Substrate concentrations are crucial and should be in the range of 0.1 to 10 times  $K_m$  which for unknown enzymes often has to be determined using trial approaches (fig. 1.8).

**Fig. 1.8.** Progress curve for an enzyme reaction. The slope in the initial rate period is the initial rate of reaction  $v$ . The Michaelis-Menten equation describes how this slope varies with the concentration of substrate.

In an enzymatic assay, one of the key parameters to check is the initial rate measured as specific activity (SA). SA gives a measure of enzyme processivity, at a specific (usually saturating) substrate concentration, and is usually constant for a pure enzyme. It is conventionally expressed in Units (U) as  $\mu\text{mol min}^{-1} \text{mg}^{-1}$  or in katal  $\text{kg}^{-1}$ . Enzyme Unit (U) is defined as the amount able to catalyse the transformation of 1 micromole of the substrate per minute under standard conditions. Turnover

number, on the other hand, is dimensionless referring to the ratio of number of moles of product per mole of catalyst used over the reaction period. On enzyme assays, depending on what methods are being used (e.g. spectrophotometry or measurement of fluorescence using a fluorometer), it may be critical to find the optimum conditions of pH, temperature, buffer concentrations (ionic strength), metal or cofactor requirements. Importantly, the enzyme concentration used has to be appropriate since accurate determination of the enzyme's SA requires the presence of excess amounts of substrate(s) and possible co-substrate(s).

## SPECIFICITY AND SELECTIVITY

One of the characteristics of an enzymatic catalysis is the specificity for substrate(s) and reactions. Enzymes are generally highly specific for one reaction type, but promiscuous activities can be found in nature or can be introduced into an enzyme by protein engineering. *Specificity* and *selectivity* are often used as synonyms to describe the ability of an enzyme to distinguish between substrates; more correctly, *substrate specificity* refers to a reaction where one (and only one) substrate can react, whereas *substrate selectivity* describes a reaction where one substrate is preferentially transformed over others. Therefore, the term *enantioselectivity* is preferentially used when the substrates are enantiomers. Enzymes also exhibit *chemoselectivity* for similar functional group, and *regioselectivity* for analogous functional groups with different chemical neighbourhood.

To better characterize the stereoselective properties of an enzyme and thus to quantitatively assess its potential for kinetic resolution<sup>36</sup> the dimensionless enantiomeric ratio ( $E$ )<sup>36</sup> was introduced. It is expressed as the quotient of the second-order rate constants ( $k_{cat}/K_m$ ) R and ( $k_{cat}/K_m$ ) S. This is a measure for the 'selectivity' of an enzymatic resolution<sup>37</sup>.  $E$  values can be experimentally calculated by measuring the enantiomeric excess ( $ee$ ) of either the residual substrate or the corresponding product at the specific degree of conversion ( $C$ ). To obtain accurate  $E$  values, the general rule is to stop the reaction at about 50% conversion.

## STABILITY

In an industrial setting, stability of a biocatalyst is one of the most important characteristics. Even the most active enzyme will be practically useless if it does not maintain its activity over the envisioned treatment or production process time. For process development, the fundamental question is whether the enzyme has to be designed to meet an existing protocol or whether the process can be designed to adapt to the enzyme's properties. One can distinguish between several forms of enzyme stability, such as chemical stability (e.g. the influence of pH, salt or solvent concentration), thermodynamic stability (e.g. reversible unfolding of the protein structure due to increasing temperature) and kinetic

stability (describing the time the enzyme remains active before undergoing irreversible denaturation)<sup>28,38</sup>. Enzyme stability studies, however, are often performed under laboratory conditions (*e.g.* in a simple buffer) and thus, although giving some insight, they only have limited value for assessing the enzyme's bioprocess suitability. Under process conditions, enzyme behaviour can be very different with substrate(s), accumulating product(s) and possible solvents modulating its activity in either way: positive (protection) or negative (destabilization)<sup>39</sup>. It should be noted that enzyme stability often depends on the concentration that it was assayed, thus adding another variable.

## ENZYME ENGINEERING

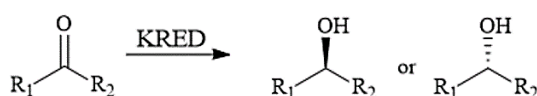
Enzymes were optimized by Darwinian evolution over millions of years to catalyse reactions while ensuring high substrate specificity, as well as exquisite enantioselectivity and stereoselectivity. However, there are often significant discrepancies between an enzyme's function in nature and the specific requirements for *ex vivo* applications envisioned by scientists and engineers.

The modification of enzymes for adaptation to the environment in a chemical process is often considered necessary, for which many strategies have been developed<sup>40</sup>. Frequently the compounds in the process are poor substrates, the enantioselectivity may be insufficient, or a more heat stable or co-solvent tolerable enzyme is desired. By using an experimentally determined structure of the enzyme (determined by X-ray crystallography or NMR) the enzyme engineer can locate specific amino acid residues suitable for mutation. This is called rational design; arguably, the amount of knowledge which is available regarding the function of a given enzyme dictates the likelihood of success with this strategy. When such attempts are unsuccessful, or a structure is unavailable, the amino acid chain can be altered in a randomised fashion and a library of mutants can be screened for the desired properties. An improved clone can be further randomised and a new library can be screened. The iterative process is repeated for the potential discovery of the required enzyme. This strategy is called *directed evolution*<sup>41-45</sup>. Further, to increase the probability of finding improved variants, semi-rational<sup>40</sup> approaches have been devised, such as CASTing<sup>46,47</sup> and saturation mutagenesis. The more recent scientific publications involving enzyme engineering contain examples of rational and semi-rational approaches with a higher frequency than in the past. This phase in biocatalytic progress was called "third wave" by Bornscheuer<sup>10</sup> as we previously reported. The method advancements, increased understanding of function and examples of successful enzyme variants have made researchers less inclined to resorting to directed evolution, which most often involves a tedious screening procedure. The choice of method is usually not straightforward, and remains a challenge for the enzyme engineering<sup>48</sup>.

For what concerns the enzyme activities taken into account, keto-reductase and transaminase activities were the main biocatalytic strategies investigated.

## KETO-REDUCTASES

Ketoreductases (KREDs) are enzymes useful for enantiomeric preparation of chiral alcohols from ketones, ketoacids and ketoesters<sup>19</sup> (scheme 1.6).

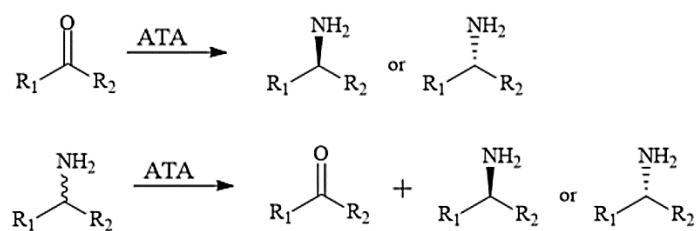


**Scheme 1.6.** Simplified catalysis by KRED.

KREDs can induce an asymmetric attack of the hydride with total or prevalent formation of one of the two enantiomers. The cofactors (mostly NADH or NADPH) provide the hydride ion giving rise to the reduction of the substrate. Yeasts are usually employed for synthetic purposes with main application in stereoselective reduction of ketones affording optically pure secondary alcohols<sup>49-52</sup>. In particular, marine yeasts have already been investigated for the production of pharmaceutical and enzymatic products, such as astaxanthin, siderophore, riboflavin, inulinase and amylases. Yet, the commercial application of marine yeasts is still limited. The current research, however, indicates the promising features of the marine yeasts for the potential industrial application and their superiority over the terrestrial ones in certain field. More direct comparison studies should be carried out to give further evidence on the advantages of marine yeasts over terrestrial yeasts<sup>53</sup>, as explained in the second chapter.

## TRANSAMINASES

Transaminases, also called amino transaminase (ATA), are enzymes capable of the enantioselective transfer of an amino group from the amino donor to the acceptor substrate. The  $\alpha$ -ATAs are able to operate on the amino moieties of the  $\alpha$ -carbon of amino acids, while the  $\omega$ -ATAs mainly accept as substrates donors with amines distal to the carboxyl moiety, as well as other amine donors and their respective non-keto acid acceptors (scheme 1.7).



**Scheme 1.7.** Simplified catalysis by  $\omega$ -ATA.

Combining ATAs with other enzymatic or chemical routes has been demonstrated to be a smart method for practical applications, particularly in regard to shortening the reaction routes, avoiding protecting steps, reducing chemical waste and achieving a high atom-efficiency. This makes these enzymes useful for synthesis of chiral amines, which are of high importance as building blocks for production of optically pure amino synthons in pharmaceutical like sitagliptin<sup>16</sup>, ethambutol<sup>54</sup>, imagabalin<sup>55</sup>, norephedrine and pseudoephedrine<sup>56</sup>, food and cosmetic additives<sup>57</sup>, agrochemical and material industries. The development of protein engineering has tried to answer to this need and it is achieving remarkable progresses through random and rational mutagenesis approach but some issues need to be completely clarify yet. The current trend in the research field is directing to the identification and designing of new  $\omega$ -transaminases with defined substrate selectivity and capable of adapting to the uncommon catalytic conditions of industrial processes. The issue will be widely discussed in the following chapters.

## TARGET MOLECULES

The range of molecules evaluated in this PhD project was selected in order to obtain asymmetric catalysis or kinetic resolution providing chiral building blocks aimed at the synthesis of biologically active molecules with a solid industrial appeal.

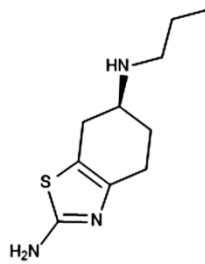
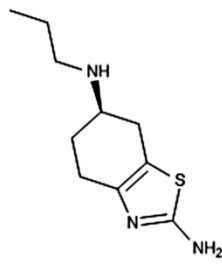
### PRAMIPEXOLE

One of the target molecules investigated in this project is pramipexole. A recent example is the preparation<sup>58</sup> of an optically pure new intermediate of (*R*)- or (*S*)-pramipexole; this thiazole derivative is endowed with anti-Parkinson activity<sup>59–61</sup> if its stereocenter is in the (*S*)-configuration, while the (*R*)-isomer is under investigation for the treatment of ALS (amyotrophic lateral sclerosis)<sup>23</sup> (fig. 1.9).



MIRAPEX

**(S)-Pramipexole** is the most prescribed dopamine agonist in the ANTI-PARKINSON THERAPY.



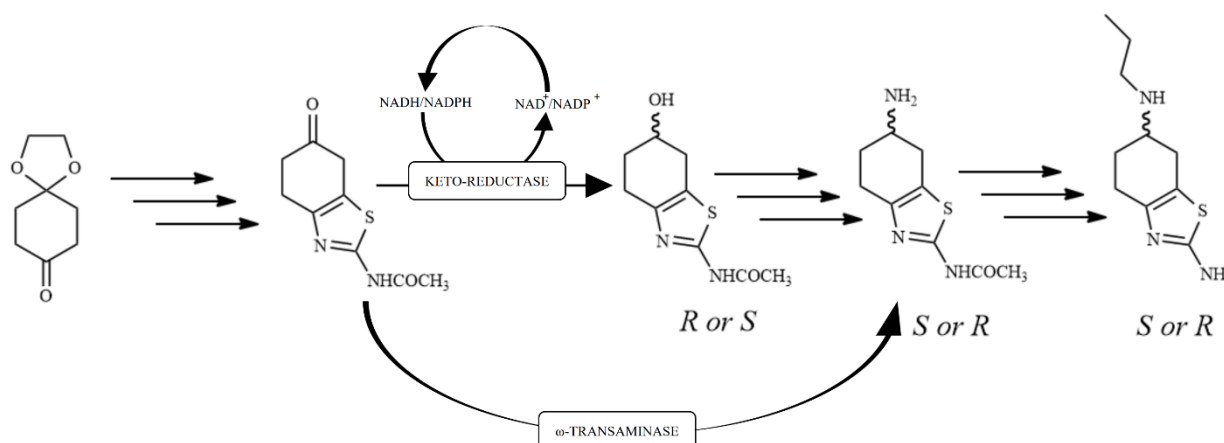
**(R)-Pramipexole** is currently under investigation for the treatment of AMYOTROPHIC LATERAL SCLEROSIS (ALS).



DEXPRAMIPEXOLE

**Fig. 1.9.** Pramipexole enantiomers could have different applications as therapeutics.

Numerous new synthetic pathways were recently developed and patented<sup>62-64</sup>. The strategy which this experimental work is based on involves a biocatalytic keto-reduction step in order to obtain an optically pure alcohol, intermediate in this new synthetic method<sup>58</sup>(scheme 1.8).



**Scheme 1.8.** This synthetic pathway based on the previous work by Ferraboschi *et al.*<sup>58</sup> combines chemical and biocatalytic steps.

MIRAPEX<sup>®</sup> by Boehringer Ingelheim<sup>®</sup> is the most common drug formulation containing as active substance (*S*)-pramipexole dihydrochloride. Currently, also the generic drug is available on the market. For what concerns anti-Parkinson drug distribution, the global prevalence in 2012 was approximately 2.18 million cases world-wide; this resulted in \$3.56 billion in global market sales of therapies, including \$1.15 billion in the U.S. market. Through advances in technology and drug development, the Parkinson treatment's market in 2022 is expected to yield \$5.26 billion in global market sales, with \$2.33 billion from the U.S. market<sup>65</sup>.

Because of the increasing spread of the disease, the global market of anti-Parkinson drugs is expanding and, consequently, Mirapex<sup>®</sup>, representing one of the most prescribed therapy, is getting an important slice of this market<sup>66</sup>.

## REFERENCES

1. Trincone, A. *Marine Enzymes for Biocatalysis*. (Woodhead Publishing, 2013).
2. Elleuche, S., Schröder, C., Sahm, K. & Antranikian, G. Extremozymes-biocatalysts with unique properties from extremophilic microorganisms. *Curr. Opin. Biotechnol.* **29**, 116–123 (2014).
3. De Vitis, V. *et al.* Marine Microorganisms as Source of Stereoselective Esterases and Ketoreductases: Kinetic Resolution of a Prostaglandin Intermediate. *Mar. Biotechnol.* **17**, 144–152 (2015).
4. Petelenz-Kurdziel, E. *et al.* Quantification of cell volume changes upon hyperosmotic stress in *Saccharomyces cerevisiae*. *Integr. Biol. Integr. Biol* **3**, 1120–1126 (1120).
5. Wood, J. M. Bacterial responses to osmotic challenges. *J. Gen. Physiol.* **145**, 381–388 (2015).
6. Graziano, G. & Merlino, A. Molecular bases of protein halotolerance. *Biochim. Biophys. Acta - Proteins Proteomics* **1844**, 850–858 (2014).
7. Ran, N., Zhao, L., Chen, Z. & Tao, J. Recent applications of biocatalysis in developing green chemistry for chemical synthesis at the industrial scale. *Green Chem.* **10**, 361–372 (2008).
8. Tao, J. & Xu, J. H. Biocatalysis in development of green pharmaceutical processes. *Curr. Opin. Chem. Biol.* **13**, 43–50 (2009).
9. Anastas, P. & Warner, J. *Green Chemistry: Theory and Practice*. (Oxford University Press, 1998).
10. Bornscheuer, U. T. *et al.* Engineering the third wave of biocatalysis. *Nature* **485**, 185–194 (2012).
11. Choi, J. M., Han, S. S. & Kim, H. S. Industrial applications of enzyme biocatalysis: Current status and future aspects. *Biotechnol. Adv.* **33**, 1443–1454 (2015).
12. Gu, Q.-M., Chen, C.-S. & Sih, C. . A facile enzymatic resolution process for the preparation of (+)-S-2-(6-hethoxy-2-naphthyl)propionic acid (Naproxen). *Tetrahedron Lett.* **27**, (1986).
13. Ciceri, S., Ciuffreda, P., Grisenti, P. & Ferraboschi, P. Synthesis of the antitumoral nucleoside capecitabine through a chemo-enzymatic approach. *Tetrahedron Lett.* **56**, 5909–5913 (2015).
14. Ferraboschi, P., Mieri, M. D. & Galimberti, F. Chemo-enzymatic approach to the synthesis of the antithrombotic clopidogrel. *Tetrahedron Asymmetry* **21**, 2136–2141 (2010).
15. Desai, A. A. Sitagliptin manufacture: A compelling tale of green chemistry, process intensification, and industrial asymmetric catalysis. *Angew. Chemie - Int. Ed.* **50**, 1974–1976 (2011).
16. Savile, C. K. *et al.* Biocatalytic Asymmetric Synthesis of Chiral Amines from Ketones Applied to Sitagliptin Manufacture. *Science (80-. )*. **329**, 305–309 (2010).

17. Truppo, M. D., Strotman, H. & Hughes, G. Development of an Immobilized Transaminase Capable of Operating in Organic Solvent. *ChemCatChem* **4**, 1071–1074 (2012).
18. Huisman, G. W. & Collier, S. J. On the development of new biocatalytic processes for practical pharmaceutical synthesis. *Curr. Opin. Chem. Biol.* **17**, 284–292 (2013).
19. Huisman, G. W., Liang, J. & Krebber, A. Practical chiral alcohol manufacture using ketoreductases. *Curr. Opin. Chem. Biol.* **14**, 122–129 (2010).
20. Liang, J. *et al.* Development of a biocatalytic process as an alternative to the (-)-DIP-Cl-mediated asymmetric reduction of a key intermediate of montelukast. *Org. Process Res. Dev.* **14**, 193–198 (2010).
21. Contente, M. L. *et al.* Development of a high-yielding bioprocess for 11- $\alpha$  hydroxylation of canrenone under conditions of oxygen-enriched air supply. *Steroids* **116**, 1–4 (2016).
22. Mitsunobu, O. The Use of Diethyl Azodicarboxylate and Triphenylphosphine in Synthesis and Transformation of Natural Products. *Synthesis (Stuttg.)* **1981**, 1–28 (1981).
23. Bozik, M. E., Mather, J. L., Kramer, W. G., Gribkoff, V. K. & Ingersoll, E. W. Safety, Tolerability, and Pharmacokinetics of KNS-760704 (Dexpramipexole) in Healthy Adult Subjects. *J. Clin. Pharmacol.* **51**, 1177–1185 (2011).
24. Schmid, A. *et al.* Industrial biocatalysis today and tomorrow. *Nature* **409**, 258–268 (2001).
25. de Carvalho, C. C. C. R. Whole cell biocatalysts: essential workers from Nature to the industry. *Microb. Biotechnol.* **10**, 250–263 (2017).
26. Roberts, R. J. *et al.* On Base Flipping Minireview. *Cell* **92**, 9–12 (1995).
27. Faber, K. *Biotransformations in Organic Chemistry: A Textbook.* (Springer Berlin Heidelberg, 2011).
28. Polizzi, K. M., Bommarius, A. S., Broering, J. M. & Chaparro-Riggers, J. F. Stability of biocatalysts. *Curr. Opin. Chem. Biol.* **11**, 220–225 (2007).
29. Morley, K. L. & Kazlauskas, R. J. Improving enzyme properties: When are closer mutations better? *Trends Biotechnol.* **23**, 231–237 (2005).
30. Eijsink, V. G. H., GÅseidnes, S., Borchert, T. V. & Van Den Burg, B. Directed evolution of enzyme stability. *Biomol. Eng.* **22**, 21–30 (2005).
31. Collins, C. H., Arnold, F. H. & Leadbetter, J. R. Directed evolution of. *Mol. Microbiol.* **55**, 712–723 (2005).
32. Michaelis, L. & Menten, M. L. Die Kinetik der Invertinwirkung. *Biochem Z* **49**, 333–369 (1913).
33. Briggs, G. E. & Haldane, J. B. S. A Further Note on the Kinetics of Enzyme Action. *Biochem. J.* **19**,

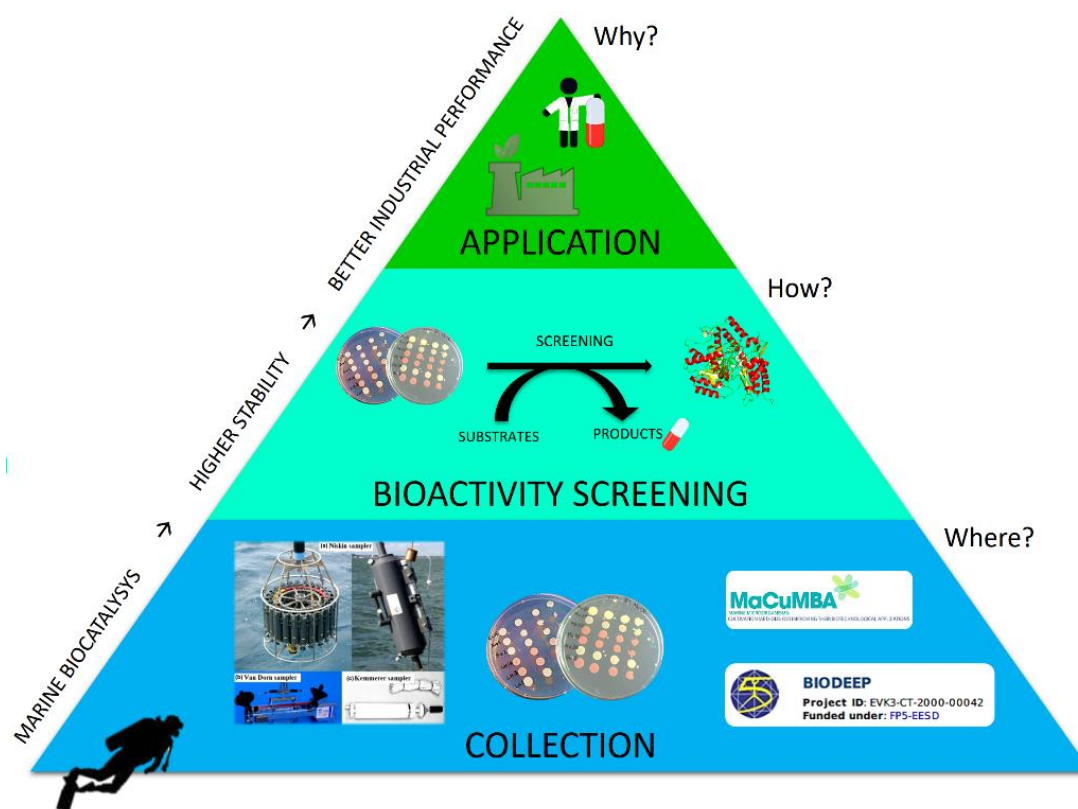
1037–1038 (1925).

34. Fersht, A. R. *et al.* Hydrogen bonding and biological specificity analysed by protein engineering. *Nature* **316**, 452–457 (1985).
35. Dean, A. M., Shiau, A. K., And, S. & Koshland, D. E. Determinants of performance in the isocitrate dehydrogenase of *Escherichia coli*. *Protein Sci.* **5**, 341–347 (1996).
36. Chen, C. S., Fujimoto, Y., Girdaukas, G. & Sih, C. J. Quantitative Analyses of Biochemical Kinetic Resolutions of Enantiomers. *J. Am. Chem. Soc.* **104**, 7294–7299 (1982).
37. Faber, K., Höning, H. & Kleewein, A. in *Preparative Biotransformations* (Wiley, 1995).
38. Illanes, A. Stability of biocatalysts. *Electron. J. Biotechnol.* **2**, 1–9 (1999).
39. Illanes, A., Altamirano, C. & Zuniga, M. E. Thermal Inactivation of Immobilized Penicillin Acylase in the Presence of Substrate and Products. *Biotechnol. Bioeng.* **50**, 609–616 (1996).
40. Lutz, S. Beyond directed evolution-semi-rational protein engineering and design. *Curr. Opin. Biotechnol.* **21**, 734–743 (2010).
41. Stemmer, W. P. DNA shuffling by random fragmentation and reassembly: in vitro recombination for molecular evolution. *Proc. Natl. Acad. Sci. U. S. A.* **91**, 10747–10751 (1994).
42. Koltermann, A. & Kettling, U. Principles and methods of evolutionary biotechnology. *Biophys. Chem.* **66**, 159–177 (1997).
43. Arnold, F. H. Design by Directed Evolution. *Acc. Chem. Res.* **31**, 125–131 (1998).
44. Turner, N. J. Directed evolution of enzymes for applied biocatalysis. *Trends Biotechnol.* **21**, 474–478 (2003).
45. Arnold, F. H. & Volkov, A. A. Directed evolution of biocatalysts. *Curr. Opin. Chem. Biol.* **3**, 54–59 (1999).
46. Reetz, M. T., Wang, L. W. & Bocola, M. Directed evolution of enantioselective enzymes: Iterative cycles of CASTing for probing protein-sequence space. *Angew. Chemie - Int. Ed.* **45**, 1236–1241 (2006).
47. Reetz, M. T., Bocola, M., Carballeira, J. D., Zha, D. & Vogel, A. Expanding the range of substrate acceptance of enzymes: Combinatorial active-site saturation test. *Angew. Chemie - Int. Ed.* **44**, 4192–4196 (2005).
48. Kazlauskas, R. J. & Bornscheuer, U. T. Finding better protein engineering strategies. *Nat. Chem. Biol.* **5**, 526–9 (2009).
49. Servi, S. Baker's Yeast as a Reagent in Organic Synthesis. *Synthesis (Stuttg.)*. (1990).

50. Kuhlmann, A. U., Bursy, J., Gimpel, S., Hoffmann, T. & Bremer, E. Synthesis of the compatible solute ectoine in *Virgibacillus pantothenicus* is triggered by high salinity and low growth temperature. *Appl. Environ. Microbiol.* **74**, 4560–4563 (2008).
51. Csuk, R. & Glänzer, B. I. Baker's Yeast Mediated Transformations in Organic Chemistry. *Chem. Rev.* **91**, 49–97 (1991).
52. Santaniello, E., Ferraboschi, P., Grisenti, P. & Manzocchi, A. The Biocatalytic Approach to the Preparation of Enantiomerically Pure Chiral Building Blocks. *Chem. Rev.* **92**, 1071–1140 (1992).
53. Zaky, A. S., Tucker, G. A., Daw, Z. Y. & Du, C. Marine yeast isolation and industrial application. *FEMS Yeast Res.* **14**, 813–825 (2014).
54. Malik, M. S., Park, E.-S. & Shin, J.-S.  $\omega$ -Transaminase-catalyzed kinetic resolution of chiral amines using l-threonine as an amino acceptor precursor. *Green Chem.* **14**, 2137 (2012).
55. Midelfort, K. S. *et al.* Redesigning and characterizing the substrate specificity and activity of *Vibrio fluvialis* aminotransferase for the synthesis of imagabalin. *Protein Eng. Des. Sel.* **26**, 25–33 (2013).
56. Sehl, T. *et al.* Efficient 2-step biocatalytic strategies for the synthesis of all nor(pseudo)ephedrine isomers. *Green Chem.* **16**, 3341–3348 (2014).
57. Contente, M. L., Dall'Oglio, F., Tamborini, L., Molinari, F. & Paradisi, F. Highly efficient oxidation of amines to aldehydes via flow-based biocatalysis. *ChemCatChem* (2017). doi:10.1002/cctc.201701147 IF:4.803
58. Ferraboschi, P. *et al.* Baker's yeast catalyzed preparation of a new enantiomerically pure synthon of (S)-pramipexole and its enantiomer (dexpramipexole). *Tetrahedron Asymmetry* **25**, 1239–1245 (2014).
59. Antonini, A. *et al.* Role of Pramipexole in the Management of Parkinson's Disease. **24**, 829–841 (2010).
60. Perez Lloret, S. & Rascol, O. Pramipexole extended-release (once-daily formulation) for the treatment of Parkinson's disease. *Expert Opin. Pharmacother.* **11**, 2221–2230 (2010).
61. Hametner, E.-M., Seppi, K. & Poewe, W. Role and clinical utility of pramipexole extended release in the treatment of early Parkinson's disease. *Clin. Interv. Aging* **7**, 83–8 (2012).
62. Patil, P., Pansare, P., Jagtap, A. & Krishnamurth, D. An improved process for the preparation of pramipexole dihydrochloride monohydrate. (2015). PATENT
63. Castaldi, G., Bologna, A., Allegrini, P., Razzetti, G. & Lucchini, V. Intermediates for the preparation of pramipexole. (2010). PATENT
64. Zivec, M., Gobec, S., Anzic, B., Zupet, R. & Kolenc, I. Novel process for synthesis of pramipexole and its pharmaceutically acceptable salts. (2008). PATENT

65. *Parkinson's Disease - Global Drug Forecast and Market Analysis to 2022*. (2014).
66. Gohil, K. Steady progress on Parkinson's disease. *PIPELINE PLUS Steady* **39**, 712–3 (2014).

## AIM OF THE WORK



This PhD project focuses on the identification, isolation and characterization of new biocatalysts able to generate biologically active molecules with significant enantioselectivity. Through screening, we identified marine strains, from MaCuMBA (Marine Culturable Microorganism for Biotechnological Applications) and BIODEEP (Biotechnologies from the deep) European project collections, which show a marked enantioselectivity on intermediates of molecules of biological interest. Once identified the strains and optimised the biotransformation conditions with whole cells, the most promising enzyme was cloned and overexpressed in a suitable host. After biochemical characterization of the biocatalyst, the final challenge was the rational engineering of the protein to improve its biocatalytic features.

Biotransformation substrate range included pramipexole, as the main target, but it also embraced other common building blocks for synthetic industrial preparation.

The following chapters are organised according to what reported below.

## WHOLE CELL SCREENING

### MARINE YEASTS ACTIVITY

Due to cofactor requirement, keto-reductase biotransformations are more efficiently carried out in whole cell system. The stereoselective reduction of structurally different ketones using halo-tolerant marine yeasts was studied using cells grown and bio-converted in seawater.

For what concerns pramipexole, the goal was to find a marine yeast able to reduce the ketone intermediate with an opposite stereochemical outcome in comparison with *Saccharomyces cerevisiae*. In order to compare biocatalytic performances, also non-marine yeasts (*Rhodotorulae* species) were tested on pramipexole intermediates.

### MARINE BACTERIA ACTIVITY

Taking into account pramipexole, firstly keto-reduction potential of thirty-three marine bacterium species was checked and afterwards the possibility to convert this substrate directly into the optically pure amine was investigated: marine bacteria were screened to identify transaminase activity. According to transaminase biocatalytic applications, where cofactor recycling is not needed, the aim in this case was to express and employ a recombinant enzyme.

## RECOMBINANT ENZYME SCREENING

### KETO-REDUCTASE ACTIVITY

A recombinant non-marine ketoreductase from *Pichia glucozyma* (KRED1-Pglu) was used for the enantioselective reduction of various cyclic ketones including pramipexole ketone intermediate. Thanks to a co-factor recycling system, the purified enzyme showed very promising results.

### ESTERASE AND LIPASE ACTIVITY

Other enzymatic activities were investigated in order to achieve optically pure intermediates for the preparation of both pramipexole enantiomers. Ten of the most common commercial lipases and one new recombinant esterase from *Bacillus coagulans* were tested on pramipexole ester intermediates.

## MARINE $\omega$ -TRANSAMINASE ACTIVITY

*Chromobacterium violaceum* and *Halomonas elongata*  $\omega$ -transaminases were screened for biocatalytic conversion of pramipexole intermediates.

## VIRGIBACILLUS PANTOTHENTICUS $\omega$ -TRANSAMINASE

Trying to improve the pramipexole synthetic pathway by a biocatalytic approach, the promising marine bacteria *Virgibacillus pantothenicus* was selected and a new  $\omega$ -TA was cloned, overexpressed and characterised.

## WHOLE CELL SCREENING - MARINE YEASTS

In this chapter, a screening for keto-reductase activity and halotolerance on a heterogeneous group of marine yeasts, recently isolated and characterized<sup>1,2</sup>, will be described.

## BACKGROUND

### MARINE YEASTS

As it was deeply discussed in the previous chapter, through million years of evolution, marine microorganisms belonging to the three kingdoms of life Bacteria, Archaea and Eukarya, have developed unique metabolic and physiological abilities in order to respond to the most extreme stresses<sup>3</sup>.

Specifically, for this experimental project, different strains of marine yeasts belonging to Basidiomycota and Ascomycota phyla have been studied and screened with biocatalytic purposes. The microorganisms were provided by MaCuMBA European research project (Marine Microorganisms: Cultivation Methods for Improving their Biotechnological Applications, FP7, Grant Agreement 311975, Brussels, Belgium), which explored unique marine ecosystems focusing on isolation and setting up culturing methods for marine microorganisms. From the biocatalytic point of view this collection offers new opportunities for studying significant enzymatic activities. The yeast strains were isolated at different depths of the Pacific and Atlantic Ocean seafloor and in particular from deep-subseafloor sediments and hydrothermal vents. These unique environments are characterized by a variety of chemical and physical properties including low availability of nutrients, exposure to high saline concentrations, high hydrostatic pressure, extreme pH and temperature changes.

The strains originating from the sediments of seafloor were isolated at different depths from the Canterbury Basin in New Zealand (44° 56 26.62 "S, 172 ° 1 36.30" E)<sup>2</sup>.

For what concerns hydrothermal springs, the samples were collected in rifts characterized by the presence of faults, magma, basalt and volcanic rocks. Water infiltration allows the dissolution of minerals in the springs. The hot winds, "black smokers"(fig. 2.1), can reach a temperature of 270-380 °C<sup>4</sup>. They are characterized by the lack of dissolved oxygen, high acidity (pH 2 or 3), high concentration of electron donor molecules (e.g. reduced compounds such as methane and hydrogen sulphide) and the presence of heavy metals<sup>5</sup>. Continuous mixing with cold ocean water (2 to 4 °C), rich in electron acceptor molecules, creates a chemical imbalance that is a source of energy for microorganisms that control the speed of redox reactions<sup>6</sup>.

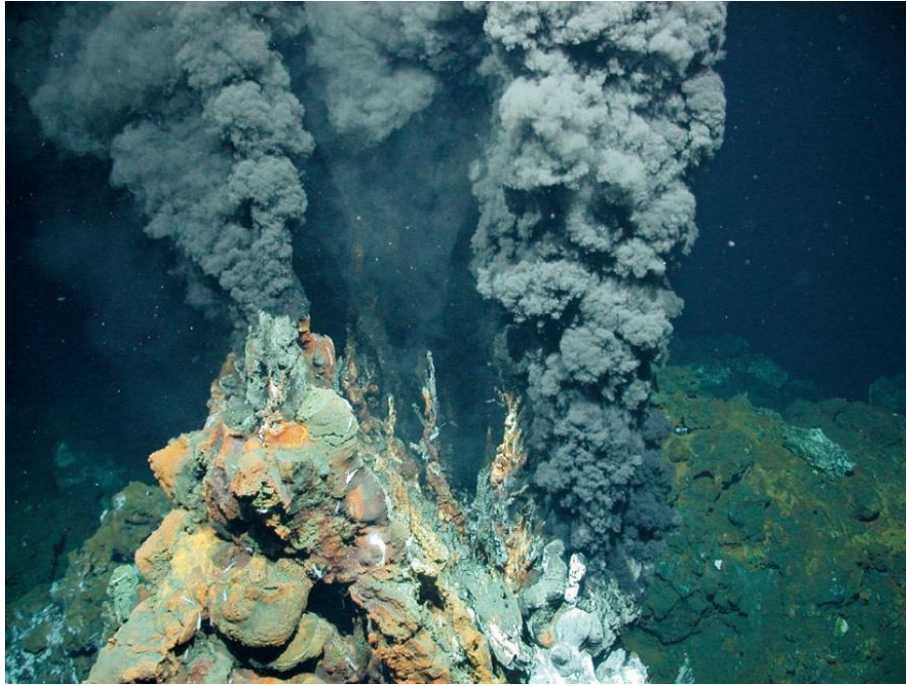


**Fig. 2.1.** “Black smokers” from hydrothermal vents on the sea floor.

## KETO-REDUCTASE

The oxidoreductases have been classified, according to the primary sequence and secondary structure folding into four main superfamilies:

- Medium-chain Dehydrogenases/Reductases (MDRs) participate in numerous oxidation reactions of alcohols, detoxification of aldehydes and alcohols and they are active in the metabolism of bile acids. Other components of this family are cinnamyl alcohol dehydrogenase (CAD), polyhydrodehydrogenase (PHD) and quinone oxidoreductase (QOR). All MDR enzymes use NADH and NAD(P)H as cofactor and not all but several members of this family possess a zinc ion for catalytic activity in the active site<sup>7</sup>.
- Flavin mononucleotide dependent reductases, also known as the old yellow enzymes (OYE) in relation to the colour associated with flavin cofactor, are exploited for stereoselective bioreduction of double bonds  $C = C$ <sup>8</sup>.
- Aldo-Keto Reductases (AKRs) are a superfamily of dependent NADP(H) oxidoreductases that can perform their action on a wide variety of both endogenous and exogenous substrates. These enzymes are made up of monomeric proteins of about 320 amino acid residues of length with an 8-barrel  $(\alpha / \beta)$  structure. Their active site contains a conserved catalytic tetrad composed of Tyr, His, Asp and Lys. They are located in most living organisms and metabolize steroids, sugars, prostaglandins, polycyclic aromatic hydrocarbons, and a large variety of non-steroidal aldehydes and ketones<sup>9</sup>.

- Short chain dehydrogenases/reductases (SDRs) are a superfamily that consists of enzymes of 250 - 300 amino acid residues. Their functionality is independent of metal cofactors and its members are easily distinguishable from the superfamily of alcohol medium and long chain dehydrogenases. They are in some cases membrane proteins mostly soluble homodimers or homotetramers with the classic  $\beta\alpha\beta$  folding pattern of Rossmann able to link both NADH and NAD(P)H cofactors. SDRs include a large and highly diverging superfamily of enzymes with over 3,000 known forms (including varieties of species), preserving a gender identity of 15-30% and covering a broad spectrum of activities on substrates such as alcohols, sugars, steroids, prostaglandins, aromatic and xenobiotic compounds<sup>10,11</sup>.

Keto-reductases (KREDs) were originally classified, based on their functionality, in the superfamily of AKRs. Subsequently, with the discovery of some homologues amino acid residues of SDR superfamily they were included in this superfamily. KREDs are structurally characterized by the typical domain involved in binding to the cofactor, called Rossmann-fold, with a GlyXXXGlyXGly preserved sequence in the N-terminal of the enzyme. Another preserved amino acid which constitutes the active site of some of these enzymes is the Tyr at position 194 which is part of the TyrXXXLys common sequence of SDRs.

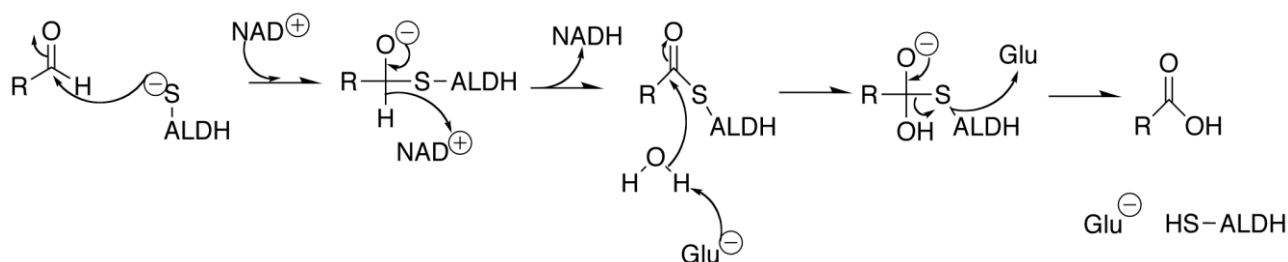
KREDs are, indeed, enzymes useful for chemo, regio, and stereoselective reductions/oxidations, being particularly useful for the synthesis of chiral alcohols from ketones, keto-acids and keto-esters. They are also able to catalyse the reaction of reduction of numerous aldehydes and more generally catalyse a series of stereoselective reactions on a wide range of substrates:

- reduction of carbonyl groups;
- oxidation of secondary alcohols;
- reduction of 2-substituted-3-ketoesters.

KREDs also usually exhibit high stereoselectivity, in fact they are able to act on molecules with two prostereogenic centers reducing only one with regioselectivity<sup>12</sup>.

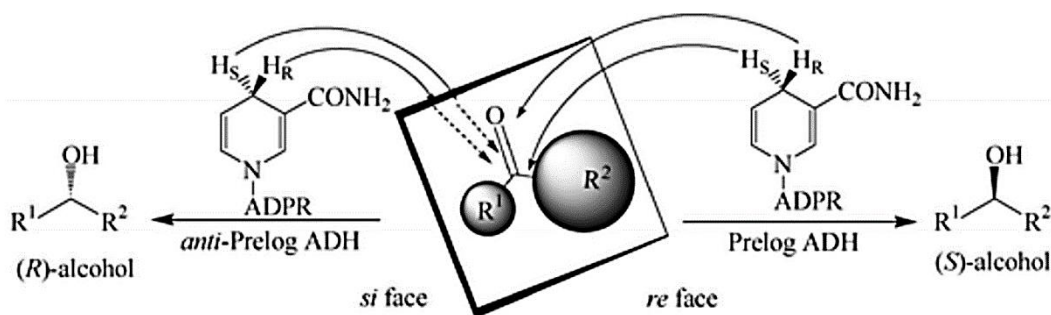
## DH CATALYTIC MECHANISM

The catalytic mechanism of carbonyl-reductase indicated by the generic term of dehydrogenase (DH) is closely related to two nicotinamide-deriving co-factor:  $\text{NAD}^+$  and  $\text{NADP}^+$ . DHs transfer electrons from the substrate to these electron carriers that are reduced and considered oxidizers of the substrate, in this way the cofactor will require its regeneration to continue the reduction of other substrate molecules (scheme 2.1).



**Scheme 2.1.** Mechanism of an aldehyde dehydrogenase, note the use of  $\text{NAD}^+$  as an electron acceptor<sup>13</sup>.

The configuration of the alcohol obtained as product generally follows an empirical rule determined by Prelog, even if the catalytic mechanisms to date are still not entirely clear. In the early 1960s, Prelog proposed a simple model to predict the stereochemistry of the products based on the steric requirements of the substrates.



**Scheme 2.2.** Stereochemistry of the hydride transfer from  $\text{NAD(P)H}$  to the carbonyl carbon on a ketone substrate. ADPR = adenosine diphosphoribose,  $\text{R}^1$  is more sterically hindered and has higher Cahn–Ingold–Prelog priority than  $\text{R}^2$ <sup>14</sup>.

In the asymmetric reduction of a prochiral ketone, there are four possible pathways to deliver the hydride from  $\text{NAD(P)H}$ , as shown in scheme 2.2. The pro-(R) or pro-(S)-hydride can attack from the re face of a prochiral ketone, to produce the (S)-alcohol, according to Prelog's Rule, or it can also attack from the si face of a ketone to produce the (R)-alcohol. (It should be noted that sometimes the products have opposite assignments because the small substituent, if alkenyl or alkynyl, has a higher Cahn–Ingold–Prelog priority than the larger alkyl one). The majority of commercially available

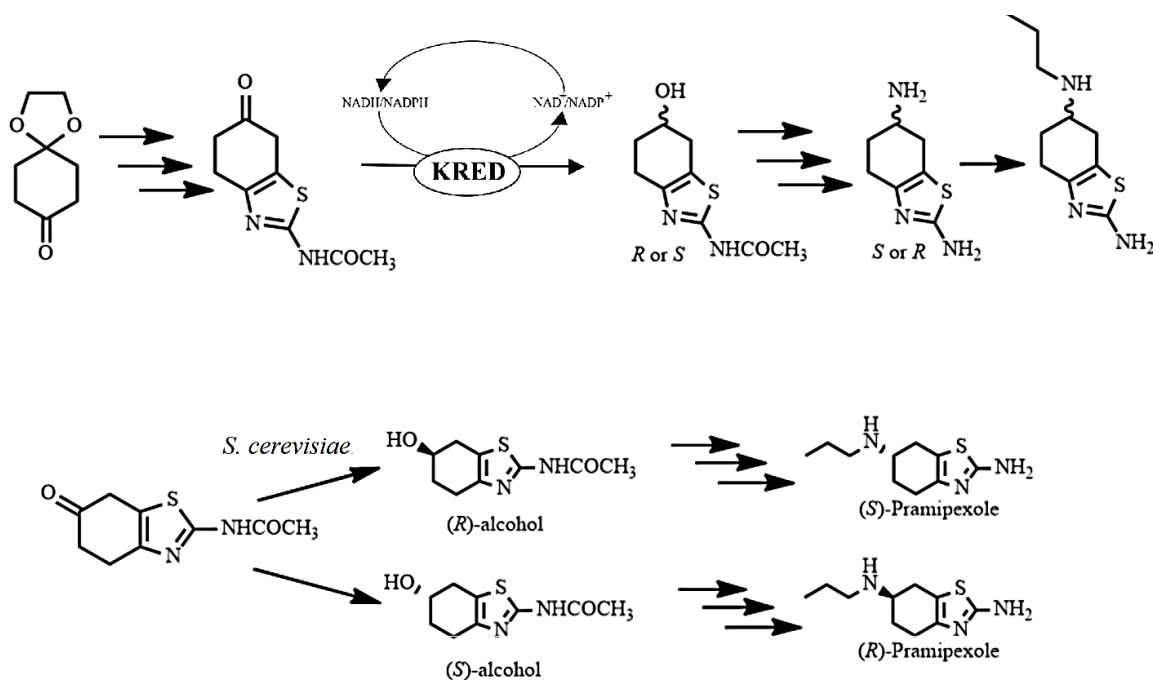
ADHs, like yeast ADH (YADH), horse liver ADH (HLADH), and *Thermoanaerobium brockii* ADH (TbADH), fall in the first category (i.e. they deliver the pro-(R)-hydride from the re face of a prochiral ketone). A few ADHs are known to have anti-Prelog stereopreference; however, very few of them are commercially available, one of which is *Lactobacillus kefir* ADH (LkADH)<sup>15</sup>.

A limit of employing recombinant ADHs is the regeneration of cofactor. These compounds are very expensive, unstable and consumed in a stoichiometric amount. For the development of an industrial application of oxidoreductases, this problem has been overcome by the *in situ* recycling techniques allowing the use of catalytic amounts of these compounds.

### PROJECT AIM

Due to cofactor requirement, keto-reductase biotransformations are more efficiently carried out in whole cell system. The stereoselective reduction of structurally different ketones using halotolerant marine yeasts was studied using cells grown and bioconverted in seawater.

For what concerns pramipexole, the goal was to find a marine yeast able to reduce the ketone intermediate with an opposite stereochemical outcome in comparison with *Saccharomyces cerevisiae* (scheme 2.3).



**Scheme 2.3.** Stereoselective reduction of keto-intermediate of pramipexole by yeasts.

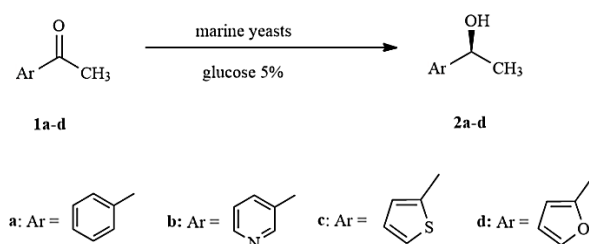
## RESULTS AND DISCUSSION

### KETO-REDUCTASE SCREENING

Enzymatic activity screening was carried out on a first more homogeneous group of marine yeasts including *genera* with already known reductive potentials<sup>16-18</sup>.

Eight strains of *Meyerozyma guilliermondii* and twelve strains of *Rhodotorula mucilaginosa* isolated previously from different deep-sub-seafloor sediment depths at Canterbury Basin (New Zealand)<sup>2</sup> were grown in a liquid YPD (yeast extract, peptone, D-glucose) prepared with purified freshwater or micro-filtered seawater. After 48h the optical density was checked and three strains appeared to be particularly halotolerant showing a similar production of biomass in freshwater- and in seawater-based media: *Meyerozyma guilliermondii* UBOCC-A-214008, *Rhodotorula mucilaginosa* UBOCC-A-214025 and *Rhodotorula mucilaginosa* UBOCC-A-214036. Therefore, the keto-reductase activity of these strains was checked towards structurally different substrates.

### ARYLMETHYLKETONES



**Scheme 2.4.** Arylmethylketones employed as substrate.

The biocatalytic potential of these three marine yeasts was first tested on arylmethylketones (**1 a–d**), substrates of choice to test stereoselective keto-reductase activity.

**Table 2.1.** Reduction of arylmethylketones **1 a–d** (10 mm) with marine yeasts.

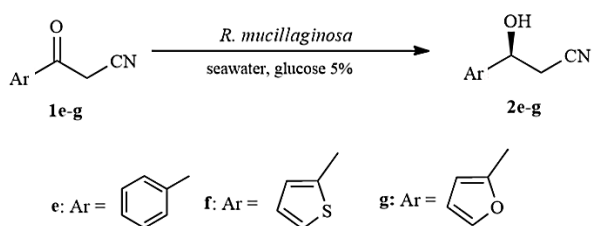
Entry	Strain	Medium	Substrate	Yield [%]	ee [%]	t [h]
1	<i>M. guilliermondii</i> UBOCC-A-214008	freshwater	<b>1 a</b>	<5	n.d.	48
2	<i>M. guilliermondii</i> UBOCC-A-214008	seawater	<b>1 a</b>	<5	n.d.	48
3	<i>M. guilliermondii</i> UBOCC-A-214008	freshwater	<b>1 b</b>	90	97	24
4	<i>M. guilliermondii</i> UBOCC-A-214008	seawater	<b>1 b</b>	65	88	48
5	<i>M. guilliermondii</i> UBOCC-A-214008	freshwater	<b>1 c</b>	<5	n.d.	48
6	<i>M. guilliermondii</i> UBOCC-A-214008	seawater	<b>1 c</b>	<5	n.d.	48
7	<i>M. guilliermondii</i> UBOCC-A-214008	freshwater	<b>1 d</b>	<5	n.d.	48
8	<i>M. guilliermondii</i> UBOCC-A-214008	seawater	<b>1 d</b>	<5	n.d.	48
9	<i>R. mucilaginosa</i> UBOCC-A-214025	freshwater	<b>1 a</b>	> 97	> 98	8
10	<i>R. mucilaginosa</i> UBOCC-A-214025	seawater	<b>1 a</b>	> 97	> 98	8
11	<i>R. mucilaginosa</i> UBOCC-A-214025	freshwater	<b>1 b</b>	<5	n.d.	48
12	<i>R. mucilaginosa</i> UBOCC-A-214025	seawater	<b>1 b</b>	<5	n.d.	48
13	<i>R. mucilaginosa</i> UBOCC-A-214025	freshwater	<b>1 c</b>	72	> 98	24
14	<i>R. mucilaginosa</i> UBOCC-A-214025	seawater	<b>1 c</b>	60	> 98	24
15	<i>R. mucilaginosa</i> UBOCC-A-214025	freshwater	<b>1 d</b>	94	> 98	3
16	<i>R. mucilaginosa</i> UBOCC-A-214025	seawater	<b>1 d</b>	87	> 98	3
17	<i>R. mucilaginosa</i> UBOCC-A-214036	freshwater	<b>1 a</b>	> 97	> 98	8
18	<i>R. mucilaginosa</i> UBOCC-A-214036	seawater	<b>1 a</b>	> 97	> 98	8
19	<i>R. mucilaginosa</i> UBOCC-A-214036	freshwater	<b>1 b</b>	<5	n.d.	48
20	<i>R. mucilaginosa</i> UBOCC-A-214036	seawater	<b>1 b</b>	<5	n.d.	48
21	<i>R. mucilaginosa</i> UBOCC-A-214036	freshwater	<b>1 c</b>	72	> 98	48
22	<i>R. mucilaginosa</i> UBOCC-A-214036	seawater	<b>1 c</b>	61	> 98	48
23	<i>R. mucilaginosa</i> UBOCC-A-214036	freshwater	<b>1 d</b>	80	>98	3
24	<i>R. mucilaginosa</i> UBOCC-A-214036	seawater	<b>1 d</b>	72	>98	3

No activity was found towards acetophenone **1 a** with strains of *Meyerozyma guilliermondii*, whereas the selected strains of *Rhodotorula mucilaginosa* gave (*S*)-1-phenylethanol with high yield and

enantioselectivity. The biotransformation of **1 a** occurred with no significant differences between freshwater or seawater. The two strains of *Rhodotorula mucilaginosa* were not active for **1 b** but reduced **1 c** and **1 d** to a different extent. 1-(Furan-2-yl)ethanone (**1 d**) was reduced enantioselectively with high yields and high rates by the two strains of *R. mucilaginosa* both in freshwater and seawater. With **1 c**, a higher efficiency in the reduction to enantiopure (*S*)-1-(thiophen-2-yl)ethanol (**2 c**) could be observed in freshwater.

From the point of view of stereoselectivity, all the tested strains gave ketone reduction that followed the so-called Prelog rule with the formation of the alcohols with an *S* configuration. Overall, bioprocesses performed entirely in seawater gave good results, although a slightly poorer activity was generally observed than for that in freshwater.

### $\beta$ - KETONITRILES



**Scheme 2.5.**  $\beta$ -Ketonitriles employed as substrate.

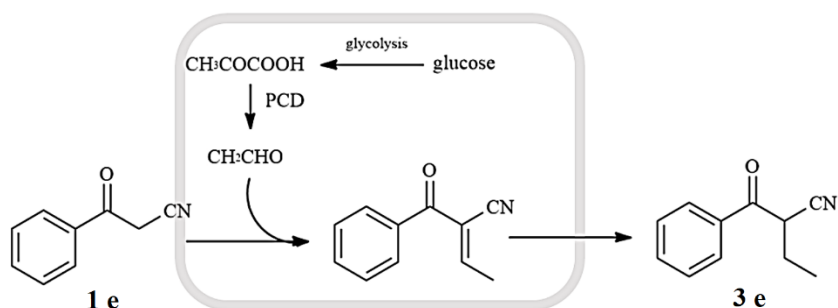
Asymmetric  $\beta$ -hydroxy nitriles are valuable chiral intermediates for the synthesis of a number of biologically active compounds; hence, we evaluated the reduction of 3-oxo-3-arylpropanenitriles **1 e–g** with marine yeasts in seawater. The biocatalytic reduction of  $\beta$ -ketonitriles has been explored using both isolated enzymes (which need systems for co-factor regeneration)<sup>19–23</sup> and whole cells<sup>24</sup>; the latter approach has the advantage of that it can supply co-factors and systems naturally for their regeneration but it is often hampered by the occurrence of competitive alkylation<sup>24</sup>, which limits the preparative scope of these biotransformations.

Entry	Strain	Substrate	Yield [%]	ee [%]
1	<i>R. mucilaginosa</i> UBOCC-A-214025	<b>1 e</b>	93	>98
2	<i>R. mucilaginosa</i> UBOCC-A-214025	<b>1 f</b>	85	>98
3	<i>R. mucilaginosa</i> UBOCC-A-214025	<b>1 g</b>	88	>98
4	<i>R. mucilaginosa</i> UBOCC-A-214036	<b>1 e</b>	92	>98

5	<i>R. mucilaginosa</i> UBOCC-A-214036	<b>1 f</b>	93	>98
6	<i>R. mucilaginosa</i> UBOCC-A-214036	<b>1 g</b>	79	>98

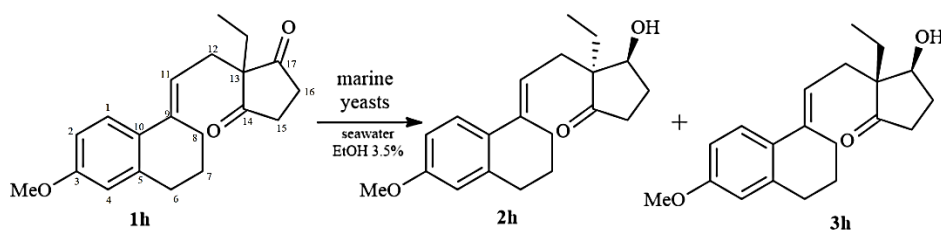
**Table 2.2.** Reduction of  $\beta$ -ketonitriles **1 e–g** (10 mM) with *R. mucilaginosa* grown in YPD-seawater medium.

Two distinct behaviours were observed for the yeasts employed: strains of *R. mucilaginosa* gave the reduction products **2 e–g** (table 2.2) as the only detectable compounds obtained by biotransformation with a high enantioselectivity to afford optically pure (*S*)-**2 e–g**. The yields and enantioselectivity obtained using the two strains are remarkable; the high selectivity (both because of the avoidance of by-products and enantioselectivity) in the reduction of aromatic  $\beta$ -ketonitriles with whole cells of yeasts was observed previously mostly with strains that belong to the genus *Rhodotorula*. However, *M. guilliermondii* UBOCC-A-214008 gave the 2-ethylketones **3 e–g** as major products and traces of (*S*)-3-hydroxy-3-arylpropanenitriles **2 e–g**. 2-Ethylketones resulted from non-enzymatic aldol condensation between aromatic  $\beta$ -ketonitriles and acetaldehyde (formed by the yeasts in the presence of glucose) followed by the reduction of activated C=C by enoate reductases (Scheme 2.5)<sup>25</sup>. This different behaviour seems to indicate the presence of pyruvate decarboxylase activity in *M. guilliermondii*, which is lacking in *R. mucilaginosa* strains. The biotransformations with cells grown and used in freshwater gave similar results (data not shown).



**Scheme 2.6.** Formation of 2-benzoylbutanenitrile (**3 e**) from 3-oxo-3-phenylpropanenitrile (**1 e**) in the presence of glucose<sup>26</sup>.

## STEROIDAL ETHYL SECODIONE



**Scheme 2.7.** Bioconversion of steroidal ethyl secodione.

To further explore the substrate range accepted by ketoreductases of the selected marine yeasts, steroidal ethyl secodione derivative **1 h** was tested as a substrate (scheme 2.7 and table 2.3). The stereoselective reduction of the diketone **1 h** provides the key chiral precursor for the synthesis of a number of hormonal contraceptives (i.e., desogestrel, norgestrel, gestodene)<sup>23</sup>. The biotransformation of **1 h** is complicated by the low solubility of the substrate in water; recently, we reported the use of different biocatalysts for the stereoselective mono-reduction of **1 h** and noticed that the use of EtOH (both to increase solubility and favour co-factor regeneration) was beneficial for biotransformations with whole microbial cells<sup>27</sup>. Thus, the reduction of **1 h** with marine yeasts was performed in the presence of different amounts of EtOH (1–5 %), and the best results were found with an EtOH concentration of 3.5 %.

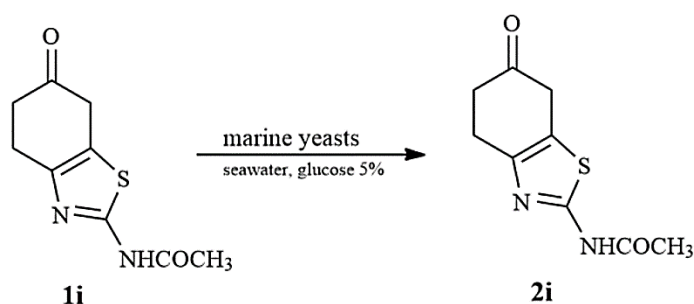
Entry	Strain	Yield [%]	2 h/3 h
1	<i>M. guilliermondii</i> UBOCC-A-214008	<5	n.d.
2	<i>R. mucilaginosa</i> UBOCC-A-214025	97	63/37
3	<i>R. mucilaginosa</i> UBOCC-A-214036	96	92/8

**Table 2.3.** Reduction of ethyl secodione **1 h** (10 mM) with marine yeasts grown in YPD-seawater medium.

The biotransformation of **1 h** in seawater occurred only with *R. mucilaginosa*; the reduction of the carbonyl occurred with high enantioselectivity to form a mixture of the stereoisomers (13*S*, 17*S*)-**2 h** and (13*R*, 17*S*)-**3 h** with a different stereoselectivity that depended on the strain employed. Reduction with *R. mucilaginosa* UBOCC-A-214036 was highly stereoselective and furnished (13*S*, 17*S*)-**2 h** as the main product.

### PRAMIPEXOLE KETO INTERMEDIATE

Scopo: sintesi R per S pramipex



**Scheme 2.8.** Reduction of keto intermediate of pramipexole.

Finally, the reduction of the pro-chiral bicyclic ketone **1 i** was evaluated (table 2.4). Enantiomerically pure 2-acetylamino-6-hydroxy-4,5,6,7-tetrahydrobenzothiazole (**2 i**) is the synthon of the anti-Parkinson (*S*)-pramipexole<sup>28</sup>. An initial screening with growing cells after 24h had led to an interesting result by *R. mucilaginosa* UBOCC-A-214025.

Microorganisms	UBOCC number	Conversion	<i>e.e.</i>	Configuration
<i>Meyerozyma guilliermondii</i> strain	UBOCC-A-214022	100%	7,5%	<i>R</i>
<i>Meyerozyma guilliermondii</i> strain	UBOCC-A-214008	100%	5%	<i>R</i>
<i>Meyerozyma guilliermondii</i> strain	UBOCC-A-214007	100%	1,3%	<i>R</i>
<i>Rhodotorula mucilaginosa</i> strain	UBOCC-A-214045	100%	40%	<i>S</i>
<i>Meyerozyma guilliermondii</i> strain	UBOCC-A-214013	100%	2%	<i>R</i>
<i>Meyerozyma guilliermondii</i> strain	UBOCC-A-214014	100%	1%	<i>R</i>
Not sequenced	UBOCC-A-214004	84%	26%	<i>R</i>
<i>Rhodotorula mucilaginosa</i> strain	UBOCC-A-214143	100%	45%	<i>S</i>
<i>Rhodotorula mucilaginosa</i> strain	UBOCC-A-214015	100%	0,15%	<i>S</i>
<i>Rhodotorula mucilaginosa</i> strain	UBOCC-A-214039	100%	42%	<i>S</i>
<i>Rhodotorula mucilaginosa</i> strain	UBOCC-A-214049	100%	62%	<i>S</i>
<i>Rhodotorula mucilaginosa</i> strain	UBOCC-A-214040	98%	50%	<i>S</i>
<i>Rhodotorula mucilaginosa</i> strain	UBOCC-A-214034	100%	56%	<i>S</i>
<i>Rhodotorula mucilaginosa</i> strain	UBOCC-A-214025	100%	64%	<i>S</i>
<i>Rhodotorula mucilaginosa</i> strain	UBOCC-A-214046	100%	48%	<i>S</i>
<i>Rhodotorula mucilaginosa</i> strain	UBOCC-A-214036	100%	38%	<i>S</i>
<i>Rhodotorula mucilaginosa</i> strain	UBOCC-A-214051	100%	48%	<i>S</i>
<i>Rhodotorula mucilaginosa</i> strain	UBOCC-A-214043	100%	50%	<i>S</i>
<i>Rhodotorula mucilaginosa</i> strain	UBOCC-A-214006	100%	50%	<i>S</i>
<i>Rhodotorula mucilaginosa</i> strain	UBOCC-A-214026	100%	49%	<i>S</i>

**Table 2.4.** Reduction of ketone **1 i** (10 mm) with marine yeasts grown in YPD-seawater medium after 24 h.

All the tested strains gave a high conversion of **1 i** into the desired alcohol with the predominant formation of (*S*)-**2 i**; *R. mucilaginosa* UBOCC-A-214025 gave the highest *ee* (64 %), whereas

reduction with *M. guilliermondii* was not enantioselective. The relatively low enantioselectivity observed in the reduction of **1 i** performed under standard conditions led us to investigate the effect of biotransformation conditions in order to improve enantioselectivity. The best results were observed using 40 mg<sub>dry weight</sub> mL<sup>-1</sup> of cells, 25 mM substrate in the presence of 7 % *i*PrOH at 27 °C; under these conditions the total conversion of the substrate was detected after 5 h with the formation of (*S*)-**2 i** in 72 % *ee*. At higher substrate concentrations (150 mM) the same enantioselectivity was observed and a recovered yield of 73 % was obtained, which shows the possibility to apply these biotransformations on a preparative scale.

## HALOTOLERANCE SCREENING

In this second part, a heterogeneous group of marine yeasts was studied from a physiological point of view in order to identify possible biocatalysts with enhanced performance.

### PRIMARY SCREENING

Having the possibility to work on a second heterogeneous group of marine yeasts<sup>29</sup>, the ability to growth at different NaCl concentrations was tested on 18 strains with different *genera/species*, plus three of previous strains with interesting biocatalytic application (table 2.5). The screened strains belong to UBO Culture Collection of marine microorganisms isolated from different basins and, consequently, they are physiologically interesting for the identification of potential candidates to implement a biocatalytic strategy in sea water. The first screening was developed in YNB (yeast nitrogen base medium) plates at various NaCl concentrations, buffered at pH 6, with glucose as the only carbon source. In this way, the growth of microorganisms was mainly influenced by the presence of NaCl and monitored day by day by observing colonies formation (table 2.5; figure 2.2).

Strain	24h					48h					120h				
	% NaCl					% NaCl8					% NaCl				
	0	3	6	9	12	0	3	6	9	12	0	3	6	9	12
(Mo 40) <i>Debaryomyces hansenii</i>	**	*	*	*		****	****	****	***		****	****	****	****	****
(Mo 29) <i>Cryptococcus sp</i>	**	*				****	****	***			****	****	****	***	
(Mo 35) <i>Rhodotorula mucilaginosa</i>	**	*				****	****	****	*		****	****	****	****	
(Mo 38) <i>Rhodospidium diobovatum</i>	**	*				****	****	***			****	****	****	***	*
(Mo 39) <i>Candida marinus</i>	**	*	*			****	****	***	***	*	****	****	****	****	****
(Ex 7) <i>Rhodotorula mucilaginosa</i>	**	*				****	****	***	*		****	****	****	****	
Ex 15 ( <i>Pichia guilliermondii</i> )	***	**	*			****	****	****	**		****	****	****	****	****
(Bio 1) <i>Candida viswanathii</i>	***	**				****	****	****	**		****	****	****	****	**

(Bio2) <i>Debaryomyces hansenii</i>	**	*	**	*		****	****	****	**	*	****	****	****	****	****
(LM 16) <i>Rhodotorula mucilaginosa</i>	**	*				****	****	***	*		****	****	****	****	
(LM18) <i>Rhodotorula mucilaginosa</i>	**	*				****	****	**	*		****	****	****	****	
(LM 2) <i>Meyerozyma guillemondi</i>	***	***	**	*		****	****	****	**		****	****	****	****	****
(Mo 36) <i>Leucosporidium scottii</i>	*					***	***	*			****	****	****	***	
(Mo 34) <i>Hortaea werneckii</i>						*	*	*			***	****	****	***	**
(Mo 31) <i>Candida atlantica</i>	*	*				****	****	****	**		****	****	****	****	****
(Mo 30) <i>Phaeothea triangularis</i>												*	**	**	
(Mo22) <i>Sporobolomyces roseus</i>						**	**				****	****	***		
(LM 9) <i>Meyerozyma guillemondi</i>	***	**	*			****	****	****	**		****	****	****	****	**

**Table 2.5.** Primary screening, colony growth (\*) at different NaCl concentrations at 24.48 and 120 hours. The \* is a qualitative indication of growth based on dilution spots.

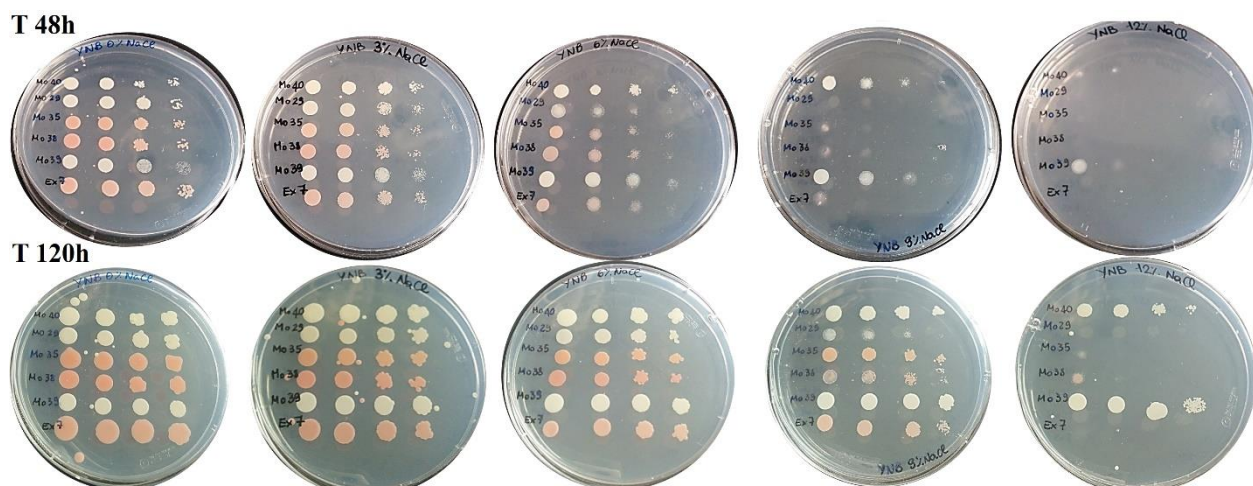


**Figure 2.2.** Plate growing was analysed at different concentrations of NaCl: 0%, 3%, 6%, 9%, 12% and at various times. The picture shows some examples.

As result of the first screening, 10 microorganisms (table 2.6) were selected for a deeper investigation under saline stress.

ID	Strain	O.D. (optical density)	Limiting [NaCl]
Bio 2	<i>Debaryomyces hansenii</i>	47	12% (A)
Mo 31	<i>Candida atlantica</i>	33	9% (B)
Mo 38	<i>Rhodospiridium diobovatum</i>	29	9% (B)
Mo 39	<i>Candida marinus</i>	48	12% (A)
Mo 40	<i>Debaryomyces hansenii</i>	36	12% (A)
Mo 34	<i>Hortaea werneckii</i>	19	9% (B)

LM 2	<i>Meyerozyma guillermondi</i>	30	12% (A)
LM 9	<i>Meyerozyma guillermondi</i>	31	9% (B)
LM 16	<i>Rhodotorula mucilaginosa</i>	28	9% (B)
LM 18	<i>Rhodotorula mucilaginosa</i>	26	9% (B)

**Table 2.6.** 48 h O.D. and limiting conditions: (A) for 12% NaCl and (B) for 9% NaCl.

## SECONDARY SCREENING

The subsequent screening was set up in liquid medium with 4% sea salts that mimic the marine mineral composition and with a limited concentration of NaCl. The selected strains were inoculated at initial concentration of 0.1 O.D. and the growth was followed for 96 hours. O.D. values were recorded every two hours at 600 nm.

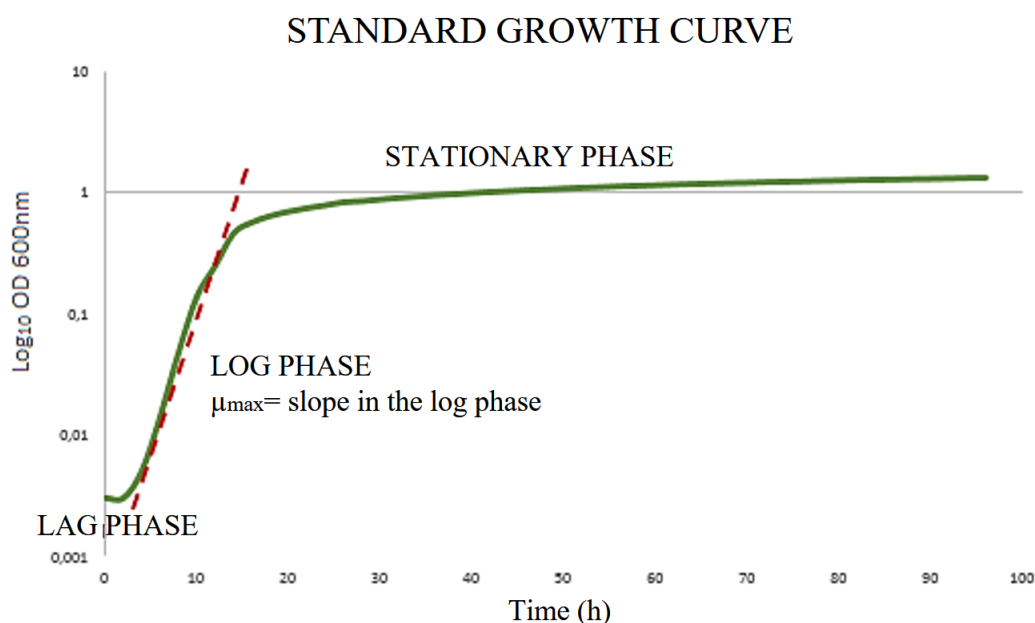
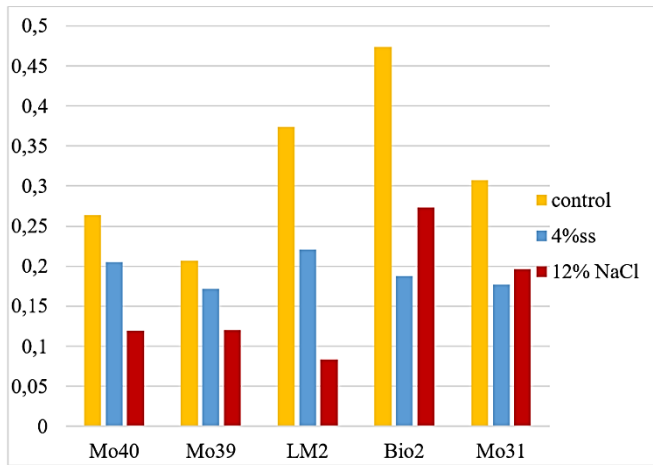


**Figure 2.3.** A standard yeast growth curve. The y axis represents the optical density at 600nm in logarithmic scale, while on the x axis there is time (h) of readings. The  $\mu_{\text{max}}$  corresponds to the slope of the line in the linear exponential phase.

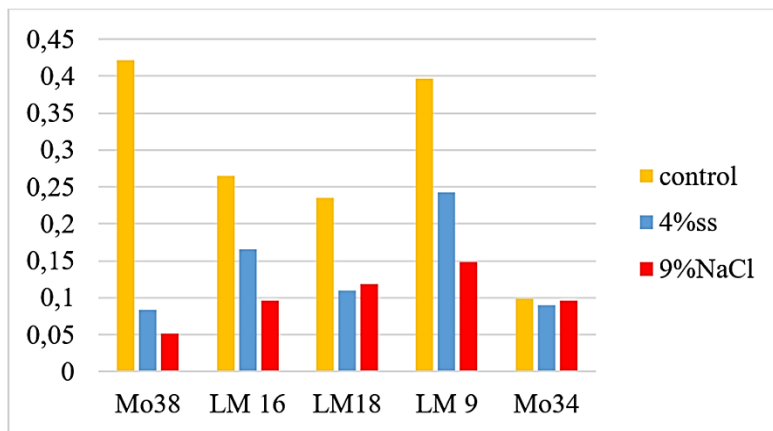
Secondary screening shows the presence of halotolerant strains. Based on the previous data, no strain has a  $\mu_{\text{max}}$  greater in the limit condition than the control.  $\mu_{\text{max}}$  is also higher in the medium with 4% sea salts than with 9% or 12% NaCl. This phenomenon is shown for all strains with the exception of *Debaryomyces hansenii* (UBOCC-A-208002) and *Candida atlantica* (UBOCC-A-208026). For these two microorganisms, the growth rate in 12% NaCl was higher than with 4% sea salts. The candidate strains for this work were chosen based on the results of the growth kinetics: *Debaryomyces hansenii*

(UBOCC-A-208002), *Candida atlantica* (UBOCC-A-208026), *Rhodospiridium diobovatum* (UBOCC-A-208033), *Hortaea werneckii* (UBOCC -A-208029) and *Phaeotheca triangularis* (UBOCC-A-208025).



Mo40	μ max	T d
control	0,2639	2,626552
4%ss	0,2049	3,382856
12% NaCl	0,1196	5,795545
Mo39	μ max	T d
control	0,207	3,348537
4%ss	0,1718	4,034617
12% NaCl	0,1203	5,761822
LM2	μ max	T d
control	0,3738	1,854326
4%ss	0,221	3,136413
12% NaCl	0,0835	8,301164
Bio2	μ max	T d
control	0,4735	1,46388
4%ss	0,1872	3,702709
12% NaCl	0,2732	2,537142
Mo31	μ max	T d
control	0,3071	2,257073
4%ss	0,1771	3,913875
12% NaCl	0,1965	3,527467

**Figure 2.4.** 12% NaCl as limiting condition: comparison of  $\mu_{\max}$  of control, 4% sea salts, 12% NaCl conditions.



Mo38	μmax	Td
control	0,422	1,642529
4%ss	0,0838	8,271446
9%NaCl	0,0512	13,53803
LM 16	μmax	Td
control	0,2653	2,61269
4%ss	0,1651	4,19835
9%NaCl	0,0962	7,20527
LM18	μmax	Td
control	0,235	2,949562
4%ss	0,1097	6,31857
9%NaCl	0,1183	5,859232
LM 9	μmax	Td
control	0,3969	1,746403
4%ss	0,2422	2,861879
9%NaCl	0,1479	4,686594
Mo34	μmax	Td
control	0,0985	7,037027
4%ss	0,0897	7,727393
9%NaCl	0,0958	7,235357

**Figure 2.5.** 9% NaCl as limiting condition: comparison of  $\mu_{\max}$  of control, 4% sea salt, 9% NaCl conditions.

### *Debaryomyces hansenii*

The strain *Debaryomyces hansenii* (UBOCC-A-208002), reported as Bio2 in figure 2.4, is one of the candidates selected in terms of  $\mu_{\max}$  and final biomass at high concentrations of NaCl. Liquid cultures were set up in YNB and YPD under different conditions: control (no NaCl), with the addition of 4% sea salts and with 12% NaCl. The growth in flasks under stirring at 28 °C was monitored for 48 hours.

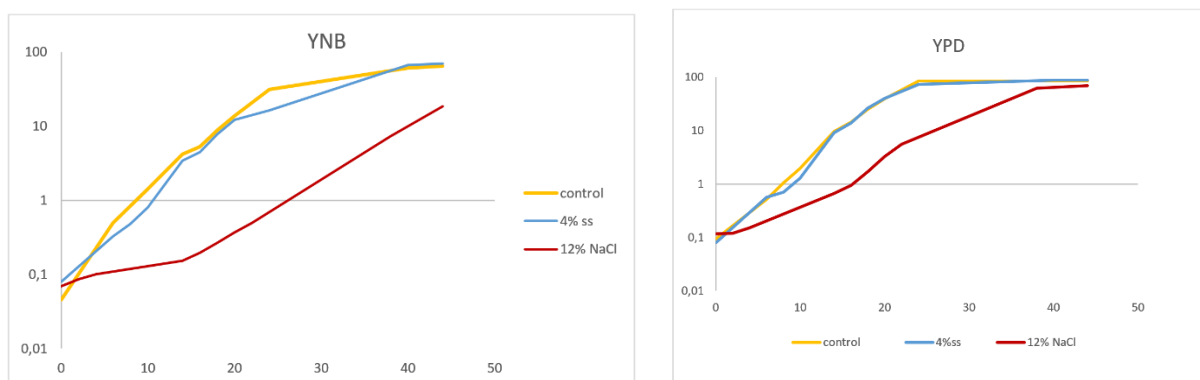


**Figure 2.6.** Growth curves in YNB and YPD in three different conditions: no NaCl (control); with the addition of 4% sea salts (4% ss) and with 12% NaCl. On the x axis there is the time (h) while on y axis the optical density at 600nm expressed in semi-logarithmic scale is reported.

Observing the curves in figure 2.6, there is a manifest difference between the two media in terms of growth rate ( $\mu_{\max}$ ), saline stress response and final biomass. The choice of employing two media, one minimal and the other one rich in nutrient elements was aimed at understanding the optimal condition for salt stress response. A greater difference was observed in limit condition, which in the case of *Debaryomyces hansenii* (UBOCC-A-208002) is represented by the culture medium (YNB / YPD) with the addition of 12% NaCl. The strain shows a faster adaptation response in rich medium resulting in a shorter latency phase in comparison with the same condition in YNB. On the contrary, for the control condition and with 4% of sea salt, for both YNB and YPD, the lag phase is absent. Moreover, the difference between  $\mu_{\max}$  of the control and  $\mu_{\max}$  of 4% sea salts is minimal and the growth curves are almost overlapped. This would suggest that both the control condition and 4% sea salts condition do not create any adjustments due to stress adaptation for the strain tested.

## MATERIALS AND METHODS

### MATERIALS

All reagents and solvents were obtained from Sigma–Aldrich-Fluka and used without further purification or drying. TLC was performed with Merck silica gel 60 F254 pre-coated plates. Silica gel column chromatography was performed on silica gel 60 (40–63  $\mu\text{m}$  particle size). Substrate **1h** was kindly gifted by Dr. Roberto Lenna (Industriale Chimica, Italy); substrate **1i** (2-acetylamino-6-oxo-4,5,6,7-tetrahydrobenzothiazole) was prepared following a procedure described previously<sup>27</sup>. For each compound, the alcohol racemic mixture was obtained by  $\text{NaBH}_4$  reduction (0.25 mmol of substrate). Natural seawater (pH 7.5) was collected from the Camogli beach (Genova, Italy) and maintained at 4 °C after microfiltration; a water salinity of 35 PSU was reported by ARPA (Agenzia Regionale Prevenzione e Ambiente) for this area.

## CHARACTERISATION

$^1\text{H}$  and  $^{13}\text{C}$  NMR spectra were recorded by using a Nuclear magnetic resonance (NMR) spectra at 300 K on a Bruker-Avance 500 MHz spectrometer operating at 500.13 and 125.76 MHz for  $^1\text{H}$  and  $^{13}\text{C}$  acquisitions, respectively. Chemical shifts ( $\delta$ ) of the  $^1\text{H}$  NMR and  $^{13}\text{C}$  NMR spectra are reported in ppm using the signal for residual solvent proton resonance as the internal standard ( $^1\text{H}$  NMR:  $\text{CDCl}_3$  7.26,  $\text{DMSO-d}_6$  2.49,  $\text{CD}_3\text{OD}$  3.31 ppm;  $^{13}\text{C}$  NMR:  $\text{CDCl}_3$  77.0 (central line),  $\text{DMSO-d}_6$  39.50 (central line),  $\text{CD}_3\text{OD}$  49.00 (central line) ppm). HPLC analyses were performed by using a Jasco Pu-980 equipped with a UV/Vis detector Jasco UV-975. Chiral HPLC columns used: Chiralcel OD (4.6x250 mm, 5 mm Daicel), Chiralcel OJ-H (4.6x250 mm, 5 mm, Daicel), Chiralcel OD-H (4.6x250 mm, 5 mm, Daicel), Chiralpak IA (4.6x250 mm, 5 mm, Daicel), Lux cellulose-2 column (4.6x250 mm, 5 mm, Phenomenex) and Lux cellulose 3 column (4.6x250 mm, 5 mm, Phenomenex). Optical rotatory power determinations were performed by a Perkin–Elmer (mod. 241) polarimeter in a 1 dm cell at 20 °C, setting the wavelength at 589 nm or at 546 nm. Elemental analyses were performed by using a Carlo Erba Model 1106 Elemental Analyzer for C, H and N, and the obtained results were within 0.4% of the theoretical values.

## MICROORGANISMS

All isolated microorganisms are available in the UBO Culture Collection (<http://www.univ-brest.fr/ubocc>).

ID	strain	Phylum	UBOCC number	Depth
LM 1	<i>Meyerozyma guillermondi</i>	Ascomycota	UBOCC-A-214022	37,1 mbsf
LM 2	<i>Meyerozyma guillermondi</i>	Ascomycota	UBOCC-A-214008	137,13 mbsf
LM 3	<i>Meyerozyma guillermondi</i>	Ascomycota	UBOCC-A-214007	24,6 mbsf
LM 4	<i>Rhodotorula mucilaginosa</i>	Basidiomycota	UBOCC-A-214045	137,13 mbsf
LM 5	<i>Meyerozyma guillermondi</i>	Ascomycota	UBOCC-A-214013	24,6 mbsf
LM 6	<i>Meyerozyma guillermondi</i>	Ascomycota	UBOCC-A-214014	24,6 mbsf
LM 7	not sequenced		UBOCC-A-214004	3,76 mbsf
LM 8	<i>Rhodotorula mucilaginosa</i>	Basidiomycota	UBOCC-A-214143	24,6 mbsf
LM 9	<i>Meyerozyma guillermondi</i>	Ascomycota	UBOCC-A-214015	21,1 mbsf
LM 10	<i>Rhodotorula mucilaginosa</i>	Basidiomycota	UBOCC-A-214039	24,6 mbsf
LM 13	<i>Rhodotorula mucilaginosa</i>	Basidiomycota	UBOCC-A-214049	21,1 mbsf
LM 14	<i>Rhodotorula mucilaginosa</i>	Basidiomycota	UBOCC-A-214040	34,1 mbsf
LM 15	<i>Rhodotorula mucilaginosa</i>	Basidiomycota	UBOCC-A-214034	37,1 mbsf
LM 16	<i>Rhodotorula mucilaginosa</i>	Basidiomycota	UBOCC-A-214025	3,76 mbsf
LM 17	<i>Rhodotorula mucilaginosa</i>	Basidiomycota	UBOCC-A-214046	345,5 mbsf
LM 18	<i>Rhodotorula mucilaginosa</i>	Basidiomycota	UBOCC-A-214036	765 mbsf

LM 19	<i>Rhodotorula mucilaginosa</i>	Basidiomycota	UBOCC-A-214051	37,1 mbsf
LM 20	<i>Rhodotorula mucilaginosa</i>	Basidiomycota	UBOCC-A-214043	34,1 mbsf
LM 21	<i>Rhodotorula mucilaginosa</i>	Basidiomycota	UBOCC-A-214006	3,76 mbsf
LM 22	<i>Rhodotorula mucilaginosa</i>	Basidiomycota	UBOCC-A-214026	34,1 mbsf
Bio1	<i>Candida viswanathii</i>	Ascomycota	UBOCC-A-208001	2620 mbsl
Bio2	<i>Debaryomyces hansenii</i>	Ascomycota	UBOCC-A-208002	2620 mbsl
Ex15	<i>Pichia guilliermondii</i>	Ascomycota	UBOCC-A-208004	700 mbsl
Ex7	<i>Rhodotorula mucilaginosa</i>	Basidiomycota	UBOCC-A-208010	2300 mbsl
Mo22	<i>Sporobolomyces roseus</i>	Basidiomycota	UBOCC-A-208018	2300 mbsl
Mo29	<i>Cryptococcus sp.</i>	Basidiomycota	UBOCC-A-208024	2300 mbsl
Mo30	<i>Phaeotheca triangularis</i>	Ascomycota	UBOCC-A-208025	2300 mbsl
Mo31	<i>Candida atlantica</i>	Ascomycota	UBOCC-A-208026	2300 mbsl
Mo34	<i>Hortaea werneckii</i>	Ascomycota	UBOCC-A-208029	2300 mbsl
Mo35	<i>Rhodotorula mucilaginosa</i>	Basidiomycota	UBOCC-A-208030	2300 mbsl
Mo36	<i>Leucosporidium scottii</i>	Basidiomycota	UBOCC-A-208031	2300 mbsl
Mo38	<i>Rhodospiridium diobovatum</i>	Basidiomycota	UBOCC-A-208033	2300 mbsl
Mo39	<i>Candida marinus</i>	Ascomycota	UBOCC-A-208034	2300 mbsl
Mo40	<i>Debaryomyces hansenii</i>	Ascomycota	UBOCC-A-208035	2300 mbsl

**Table 2.7.** Marine yeasts employed and and sampling depths: mbsf = meter below seafloor; mbsl = meter below sea level.

The first group presents 8 strains of *Meyerozyma guilliermondii* and 12 strains of *Rhodotorula mucilaginosa* isolated previously<sup>2</sup> from different deep-sub-seafloor sediment depths (mbsf= meter below the seafloor) at Canterbury Basin (New Zealand 44°56' 26.62"S, 172°1' 36.30"E).

The second group, on the other hand, derives from a second collection of marine microorganisms of different origins: South Pacific West (Lau Basin), Mid-Atlantic Ridge (Rainbow), Mid-Atlantic Ridge (Lost City). These strains were isolated from marine fauna present in "hydrothermal vents" (table 2.8).

Locations (depth)	Sample processed (type)	Strains
South Pacific West (Lau Basin, – 2620 m)	B2E07: seawater surrounding mussels	Bio1
	B9E07: gastropod ( <i>Ifrimeria nautilei</i> ) gills	Bio2
Mid-Atlantic Ridge (Rainbow, – 2300 m)	EX6E01 to EX6E04: <i>Rimicaris exoculata</i>	Ex7
	MoPR2: <i>Rimicaris exoculata</i>	Mo22
	MoPR5: colonization module TRAC (carbonates)	Mo29
	MoPR6: <i>Bathymodiolus azoricus</i>	Mo30–Mo36
	MoPR9: sponge	Mo38 and Mo39
	MoPR9: coral	Mo40
Mid-Atlantic Ridge (Lost City, – 700 m)	EX18E02: siliceous sponge	Ex15

**Table 2.8.** Collection of marine yeasts associated with fauna in the hydrothermal vents<sup>1</sup>.

## GROWING MEDIUM

### *YNB (YEAST NITROGEN BASE) MEDIUM*

It is a defined mineral medium containing specific concentrations of mineral salts, vitamins and other elements (traces). As nitrogen source, ammonium sulphate can be added.

COMPOSITION	CONCENTRATION
<b>YNB (BD-Difco)</b>	1.7 g/L
<b>MES buffer</b>	1 M
<b>Glucose</b>	20 g/L
<b>(NH<sub>4</sub>)<sub>2</sub>SO<sub>4</sub></b>	5 g/L

### *YPD MEDIUM*

It is a rich medium in nitrogen sources.

term of carbon and

COMPOSITION	CONCENTRATION
Yeast extract	10 g/L
Tryptone	20 g/L
Glucose	20 g/L

## HALOTOLERANCE SCREENING

### *SCREENING ON PLATE*

Plate screening was set up for 18 yeast strains and allowed a first analysis of strain growth and strain patterns at different NaCl concentrations. For this preliminary analysis YNB plates were prepared at all different concentrations of NaCl and growth was evaluated up to 120 hours.

From glycerol stocks, the yeasts were re-activated on YPD Solid Broth and grown to 28 °C for 48 hours. They were then pre-inoculated in buffered YNB in Erlenmeyer flasks, allowed to grow at 28 °C, 150 rpm for 48 hours. Growth was evaluated by reading optical density (O.D.) at 600 nm. Each strain was deposited on plate in four dilutions: 10<sup>5</sup>, 10<sup>4</sup>, 10<sup>3</sup>, 10<sup>2</sup> cell number (figure 2.2). The protocol was repeated for all the four conditions of increasing salinity: 0% NaCl, 3% NaCl, 6% NaCl, 9% NaCl, 12% NaCl.

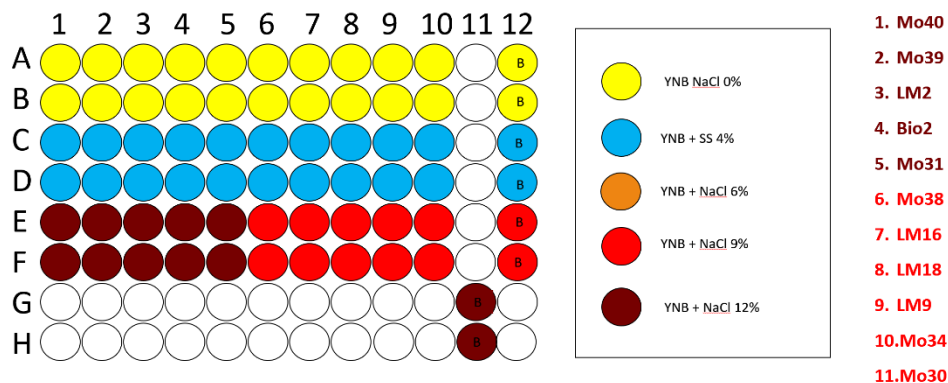
## SCREENING IN LIQUID AND GROWTH KINETICS

A liquid screening was then performed on the 10 strains with the most interesting results in terms of tolerance at high NaCl concentrations. Growth kinetics analysis was performed in microtiter (96-wells of multiwell plate) and for each strain three different conditions were analysed:

- YNB + 0% NaCl (control)
- YNB + 4% sea salts (sea water control)
- YNB + 9% (limit condition)
- YNB + 12% NaCl (limit condition)

For each strain, each condition was in duplicate.

The selected strains were pre-inoculated in buffered YNB Erlenmeyer flasks. Growth was monitored by reading the O.D. at 600 nm after 48 hours (table 2.6). After the inoculum at O.D. of 0.1 (about  $1 \times 10^6$  cells/mL) the growth was followed for about 96 hours.



**Scheme 2.9.** Design of the first liquid screening in 96 multiwell plate (B stands for blank).

Gene 5 microplate reader (Biotek) was set to record the optical density of the culture every two hours; although static, the cell suspension was mixed by rapid agitation before each reading. Once all the values for each strain and each conditions, the growth curves were designed and for each one the rate and duplication time were calculated.

## FLASK CELL GROWTH

The growth of the most promising strains in term of halotolerance was followed also in flask employing a Pharmacia®Biotek Ultrospec 1000 spectrophotometer. Based on the results obtained from these screenings, the best candidates in terms of halotolerance were selected for a deeper physiological characterization and investigated from biocatalytic point of view.

## BIOTRANSFORMATIONS

The screening of growth was performed in Erlenmeyer flasks (100 mL) that contained 10 mL of YPD liquid prepared with freshwater or natural seawater<sup>30</sup> and incubated in an orbital shaker at 180 rpm at 28 °C for 48 h. Samples were withdrawn at appropriate intervals and used to monitor the cell growth by measuring the O.D. at 600 nm by using a spectrophotometer after appropriate dilution. For dry weight determination, washed culture samples were filtered through a 0.45 µm glass microfiber GF/A filter (Whatman) and dried for 24 h at 110 °C. The results were an average of five replicates. Reductions of all substrates were performed with freshly prepared cells, grown in freshwater-YPD or in YPD-seawater. Cells grown in freshwater-YPD medium (50 mg dry weight/mL) were suspended in phosphate buffer (pH 7.5, 0.1M), whereas cells grown in seawater-YPD medium (50 mg dry weight/mL) were suspended in natural microfiltered seawater. The biotransformations of **1a–g** were performed in the presence of 5% glucose by adding the substrates as concentrated solution in DMSO (final concentration of co-solvent 1%). The biotransformations of ethyl secodione derivative **1h** was performed using freshly cells suspended in seawater in the presence of 3.5% EtOH both to increase the solubility and to favour cofactor regeneration. The biotransformations of **1i** were performed using fresh cells suspended in seawater in the presence of different co-solvents.

The biotransformations were performed on a 25 mL scale and kept under reciprocal shaking (150 rpm) at the desired temperature. Once the reaction was over, EtOAc (12 mL) was added, and the resulting mixture was shaken and centrifuged; the aqueous phase was extracted twice more with 12 mL of EtOAc. The organic phases were collected and dried over Na<sub>2</sub>SO<sub>4</sub> and the solvent was evaporated. The crude residues were purified by flash chromatography.

### *ARYL METHYLKETONI*

Cells were grown in freshwater-YPD or in seawater-YPD medium. Biotransformations were performed for 24 h with freshly prepared cells (50 mg dry weight mL<sup>-1</sup>). Cells grown in freshwater-YPD medium were suspended in phosphate buffer (pH 7.5, 0.1 M), whereas cells grown in seawater-YPD medium were suspended in seawater. Biotransformations were performed in the presence of 5 % glucose.

### *β – KETONITRILES*

Biotransformations were performed for 24 h with freshly prepared cells (50 mg dry weight mL<sup>-1</sup>) suspended in seawater in the presence of 5 % glucose. Yields and enantioselectivity after 24 h.

## ETHYL SECODIONE DERIVATIVE

Biotransformations were performed for 24 h with freshly prepared cells (50 mg dry weight mL<sup>-1</sup>) suspended in seawater in the presence of 3.5 % EtOH. Yields and diastereoselectivity after 24 h.

## PRAMIPEXOLE KETO INTERMEDIATE

Biotransformations were performed for 24 h with freshly prepared cells (50 mg dry weight mL<sup>-1</sup>) suspended in seawater (pH 5.6) in the presence of 5 % glucose. Yields and enantioselectivity were determined after 24 h. In this case, seawater was used at pH 5.6 because of the low stability of the substrate at a higher pH.

## PURIFICATION AND CHEMICAL CHARACTERISATION

### (S)-1-Phenylethanol (2 a)

The reaction progress and *ee* were determined by using HPLC using a Chiralcel OD column (*n*-hexane/*i*PrOH 95:5, 0.7 mL min<sup>-1</sup>, 254 nm): *t*<sub>r</sub> (R)-2 a 14.2 min, *t*<sub>r</sub> (S)-2 a 18.0 min.<sup>31</sup> Oil. *R*<sub>f</sub>=0.4 (hexane/EtOAc=8:2); [α]<sub>D</sub><sup>25</sup> = -40.0 (*c*=0.5 chloroform) lit<sup>32</sup>. [α]<sub>D</sub><sup>25</sup> = -39.2 (*c*=2.54 chloroform); <sup>1</sup>H NMR (300 MHz, CDCl<sub>3</sub>): δ=7.20–7.35 (m, 5 H), 4.85 (q, *J*=6.4 Hz, 1 H), 1.46 ppm (d, *J*=6.4 Hz, 3 H); <sup>13</sup>C NMR (75 MHz, CDCl<sub>3</sub>): δ=145.9, 128.5, 127.5, 125.4, 70.4, 25.2 ppm; elemental analysis calcd (%) for C<sub>8</sub>H<sub>10</sub>O (122.07): C 78.65, H 8.25; found: C 78.38, H 8.01.

### (S)-1-Pyridin-3-yl-ethanol (2 b)

The reaction progress and *ee* were determined by using HPLC using a Phenomenex Lux cellulose 2 column (*n*-hexane/*i*PrOH 90:10, 0.7 mL min<sup>-1</sup>, 254 nm): *t*<sub>r</sub> (R)-2 b 20.46 min, *t*<sub>r</sub> (S)-2 b 25.30 min.<sup>33</sup> Oil. *R*<sub>f</sub>=0.3 (EtOAc); [α]<sub>D</sub><sup>25</sup> = -38.04 (*c*=0.4 ethanol) lit<sup>34</sup>. -39.0 (*c*=0.93 ethanol); <sup>1</sup>H NMR (300 MHz, CDCl<sub>3</sub>): δ=8.46–8.33 (m, 2 H), 7.75–7.70 (m, 1 H), 7.24 (dd, *J*=8.0, 5.0 Hz, 1 H), 4.90 (q, *J*=6.5 Hz, 1 H), 4.5 (br s, 1 H, OH), 1.49 ppm (d, *J*=6.5 Hz, 3 H); <sup>13</sup>C NMR (75 MHz, CDCl<sub>3</sub>): δ=148.0, 147.0, 141.8, 133.5, 123.5, 67.5 25.1 ppm; elemental analysis calcd (%) for C<sub>7</sub>H<sub>9</sub>ON (123.07): C 68.27, H 7.37, N 11.37; found: C 68.55, H 7.67, N 11.10.

### (S)-(1-Thiophen-2-yl)ethanol (2 c)

The reaction progress and *ee* were determined by using HPLC using a Phenomenex Lux cellulose-3 column (*n*-hexane/*i*PrOH 90:10, 0.5 mL min<sup>-1</sup>, 254 nm): *t*<sub>r</sub> (S)-2 c 13.5 min, *t*<sub>r</sub> (R)-2 c 15.90 min.<sup>35</sup> Oil. *R*<sub>f</sub>=0.3 (hexane/EtOAc=8:2); [α]<sub>D</sub><sup>25</sup> = -20.80 (*c*=0.2 chloroform) lit<sup>35</sup>. [α]<sub>D</sub><sup>20</sup> = -23.2 (*c*=0.79 chloroform); <sup>1</sup>H NMR (300 MHz, CDCl<sub>3</sub>): δ=7.25–7.18 (m, 1 H), 6.95–6.92 (m, 2 H), 5.07 (q, *J*=6.5 Hz, 1 H), 2.54 (br s, 1 H, OH), 1.56 ppm (d, *J*=6.5 Hz, 3 H); <sup>13</sup>C NMR (75 MHz, CDCl<sub>3</sub>): δ=150.0, 126.6, 124.4, 123.2, 66.2, 25.2 ppm; elemental analysis calcd (%) for C<sub>6</sub>H<sub>8</sub>OS (128.03): C 56.22, H 6.29; found: C 56.04, H 6.58.

### *(S)*-(1-Furan-2-yl)ethanol (**2 d**)

The reaction progress and *ee* were determined by using HPLC using a Phenomenex Lux cellulose-3 column (*n*-hexane/*i*PrOH 98:2, 0.5 mL min<sup>-1</sup>, 220 nm): *t<sub>r</sub>* (*S*)-**2 d** 19.3 min, *t<sub>r</sub>* (*R*)-**2 d** 21.3 min.<sup>35</sup> Oil. *R<sub>f</sub>*=0.3 (hexane/EtOAc=8:2); [ $\alpha$ ]<sub>D</sub><sup>25</sup> = -20.5 (*c*=0.2 chloroform) lit.<sup>34</sup>. [ $\alpha$ ]<sub>D</sub><sup>20</sup> = -13.6 (*c*=0.55 chloroform); <sup>1</sup>H NMR (400 MHz, CDCl<sub>3</sub>):  $\delta$ =7.36 (dd, *J*=2.0, 1.0 Hz, 1 H), 6.32 (dd, *J*=3.0, 2.0 Hz, 1 H), 6.22 (d, *J*=3.0 Hz, 1 H), 4.86 (q, *J*=6.5 Hz, 1 H), 2.35 (br s, 1 H, OH), 1.52 ppm (d, *J*=6.5 Hz, 3 H); <sup>13</sup>C NMR (100 MHz, CDCl<sub>3</sub>):  $\delta$ =157.7, 141.8, 110.1, 105.1, 63.6, 21.2 ppm<sup>26</sup>; elemental analysis calcd (%) for C<sub>6</sub>H<sub>8</sub>O<sub>2</sub> (112.05): C 64.27, H 7.19; found: C 63.97, H 7.34.

### *(S)*-3-Hydroxy-3-phenylpropanenitrile (**2 e**)

The reaction progress and *ee* were determined by using HPLC using a Chiralcel OJ-H column (*n*-hexane/*i*PrOH 90:10, 1.0 mL min<sup>-1</sup>, 220 nm), *t<sub>r</sub>* (*S*)-**2 e** 24.5, *t<sub>r</sub>* (*R*)-**2 e** 31.1 min.<sup>23</sup> Oil. *R<sub>f</sub>*=0.4 (hexane/EtOAc=7:3); [ $\alpha$ ]<sub>D</sub><sup>20</sup> = -58.5 (*c*=1.0, EtOH) lit.<sup>24</sup> [ $\alpha$ ]<sub>D</sub><sup>20</sup> = -57.7 (*c*=2.6, EtOH)]; <sup>1</sup>H NMR (300 MHz, CDCl<sub>3</sub>):  $\delta$ =2.74 (d, *J*=6.1 Hz, 2 H), 5.01 (t, *J*=6.1 Hz, 1 H), 7.36–7.39 ppm (m, 5 H); <sup>13</sup>C NMR (75 MHz, CDCl<sub>3</sub>):  $\delta$ =27.9, 70.0, 117.4, 125.5, 128.8, 128.9, 141.1 ppm; elemental analysis calcd (%) for C<sub>9</sub>H<sub>9</sub>ON (147.07): C 73.45, H 6.16, N 9.52; found: C 73.01, H 6.31, 9.32.

### *(S)*-3-(2-Thienyl)-3-hydroxypropanenitrile (**2 f**)

The reaction progress and *ee* were determined by using HPLC using a Chiralcel OJ-H column (*n*-hexane/*i*PrOH=90:10, 1.0 mL min<sup>-1</sup>, 220 nm), *t<sub>r</sub>* (*S*)-**2 f** 27.0, *t<sub>r</sub>* (*R*)-**2 f** 32.3 min.<sup>23</sup> Oil. *R<sub>f</sub>*=0.3 (hexane/EtOAc=7:3); [ $\alpha$ ]<sub>D</sub><sup>28</sup> = -19.4 (*c*=1.0, CHCl<sub>3</sub>) lit.<sup>34</sup> [ $\alpha$ ]<sub>D</sub><sup>28</sup> = -16.71 (*c*=1.01, CHCl<sub>3</sub>); <sup>1</sup>H NMR (300 MHz, CDCl<sub>3</sub>):  $\delta$ =2.85 (d, *J*=6.2 Hz, 2H), 3.04 (s, br, OH), 5.26 (t, *J*=6.2 Hz, 1 H), 6.98–7.00 (m, 2 H), 7.06–7.07 (d, *J*=3.5 Hz, 1 H), 7.29–7.32 ppm (m, 1 H); <sup>13</sup>C NMR (75 MHz, CDCl<sub>3</sub>):  $\delta$ =28.2, 66.2, 117.1, 124.7, 125.7, 127.1, 144.5 ppm; elemental analysis calcd (%) for C<sub>7</sub>H<sub>7</sub>ONS (153.02): C 54.88, H 4.61, N 9.14; found: C 54.81, H 4.81, 8.92.

### *(S)*-3-(2-Furyl)-3-hydroxypropanenitrile (**2 g**)

The *ee* was determined by using HPLC using a Chiralcel OJ-H column (*n*-hexane/*i*PrOH=90:10, 1.0 mL min<sup>-1</sup>, 220 nm), *t<sub>r</sub>* (*S*)-**2 g** 21.9, *t<sub>r</sub>* (*R*)-**2 g** 25.6 min.<sup>23</sup> Oil. *R<sub>f</sub>*=0.3 (hexane/EtOAc=7:3); [ $\alpha$ ]<sub>D</sub><sup>28</sup> = -40.2 (*c*=1.0, EtOH) lit.<sup>24</sup> [ $\alpha$ ]<sub>D</sub><sup>20</sup> = -38.6 (*c*=1.3, CHCl<sub>3</sub>); <sup>1</sup>H NMR (300 MHz, CDCl<sub>3</sub>):  $\delta$ =2.57 (s, br, OH), 2.88 (d, *J*=6.2 Hz, 2 H), 5.05 (t, *J*=6.2 Hz, 1 H), 6.37–6.41 (m, 2 H), 7.41–7.42 ppm (m, 1 H); <sup>13</sup>C NMR (75 MHz, CDCl<sub>3</sub>):  $\delta$ =24.9, 63.8, 107.5, 110.6, 116.9, 142.9, 152.8 ppm; elemental analysis calcd (%) for C<sub>7</sub>H<sub>7</sub>O<sub>2</sub>N (137.05): C 61.31, H 5.14, N 10.21; found: C 61.06, H 5.36, 9.94.

### *1*-Benzoylbutanenitrile (**3 e**)

Oil. *R<sub>f</sub>*=0.4 (hexane/EtOAc=7:3). <sup>1</sup>H NMR (300 MHz, CDCl<sub>3</sub>):  $\delta$ =1.16 (t, *J*=7.7 Hz, 3 H), 2.02–2.15 (m, 2 H), 4.30 (dd, *J*=6.2, 4.3 Hz, 1), 7.49–7.56 (m, 2 H), 7.65 (d, *J*=7.6 Hz, 1 H), 7.95 ppm (d, *J*=6.7 Hz, 2 H); <sup>13</sup>C NMR (75 MHz, CDCl<sub>3</sub>):  $\delta$ =11.89, 23.77, 41.38, 128.68, 128.92, 129.31, 130.38, 133.93, 134.63, 170.91, 190.88 ppm; elemental analysis calcd (%) for C<sub>11</sub>H<sub>11</sub>ON (173.08): C 76.28, H 6.40, N 8.09; found: C 75.92, H 6.50, 7.97.

*(13S,17S)-E-13-Ethyl-3-methoxy-8,14-secogona-1,3,5(10),9(11)-tetraene-17-ol-14-one (2 h)*

The reaction progress, *ee* and diastereomeric excess (*de*) were determined by HPLC using a Lux Cellulose-2 column (*n*-hexane/*i*PrOH 85:15; 0.5 mL min<sup>-1</sup> 254 nm); *t<sub>r</sub>* (13*S*, 17*S*)-**2 h** 18.87 min, (13*S*, 17*R*)-**2 h** 20.62 min, (13*R*, 17*S*)-**2 h** 23.34 min, (13*R*, 17*S*)-**2 h**, 24.61 min.<sup>27</sup> White solid. *R<sub>f</sub>*=0.3 (hexane/EtOAc=1:1). *ee*=84 %. <sup>1</sup>H NMR (300 MHz, C<sub>3</sub>D<sub>6</sub>O): δ=0.82 (t, *J*=7.5 Hz, 3 H), 1.53 (non, *J*=7.5 Hz, 2 H), 1.78 (qui, *J*=6.2 Hz, 2 H), 1.95–2.07 (m, 1 H), 2.23–2.31 (m, 3 H); 2.43–2.46 (m, 2 H; CH<sub>2</sub>), 2.51 (t, *J*=6.2 Hz, 2 H), 2.74 (t, *J*=6.2 Hz, 2 H), 3.77 (s, 3 H), 4.13 (d, *J*=4.2 Hz, 1 H; OH), 4.32 (q, *J*=5.3 Hz, 1 H), 6.0 (t, *J*=7.5 Hz, 1 H), 6.64 (d, *J*=2.8 Hz, 1 H), 6.72 (dd, *J*=2.8, 8.7 Hz, 1 H), 7.50 ppm (d, *J*=8.7 Hz, 1 H); <sup>13</sup>C NMR (300 MHz, C<sub>3</sub>D<sub>6</sub>O): δ=8.2, 23.6, 25.3, 26.6, 26.8, 28.4, 30.9, 34.8, 54.9, 57.2, 75.1, 112.8, 113.2, 118.1, 125.3, 129.6, 135.4, 138.7, 159.0, 219.1 ppm; elemental analysis calcd (%) for C<sub>20</sub>H<sub>26</sub>O<sub>3</sub> (314.19): C 76.40, H 8.33; found: C 76.11, H 8.39.

*(S)-2-Acetylamino-6-hydroxy-4,5,6,7-tetrahydrobenzothiazole (2 i)*

The reaction progress and *ee* were determined by using HPLC using a Chiralpak IA column (*n*-hexane/*i*PrOH 8:2 as eluent, flow rate: 0.7 mL min<sup>-1</sup>, 254 nm), *t<sub>r</sub>* (*R*)-**2 i** 10.9 min, *t<sub>r</sub>* (*S*)-**2 i** 14.8 min<sup>27</sup>. Yellowish solid. *R<sub>f</sub>*=0.25 (CH<sub>2</sub>Cl<sub>2</sub>/MeOH, 95:5). *ee*=64 %. <sup>1</sup>H NMR (300 MHz, CD<sub>3</sub>OD): δ=1.91 (dddd, *J*=14.2, 8.6, 7.7, 5.9 Hz, 1 H), 2.04 (dddd, *J*=14.2, 6.2, 5.9, 2.9 Hz, 1 H), 2.26 (s, CH<sub>3</sub>, 3 H), 2.61–2.71 (m, 2 h), 2.79 (dddd, *J*=16.5, 5.9, 5.9, 1.8 Hz, 1 H), 2.99 (ddd, *J*=15.7, 4.7, 1.8 Hz, 1 H), 4.15 ppm (dddd, *J*=8.6, 6.9, 4.7, 2.9 Hz, 1 H); <sup>13</sup>C NMR (300 MHz, CD<sub>3</sub>OD): δ=21.2, 23.2, 30.5, 30.7, 66.2, 120.9, 143.2, 156.4, 169.1 ppm; elemental analysis calcd (%) for C<sub>9</sub>H<sub>12</sub>O<sub>2</sub>N<sub>2</sub>S (212.06): C 50.92, H 5.70, N 13.20; found: C 50.96, H 5.89 N 12.85.

## REFERENCES

1. Burgaud, G., Arzur, D., Durand, L., Cambon-Bonavita, M. A. & Barbier, G. Marine culturable yeasts in deep-sea hydrothermal vents: Species richness and association with fauna. *FEMS Microbiol. Ecol.* **73**, 121–133 (2010).
2. Rédou, V., Navarri, M., Meslet-Cladière, L., Barbier, G. & Burgaud, G. Species richness and adaptation of marine fungi from deep-subseafloor sediments. *Appl. Environ. Microbiol.* **81**, 3571–3583 (2015).
3. Trincone, A. *Marine enzymes for biocatalysis*.
4. Munn, C. B. *Marine Microbiology – Ecology and Applications*. (Bios-Garland Scientific, 2003).
5. Tivey, M. K. Generation of Seafloor Hydrothermal Vent Fluids and Associated Mineral Deposits. *Oceanography* **20**, 50–65 (2007).
6. Jørgensen, B. B. & Boetius, A. Feast and famine — microbial life in the deep-sea bed. *Nat. Rev. Microbiol.* **5**, 770–781 (2007).
7. Nordling, E., Jörnvall, H. & Persson, B. Medium-chain dehydrogenases/reductases (MDR): Family characterizations including genome comparisons and active site modelling. *Eur. J. Biochem.* **269**, 4267–4276 (2002).
8. Stuermer, R., Hauer, B., Hall, M. & Faber, K. Asymmetric bioreduction of activated C=C bonds using enoate reductases from the old yellow enzyme family. *Curr. Opin. Chem. Biol.* **11**, 203–213 (2007).
9. Hoffmann, F. & Maser, E. Carbonyl reductases and pluripotent hydroxysteroid dehydrogenases of the short-chain dehydrogenase/reductase superfamily. *Drug Metab. Rev.* **39**, 87–144 (2007).
10. Kallberg, Y., Oppermann, U. & Persson, B. Classification of the short-chain dehydrogenase/reductase superfamily using hidden Markov models. *FEBS J.* **277**, 2375–2386 (2010).

11. Forrest, G. L. & Gonzalez, B. Carbonyl reductase. *Chem. Biol. Interact.* **129**, 21–40 (2000).
12. Zhu, D. & Hua, L. How carbonyl reductases control stereoselectivity: Approaching the goal of rational design. *Pure Appl. Chem.* **82**, 117–128 (2010).
13. Liu, Z.-J. *et al.* The first structure of an aldehyde dehydrogenase reveals novel interactions between NAD and the Rossmann fold. *Nat. Struct. Biol.* **4**, 317–326 (1997).
14. V. Prelog. Specification of the stereospecificity of some oxido-reductases by diamond lattice sections. *Pure Appl. Chem.* **9**, 119–130 (1964).
15. Musa, M. M. & Phillips, R. S. Recent advances in alcohol dehydrogenase-catalyzed asymmetric production of hydrophobic alcohols. *Catal. Sci. Technol.* **1**, 1311 (2011).
16. Kurbanoglu, E. B., Zilbeyaz, K., Ozdal, M., Taskin, M. & Kurbanoglu, N. I. Asymmetric reduction of substituted acetophenones using once immobilized *Rhodotorula glutinis* cells. *Bioresour. Technol.* **101**, 3825–3829 (2010).
17. Papon, N. *et al.* *Candida guilliermondii*: Biotechnological applications, perspectives for biological control, emerging clinical importance and recent advances in genetics. *Curr. Genet.* **59**, 73–90 (2013).
18. Zhang, B., Zheng, L., Lin, J. & Wei, D. Characterization of an ene-reductase from *Meyerozyma guilliermondii* for asymmetric bioreduction of a,b-unsaturated compounds. *Biotechnol. Lett.* **38**, 1527–1534 (2016).
19. Zhu, D. *et al.* Asymmetric reduction of  $\beta$ -ketonitriles with a recombinant carbonyl reductase and enzymatic transformation to optically pure  $\beta$ -hydroxy carboxylic acids. *Org. Lett.* **9**, 2560–2563 (2007).
20. Ankati, H., Zhu, D., Yang, Y., Biehl, E. R. & Hua, L. Asymmetric synthesis of both antipodes of beta-hydroxy nitriles and beta-hydroxy carboxylic acids via enzymatic reduction or sequential reduction/hydrolysis. *J. Org. Chem.* **74**, 1658–1662 (2009).
21. Nowill, R. W. *et al.* Biocatalytic strategy toward asymmetric  $\beta$ -hydroxy nitriles and  $\beta$ -amino alcohols. *Tetrahedron Lett.* **52**, 2440–2442 (2011).
22. Xu, G. C., Yu, H. L., Zhang, Z. J. & Xu, J. H. Stereocomplementary bioreduction of  $\beta$ -ketonitrile without ethylated byproduct. *Org. Lett.* **15**, 5408–5411 (2013).
23. Contente, M. L. *et al.* Preparation of enantiomerically enriched aromatic  $\beta$ -hydroxynitriles and halohydrins by ketone reduction with recombinant ketoreductase KRED1-Pglu. *Tetrahedron* **72**, 3974–3979 (2016).
24. Dehli, J. R. & Gotor, V. Enantio- and chemoselective bioreduction of  $\beta$ -keto nitriles by the fungus *Curvularia lunata*. *Tetrahedron Asymmetry* **11**, 3693–3700 (2000).
25. Aguirre-Pranzoni, C., Bisogno, F. R., Orden, A. A. & Kurina-Sanz, M. Lyophilized *Rhodotorula* yeast as all-in-one redox biocatalyst: Access to enantiopure building blocks by simple chemoenzymatic one-pot procedures Dedicated to Professor Carlos E. Tonn for his great contribution to the development of the chemistry of natura. *J. Mol. Catal. B Enzym.* **114**, 19–24 (2015).
26. Gotor, V., Dehli, J. R. & Rebolledo, F. Biotransformations of benzoylacetone nitrile with the fungus. *R. Soc. Chem.* **8**, 307–309 (2000).
27. Ferraboschi, P. *et al.* Baker's yeast catalyzed preparation of a new enantiomerically pure synthon of (S)-pramipexole and its enantiomer (dexpramipexole). *Tetrahedron Asymmetry* **25**, 1239–1245 (2014).
28. Romano, D., Gandolfi, R., Guglielmetti, S. & Molinari, F. Enzymatic hydrolysis of capsaicins for the production of vanillylamine using ECB deacylase from *Actinoplanes utahensis*. *Food Chem.* **124**, 1096–1098 (2011).
29. Burgaud, G., Arzur, D., Durand, L., Cambon-Bonavita, M. A. & Barbier, G. Marine culturable yeasts in deep-sea hydrothermal vents: Species richness and association with fauna. *FEMS Microbiol. Ecol.* **73**, 121–133 (2010).
30. Chi, Z., Ma, C., Wang, P. & Li, H. F. Optimization of medium and cultivation conditions for alkaline protease production by the marine yeast *Aureobasidium pullulans*. *Bioresour. Technol.* **98**, 534–538

(2007).

31. Contente, M. L. *et al.* Biotransformation of aromatic ketones and ketoesters with the non-conventional yeast *Pichia glucozyma*. *Tetrahedron Lett.* **55**, 7051–7053 (2014).
32. Kantam, M. L. *et al.* Asymmetric Hydrosilylation of Ketones Catalyzed by magnetically recoverable and reusable copper ferrite nanoparticles. *J. Org. Chem* 4608–4611 (2009).
33. Contente, M. L. *et al.* Stereoselective reduction of aromatic ketones by a new ketoreductase from *Pichia glucozyma*. *Appl. Microbiol. Biotechnol.* **100**, 193–201 (2016).
34. Vázquez-Villa, H., Reber, S., Ariger, M. A. & Carreira, E. M. Iridium diamine catalyst for the asymmetric transfer hydrogenation of ketones. *Angew. Chemie - Int. Ed.* **50**, 8979–8981 (2011).
35. Li, Y. *et al.* Iron catalyzed asymmetric hydrogenation of ketones. *J. Am. Chem. Soc.* **136**, 4031–4039 (2014).

## WHOLE CELL SCREENING – MARINE BACTERIA

In this section the focus will be on biocatalytic potential of varied range of bacterial strains collected from one of the most peculiar marine habitats. Keto-reductase and transaminase enzymatic activities were investigated with whole cells in order to identify a possible gene target to express as recombinant enzyme with enhanced performances.

## BACKGROUND

### MARINE BACTERIA

In the context of this doctoral thesis, the enzymatic activities of 33 marine strains from four different deep hypersaline anoxic basins (DHABs) located in the eastern area of the Mediterranean Sea have been studied. This project was involved in the European research project BIODEEP<sup>1</sup> (Biotechnologies from the Deep), which aimed to explore unique marine habitats in order to isolate and cultivate marine microorganisms, offering new opportunities for the study of new significant enzymatic activities. The bacteria collected from DHABs have adapted to high salinity, anoxia and high pressures that may have affected the expression of unique cellular features of interest in many industrial applications.

The DHABs are located in an area of the Mediterranean called Mediterranean Ridge (figure 3.1); it is the result of the convergence between the African, European and Aegean platforms. The hypersaline basins are probably the result of the melting of underground deposits (3200-3600m of depth) of salt (Messinians evaporites) that were exposed to seawater because of tectonic activities during Miocene period (from 26 million to 2.5 million years ago). The brine in DHABs is characterized by anoxia conditions, high pressure ( $\approx 35$  MPa), saturated salts concentrations<sup>2-5</sup>, high concentrations of  $MgCl_2$  ( $\approx 5$  M) and no light that make them some of the most extreme habitats on earth<sup>5,6</sup>.

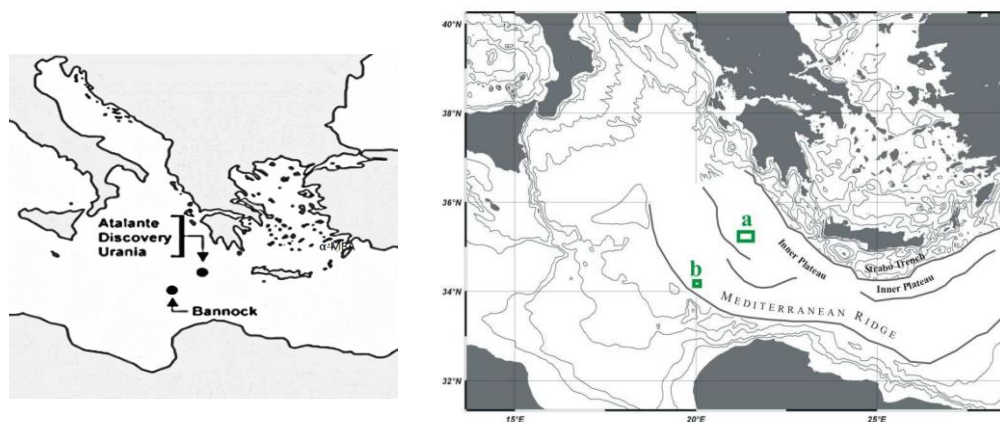


**Figure 3.1.** Localisation of deep hypersaline anoxic basins in Mediterranean Sea. The L'Atalante, Urania and Discovery are located in **a** and Bannock in **b**.

The brine high density limits the mixing with the overlying oxygen-rich waters, creating a chemocline of 1-3 m of the thickness. It is clear from previous studies that every DHABs have distinct

geochemical characteristics from the other ones<sup>2,4,7</sup>. The L'Atalante, Bannock and Urania brine has a similar ionic composition, but the salinity of Urania is lower in contrast to the concentration of methane and sulphate which is, however, considerably higher than the other two. The main difference with the Discovery basin lies in its high concentration of Mg<sup>2+</sup> ions (about 5M) and a lower concentration of Na<sup>+</sup> ions.

	Atalante	Bannock	Urania	Discovery	Sea Water
<b>Density</b> (g cm <sup>-3</sup> )	1.23	1.21	1.13	1.35	1.03
<b>Na<sup>+</sup></b> (M)	4.7	3.2	3.5	0.07	0.53
<b>Cl</b> (M)	5.3	5.4	3.7	9.5	0.62
<b>Mg<sup>2+</sup></b> (M)	0.41	0.65	0.32	5	0.06
<b>SO<sub>4</sub><sup>2-</sup></b> (mM)	397	137	107	96	31.8
<b>HS<sup>-</sup></b> (mM)	2.9	3	16	0.7	2.6*10 <sup>-6</sup>
<b>CH<sub>4</sub></b> (mM)	0.52	0.45	5.56	0.03	1.5*10 <sup>-6</sup>

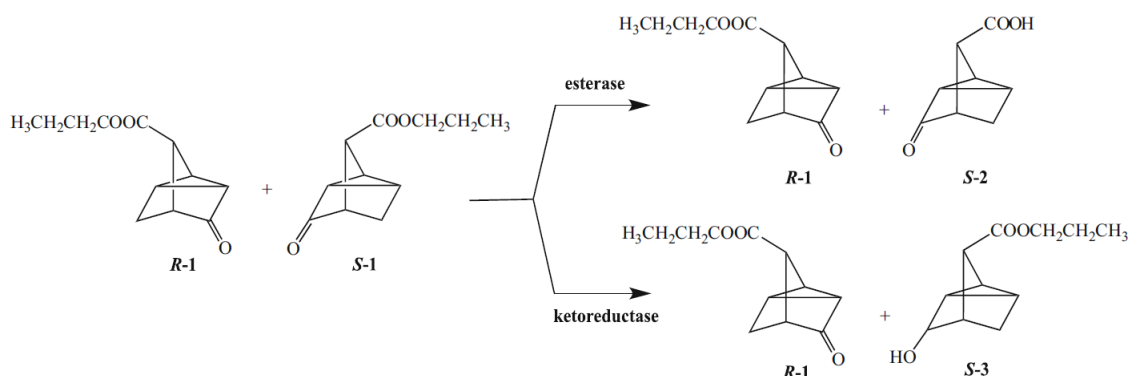
**Table 3.1.** Element composition of deep hypersaline anoxic basins and sea water<sup>6</sup>.

Physical separation due to different water density and thousands of year of evolutionary pathway have probably made possible the development of specific and diverse microbial communities in the four different basins. In the past, these high cation concentrations convinced the researchers that this condition was incompatible with life<sup>8,9</sup>, but recently the presence of metabolically active microbial communities has been demonstrated<sup>6</sup>. Through the combined study of 16S rRNA and enzymatic tests, in all four basins, an active reduction of methane, sulfate and an important heterotrophic and chemoautotrophic activities has been demonstrated. Instead, the waters above them show a different structure of the microbial community<sup>10</sup>. Microbial communities prevailing in the Discovery basin belong to the Bacteria kingdom and same happens for L'Atalante and Bannock basins, while in Urania basin there is a prevalent prevalence of the Archaea microorganisms.

In all four hypersaline anoxic basins, a microbial population belonging to Bacteria kingdom is highly diversified compared to the Archaea one; a biodiversity that was not found in the Urania basin. After a more specific analysis of 16S rRNA gene sequences, it has also emerged that hypersaline anoxic basins are populated by high percentages of microbial species belonging to  $\gamma$ -,  $\delta$ -, and  $\epsilon$ -proteobacteria, sphingobacteria and halobacteria. This isolation may have resulted in the evolution of specific microbial communities in each DHAB. In fact, through biodiversity analysis of the seawater interface, several taxonomic categories have been identified, including new phylogenetic groups, organized in colonies and heavily stratified in the "deep-water ecosystem"<sup>11-16</sup>.

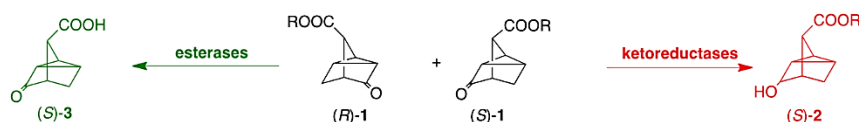
## MARINE BACTERIA BIOCATALYSIS

As fairly described by De Vitis *et al.*<sup>17</sup> these peculiar microorganisms isolated from DHABs on the Mediterranean Ridge have already showed interesting biocatalytic features applied in a kinetic resolution of the propyl ester of *anti*-2-oxotricyclo[2.2.1.0]heptan-7-carboxylic acid, a key intermediate for the prostaglandin D-cloprostenol<sup>18</sup> (scheme 3.1).



**Scheme 3.1.** Kinetic resolution of *anti*-2-oxotricyclo[2.2.1.0]heptan-7-carboxylic acid by newly isolated marine bacteria<sup>17</sup>.

The 33 strains were screened on racemic (*R,S*)-**1** and some of them have showed enantioselective keto-reductase and esterase activity. *Virgibacillus pantothenicus* 21D showed high halotolerance, enantioselective keto-reductase activity in the presence of glucose, and esterase activity was prevalent in the absence of glucose.



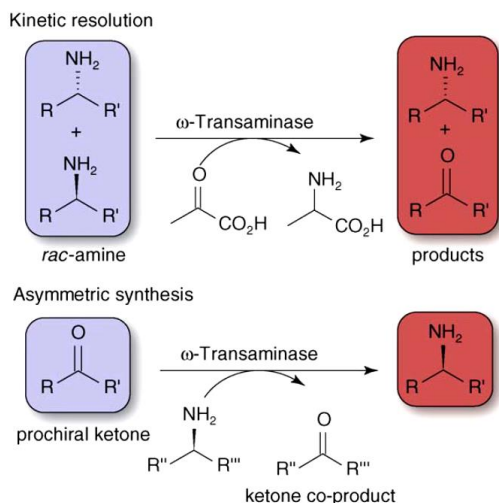
Strain	Growth optimum (NaCl %)	<b>3</b>		<b>2</b>		Time (h)
		(%)	ee (%)	(%)	ee (%)	
<i>Bacillus horneckiae</i> 15A <sup>a</sup>	0-3	< 5	n. d.	58	100	3
<i>Halomonas aquamarina</i> 9B <sup>a</sup>	3	57	100	< 5	n.d.	5
<i>Virgibacillus pantothenicus</i> 21D <sup>a</sup>	6-9	< 5	n. d.	58	100	6
<i>Virgibacillus pantothenicus</i> 21D <sup>b</sup>	6-9	46	88	7	n.d.	6

**Table 3.2.** Activity on racemic propyl ester **1** of whole cells of marine bacteria. <sup>a</sup> Biotransformation in the presence of glucose (5%); <sup>b</sup> Biotransformation in the absence of glucose.

In both cases, enantiomerically pure unreacted substrate could be easily recovered and purified at molar conversion below 57–58 %.

## $\omega$ -TRANSAMINASE

As it was reported in the introduction of this PhD thesis,  $\omega$ -transaminases ( $\omega$ -TAs), also called aminotransferases, are enzymes that transfers an amino group from an amino-donor into a carbonyl moiety of an amino-acceptor, whereby at least one of the two substances is not an  $\alpha$ -amino acid or an  $\alpha$ -keto acid.  $\omega$ -TAs offer a unique opportunity for the asymmetric synthesis or kinetic resolution (scheme 3.2) of bioactive compounds that possess a chiral amine moiety, starting from prochiral ketones or low-cost racemic amines<sup>19</sup>.

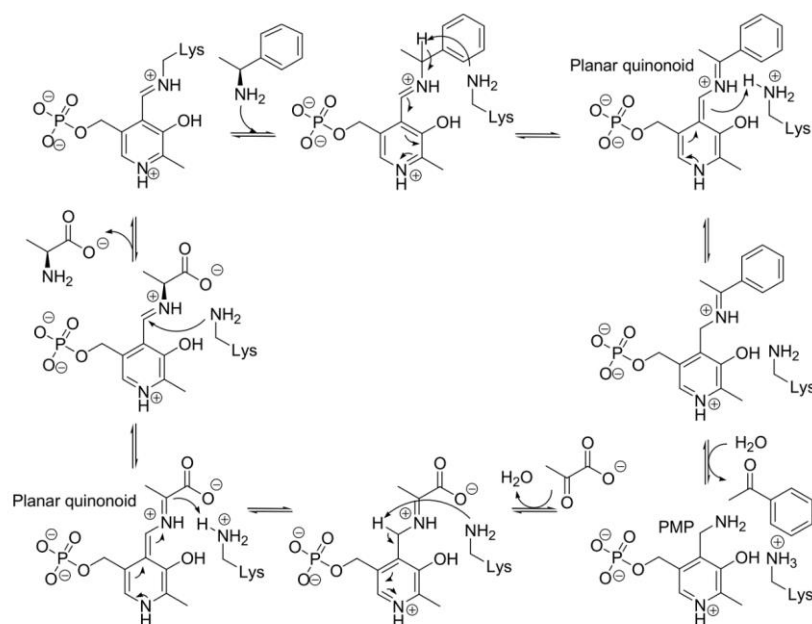


**Scheme 3.2.** Kinetic resolution starting with racemic amines is limited by 50% maximum yield. Theoretically, a 100% yield is possible in asymmetric synthesis from prochiral ketones if the equilibrium can be shifted appropriately<sup>19</sup>.

This enzymatic catalysis consists of two steps:

- deamination of an amino acid or amine (amino-donor) releasing amino-donor product;
- amination of a keto acid, ketone or aldehyde (amino-acceptor) producing a new amino acid or amine.

All aminotransferases (EC 2.6.1.X) reported to date require the same coenzyme, namely pyridoxal-5'-phosphate (PLP), which serves as a molecular shuttle for ammonia and electrons between the amino donor and the amino acceptor (scheme 3.3). During the reaction, PLP is reversibly interconverted to pyridoxamine (PMP). In the catalytic cycle, the amino donor binds first to the enzyme, PLP is aminated to PMP, and the respective keto product of the amino donor is released. The transamination is finalized by transferring the amino group from PMP to the acceptor molecule, thereby closing the catalytic cycle through the liberation of PLP.



**Scheme 3.3.** Proposed reaction mechanism of an (*S*)-selective  $\omega$ -transaminase<sup>20</sup>. PLP is, in the holo-enzyme, covalently bound to a lysine residue (top left) as an internal aldimine. An amino donor, here (*S*)-1-phenylethylamine, reacts with the internal aldimine to form PMP and a keto compound (here acetophenone). Then, a keto substrate, here pyruvate, reacts with PMP to form alanine. This equilibrium reaction in this case strongly favours the products. Adapted from the mechanism deduced for aspartate  $\alpha$ -transaminase<sup>21,22</sup>.

## STEREOSELECTIVITY

Another appealing property of TAs is their extraordinary stereoselectivity<sup>19</sup>. With the almost exclusive substrate-binding mode constrained by the relative position of PLP and two substrate-binding pockets of different sizes (figure 3.2), the enantiomeric excess of the chiral products is remarkably high. These distinguished natural properties have brought TAs to the attention of the biocatalysis community<sup>23–25</sup>.

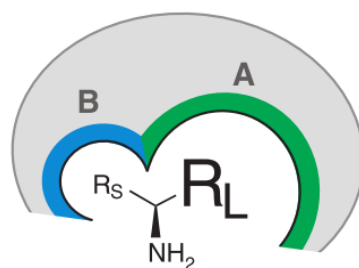


**Figure 3.2.** PLP-dependent fold class I (*S*)-amine transaminase binding pocket: small (B) and large (A) binding pocket<sup>26</sup>.

A more detailed description of  $\omega$ -TAs is presented in the chapter about *Virgibacillus pantothenicus*  $\omega$ -transaminase.

## PROJECT AIM

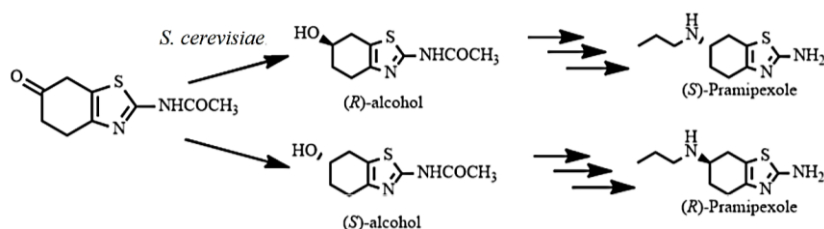
Starting from the encouraging results achieved by marine bacteria keto-reductions, the idea was to exploit this ability on pramipexole keto-intermediate, as done with marine yeasts previously.

On the other hand, the possibility to convert pramipexole ketone intermediate into the optically pure amine could be realised by a  $\omega$ -transaminase enzyme ( $\omega$ -TA) in a one-pot bioreaction instead of a multi-step synthetic pathway. Therefore, thirty-three marine bacteria species were screened to identify a transaminase activity. According to transaminase biocatalytic applications, where cofactor recycling is not needed, the aim in this case was to express and employ a recombinant enzyme.

## RESULTS AND DISCUSSION

### KETO-REDUCTASE

The most promising strains belonging to BIODEEP collection were selected and screened on keto-intermediate of pramipexole. The results showed a no particular enantioselectivity, with a general preference for (*R*)-enantiomer formation like *Saccharomyces cerevisiae* (table 3.3).

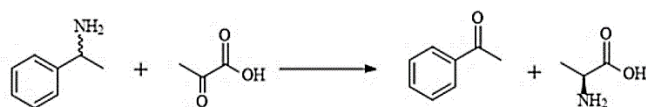


STRAIN	C (%)	e.e.(%)	SPECIFICITY
11D	100	47	<i>S</i>
15A	100	74	<i>R</i>
3U	100	45	<i>R</i>
3B	46,57	47	<i>R</i>
5B tris	20	46	<i>S</i>
6B	35,97	75	<i>R</i>
7B	41,67	52	<i>R</i>
26A	99	25	<i>S</i>
9A	100	55	<i>R</i>
12D	100	35	<i>R</i>
21D	100	29	<i>S</i>

**Table 3.3.** Bioconversion data with marine yeasts.

## $\omega$ -TRANSAMINASE

The aim was to identify marine bacteria able to convert the keto-intermediate of pramipexole directly into the optically pure amine. Providing as amino acceptor the keto-intermediate and as amino donor methyl benzylamine the main activity seen was the keto-reductase one. For this reason, the subsequent approach was to try with model substrate<sup>27</sup> (scheme 3.4). Hence, the thirty-three marine bacteria species were screened on a model substrates as pyruvate and racemic methyl benzylamine.



**Scheme 3.4.** A transamination reaction where acetophenone and L-alanine is produced from *rac*-1-phenylethylamine and pyruvate, catalysed by an  $\omega$ -transaminase ( $\omega$ -TA).

The data showed here are a qualitative evaluation of presence of the product acetophenone after 6 h (due to volatile product) of bioconversion. All products from biotransformations were extracted in the same way and the samples injected in HPLC with the same dilution. This methodology was intentionally a rough screening because of whole cell metabolism that could hamper the conversion of pyruvate into L-alanine.

STRAIN	ACETOPHENONE	STRAIN	ACETOPHENONE	STRAIN	ACETOPHENONE
11D	-	3U	**	3B	*
15A	-	9U	-	5B tris	-
20D	*	9B	-	6B	-
15D	-	13U	**	7B	*
17B	*	18D	-	5U	-
19B	-	8B	*	24U	*
11U bis 2	-	15B	-	13A	-
12D	*	13D	-	14A	-
16U	-	1U	*	21D	**
16U bis 2	-	2U	*	26A	-
16A	-	23U	*	9A	-

**Table 3. 4.** Qualitative evaluation of acetophenone production by marine bacteria. \* represents roughly the formation of trace of acetophenone.

## *VIRGIBACILLUS PANTOTHENTICUS*

Based on the previous results<sup>17</sup> in terms of halotolerance and keto-reductase activity, and on transaminase screening previously reported, the marine bacterium strain *Virgibacillus pantothenticus* 21D was selected for the genome sequencing (next generation sequencing) in order to clone and express an  $\omega$ -transaminase enzyme.

The strain 21D isolated from seawater-brine interface of the deep hypersaline anoxic basin Discovery (35° 17' N, 21° 41' E), on the Mediterranean Ridge<sup>6</sup>. The isolate grows in presence of NaCl and MgCl<sub>2</sub> at concentrations up to 9% and 9.52%, respectively, with optimum growth at 6-9% NaCl and 4.76% MgCl<sub>2</sub>; pH optimum (8-9) and temperature optimum (30-37°C) have been also determined.

Genome sequencing data were deposited in The Seed database and genes were annotated by RAST software<sup>28</sup>. Automatic annotation of the genome showed that it contains genes that could help the bacterium to thrive osmotic stresses typically of extreme environments (osmotically activated L-carnitine/choline ABC transporters, glycine betaine transporters, choline uptake and an ectoine synthase). The complete genome sequence of *Virgibacillus pantothenicus* 21D has been deposited in EMBL database (accession numbers: HG799644) and GenBank database (accession number: CP018622).

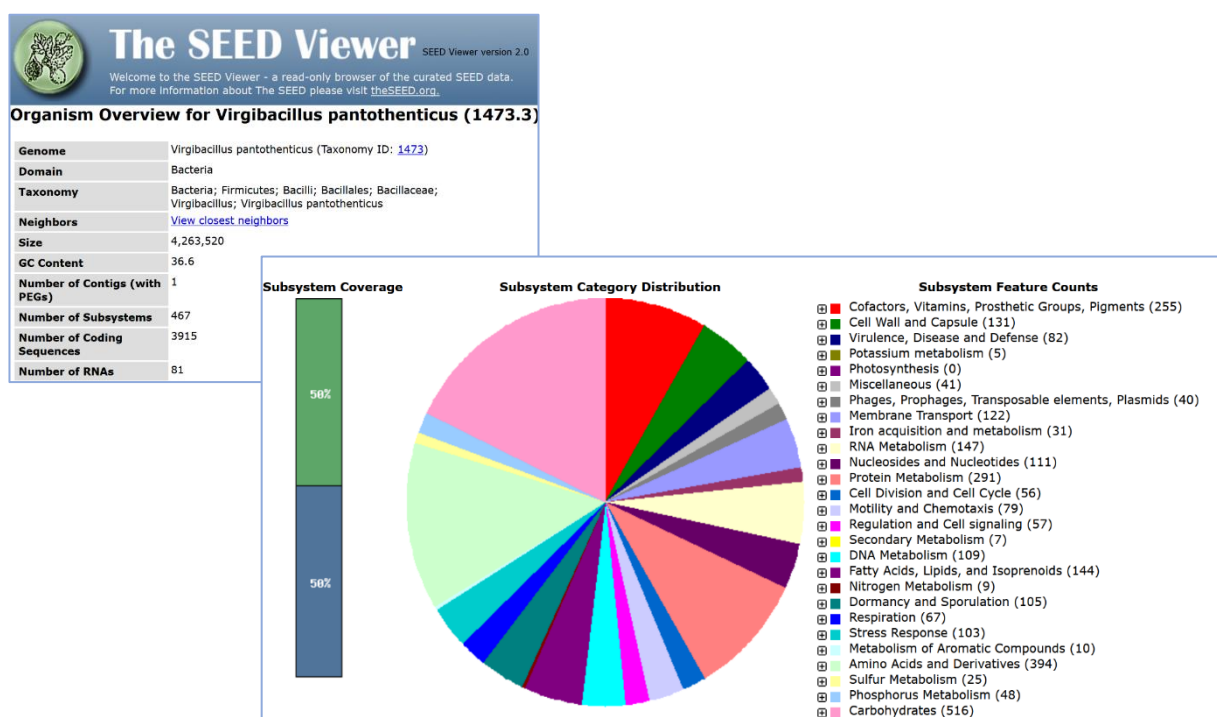


**Figure 3.3.** The Seed representation of Rast Genome Annotations System of *Virgibacillus pantothenicus* 21D.

## MATERIALS AND METHODS

### MATERIALS

All reagents and solvents were obtained from Sigma–Aldrich-Fluka and used without further purification or drying. TLC was performed with Merck silica gel 60 F254 pre-coated plates. Silica gel column chromatography was performed on silica gel 60 (40–63 mm particle size). Pramipexole keto intermediate (2-acetyl-amino-6-oxo-4,5,6,7- tetrahydrobenzothiazole) was prepared following a procedure previously described by Ferraboschi *et al.*<sup>29</sup>

## CHARACTERISATION

$^1\text{H}$  and  $^{13}\text{C}$  NMR spectra were recorded by using a Nuclear magnetic resonance (NMR) spectra were recorded at 300 K on a Bruker-Avance 500 MHz spectrometer operating at 500.13 and 125.76 MHz for  $^1\text{H}$  and  $^{13}\text{C}$  acquisitions, respectively. Chemical shifts ( $\delta$ ) of the  $^1\text{H}$  NMR and  $^{13}\text{C}$  NMR spectra are reported in ppm using the signal for residual solvent proton resonance as the internal standard ( $^1\text{H}$  NMR:  $\text{CDCl}_3$  7.26,  $\text{DMSO-d}_6$  2.49,  $\text{CD}_3\text{OD}$  3.31 ppm;  $^{13}\text{C}$  NMR:  $\text{CDCl}_3$  77.0 (central line),  $\text{DMSO-d}_6$  39.50 (central line),  $\text{CD}_3\text{OD}$  49.00 (central line) ppm). HPLC analyses were performed by using a Jasco Pu-980 equipped with a UV/Vis detector Jasco UV-975. Chiral HPLC columns used: Chiralpak IA (4.6x250 mm, 5 mm, Daicel), Chiralcell OD (4.6x250 mm, 5 mm, Daicel). Optical rotatory power determinations were performed by a Perkin–Elmer (mod. 241) polarimeter in a 1 dm cell at 20 °C, setting the wavelength at 589 nm or at 546 nm.

## MICROORGANISMS

All microorganisms employed were isolated for BIODEEP project from four different deep hypersaline anoxic basins on Mediterranean Ridge.

Strain code	DHABs	Closest described species (acc. no.)	Phylum/Class	% Identity	ITS haplotype	Growth opt (NaCl %)
3B	Bannock	<i>Oceanobacillus profundus</i> (HQ595230)	Firmicutes	99	19	0–3–6
5Bt	Bannock	<i>Oceanobacillus profundus</i> (HQ595230)	Firmicutes	99	19	n.d.
6B	Bannock	<i>Oceanobacillus profundus</i> (HQ595230)	Firmicutes	99	19	n.d.
7B	Bannock	<i>Oceanobacillus profundus</i> (HQ595230)	Firmicutes	99	19	n.d.
17B	Bannock	<i>Bacillus selenatarsenatis</i> (JF506004)	Firmicutes	99	23	6
19B	Bannock	<i>Bacillus selenatarsenatis</i> (JF506004)	Firmicutes	99	23	n.d.
8B	Bannock	<i>Halomonas meridiana</i> (EU441001)	Gammaproteobacteria	99	20	n.d.
9B	Bannock	<i>Halomonas aquamarina</i> (EU440965)	Gammaproteobacteria	99	21	3
15B	Bannock	<i>Halomonas meridiana</i> (EU441001)	Gammaproteobacteria	99	22	n.d.
11D	Discovery	<i>Bacillus firmus</i> (DQ089748)	Firmicutes	99	13	n.d.
12D	Discovery	<i>Bacillus firmus</i> (DQ089748)	Firmicutes	99	13	3
13D	Discovery	<i>Halobacillus trueperi</i> (HM179214)	Firmicutes	99	14	3
15D	Discovery	<i>Bacillus selenatarsenatis</i> (JF506004)	Firmicutes	99	15	n.d.
20D	Discovery	<i>Bacillus lehensis</i> (NR_036940)	Firmicutes	99	17	n.d.
21D	Discovery	<i>Virgibacillus pantothenicus</i> (JN791392)	Firmicutes	100	18	6–9
18D	Discovery	<i>Halomonas cupida</i> (AB681327)	Gammaproteobacteria	99	16	3
13A	L'Atalante	<i>Virgibacillus halodenitrificans</i> (AB697714)	Firmicutes	97	9	3–6
14A	L'Atalante	<i>Virgibacillus halodenitrificans</i> (AB697714)	Firmicutes	97	9	3–6
15A	L'Atalante	<i>Bacillus horneckiae</i> (JN002383)	Firmicutes	99	10	0–3
16A	L'Atalante	<i>Virgibacillus proomii</i> (FN397532)	Firmicutes	99	11	n.d.
26A	L'Atalante	<i>Virgibacillus pantothenicus</i> (JN791392)	Firmicutes	99	12	3–6
9A	L'Atalante	<i>Halomonas aquamarina</i> (EU430083)	Gammaproteobacteria	99	5	n.d.
9U	Urania	<i>Exiguobacterium acetylicum</i> (JN852813)	Firmicutes	99	4	n.d.
11Ub	Urania	<i>Bacillus thioeparans</i> (NR_043762)	Firmicutes	99	6	n.d.
16U	Urania	<i>Bacillus thioeparans</i> (NR_043762)	Firmicutes	99	6	n.d.
16Ub	Urania	<i>Bacillus thioeparans</i> (NR_043762)	Firmicutes	99	6	n.d.
23U	Urania	<i>Virgibacillus salinus</i> (FM205010)	Firmicutes	99	7	n.d.
1U	Urania	<i>Idiomarina loihiensis</i> (AY505529)	Gammaproteobacteria	99	1	3–6
2U	Urania	<i>Idiomarina loihiensis</i> (NR_025119)	Gammaproteobacteria	99	1	n.d.
3U	Urania	<i>Enterobacter aerogenes</i> (JQ682634)	Gammaproteobacteria	99	2	n.d.
5U	Urania	<i>Pseudoalteromonas ganghwensis</i> (DQ011614)	Gammaproteobacteria	100	3	n.d.
13U	Urania	<i>Halomonas aquamarina</i> (AB681582)	Gammaproteobacteria	99	5	3
24U	Urania	<i>Salinisphaera shabanensis</i> (JF281734)	Gammaproteobacteria	99	8	n.d.

**Table 3.5.** List of all the marine bacterium strains employed in this research project with their identification number.

## MEDIA AND GROWING CONDITIONS

### *CYSP (Casitone, Yeast extract, Soytone, Peptone) MEDIUM + 3% NaCl*

For both solid and liquid growing broth, the medium employed was CYSP<sup>18</sup> medium + 3% NaCl to mimic the ionic strength of a marine environment. The growth in liquid was evaluated by measuring optical density (O.D.) at 600 nm with a single-ray Pharmacia<sup>®</sup>Biotech Ultrospec 1000 spectrophotometer.

COMPOSITION	CONCENTRATION
-------------	---------------

casitone	15 g/L
yeast extract	5 g/L
soitone	3 g/L
peptone	2 g/L
MgSO <sub>4</sub> *7H <sub>2</sub> O	15 mg/L
FeCl <sub>3</sub> *6H <sub>2</sub> O	116 mg/L
MnCl <sub>2</sub> *4H <sub>2</sub> O	20 mg/L
NaCl	30 g/L (3%)

## BIOTRANSFORMATION

Cells were grown in CYSP medium + 3% NaCl for 24h in an orbital shaker at 180 rpm at 28 °C for 24 h. Biotransformations were performed suspending freshly prepared cells (50 mg<sub>dry weight</sub> mL<sup>-1</sup>) in 10 mL of phosphate buffer (pH 7.5, 0.1 M) in Erlenmeyer flasks (100 mL). Bioconversions were kept at 28 °C at 180 rpm for 24h. Yields and enantioselectivity were checked during this time.

For dry weight determination, washed culture samples were filtered through a 0.45 µm glass microfiber GF/A filter (Whatman) and dried for 24 h at 110 °C. The results were an average of five replicates.

The biotransformation of pramipexole keto intermediate (5 mM) were performed by adding the substrate as concentrated solution in 2-propanol (final concentration of co-solvent 5%).

The biotransformation of *rac*-1-phenylethylamine and sodium pyruvate were performed in the presence of 1% DMSO to increase the solubility and 50 g/L glucose.

For extraction, EtOAc was added in each sample collected at various time for monitoring conversion and the resulting mixture was shaken and centrifuged; the organic phases were collected, dried under N<sub>2</sub> and analysed by HPLC.

## PURIFICATION AND CHEMICAL CHARACTERISATION

### *2-Acetylamino-6-hydroxy-4,5,6,7-tetrahydrobenzothiazole*

The reaction progress and *ee* were determined by HPLC using a Chiralpak IA column (*n*-hexane/*i*PrOH 8:2 as eluent, flow rate: 0.7 mL min<sup>-1</sup>, 254 nm), *t<sub>r</sub>* (*R*)-**2** i 10.9 min, *t<sub>r</sub>* (*S*)-**2** i 14.8 min.<sup>29</sup> Yellowish solid. *R<sub>f</sub>*=0.25 (CH<sub>2</sub>Cl<sub>2</sub>/MeOH, 95:5). <sup>1</sup>H NMR (300 MHz, CD<sub>3</sub>OD): δ=1.91 (dddd, *J*=14.2, 8.6, 7.7, 5.9 Hz, 1 H), 2.04 (dddd, *J*=14.2, 6.2, 5.9, 2.9 Hz, 1 H), 2.26 (s, CH<sub>3</sub>, 3 H), 2.61–2.71 (m, 2 h), 2.79 (dddd, *J*=16.5, 5.9, 5.9, 1.8 Hz, 1 H), 2.99 (ddd, *J*=15.7, 4.7, 1.8 Hz, 1 H), 4.15

ppm (dddd,  $J=8.6, 6.9, 4.7, 2.9$  Hz, 1 H);  $^{13}\text{C}$  NMR (300 MHz,  $\text{CD}_3\text{OD}$ ):  $\delta=21.2, 23.2, 30.5, 30.7, 66.2, 120.9, 143.2, 156.4, 169.1$  ppm; elemental analysis calcd (%) for  $\text{C}_9\text{H}_{12}\text{O}_2\text{N}_2\text{S}$  (212.06): C 50.92, H 5.70, N 13.20; found: C 50.96, H 5.89 N 12.85.

### Acetophenone

The reaction progress and *e.e.* were determined by using HPLC using a Chiralcell OD column (n-hexane/iPrOH 95:5 as eluent, flow rate:  $0.7\text{ mL min}^{-1}$ , 254 nm), *tr* 7.6 min.

## REFERENCES

1. BIODEEP. Available at: [http://cordis.europa.eu/project/rcn/57219\\_it.html](http://cordis.europa.eu/project/rcn/57219_it.html).
2. Camerlenghi, A. Anoxic basins of the eastern Mediterranean: geological framework. *Mar. Chem.* **31**, 1–19 (1990).
3. Jongsma, D. *et al.* Discovery of an anoxic basin within the Strabo Trench, eastern Mediterranean. *Lett. to Nat.* **305**, (1983).
4. Langendijk, P. S., Hanssen, J. T. & Van der Hoeven, J. S. Sulfate-reducing bacteria in association with human periodontitis. *J. Clin. Periodontol.* **27**, 943–950 (2000).
5. Wallmann, K., Suess, E., Westbrook, G. H., Winckler, G. & Cita, M. B. Salty brines on the Mediterranean sea floor. *Nat. - Sci. Corresp.* **387**, (1997).
6. Daffonchio, D. *et al.* The Enigma of Prokaryotic Life in Deep Hypersaline Anoxic Basins. *Science* **4**, 121–123 (2005).
7. Henneke, E. & Lange, G. J. D. The distribution of DOC and POC in the water column and brines of the Tyro and Bannock Basins. *Mar. Chem.* **31**, (1990).
8. Horowitz, N. H., Cameron, R. E. & Hubbard, J. S. Microbiology of the Dry Valleys of Antarctica. *Science (80-. )*. **176**, 242–245 (1972).
9. Siegel, B. Z., Mcmurty, G., Siegel, S. M., Chen, J. & Larock, P. Life in the calcium chloride environment of Don Juan Pond, Antarctica. *Nature* **280**, 828–829 (1979).
10. Sørensen, K. B., Canfield, D. E., Teske, A. P. & Oren, A. Community Composition of a Hypersaline Endoevaporitic Microbial Mat Community Composition of a Hypersaline Endoevaporitic Microbial Mat. *Appl. Environ. Microbiol.* **71**, 7352–7365 (2005).
11. Daffonchio, D. *et al.* Stratified prokaryote network in the oxic–anoxic transition of a deep-sea halocline. *Nature* **440**, 203–207 (2006).
12. Yakimov, M. M., Giuliano, L., Cappello, S., Denaro, R. & Golyshin, P. N. Microbial community of a hydrothermal mud vent underneath the deep-sea anoxic brine lake Urania (Eastern Mediterranean). *Orig. Life Evol. Biosph.* **37**, 177–188 (2007).
13. Borin, S. *et al.* Sulfur cycling and methanogenesis primarily drive microbial colonization of the highly sulfidic Urania deep hypersaline basin. *Proc. Natl. Acad. Sci. U. S. A.* **106**, 9151–9156 (2009).
14. Danovaro, R. *et al.* Deep-sea biodiversity in the Mediterranean Sea: The known, the unknown, and the unknowable. *PLoS One* **5**, (2010).
15. Sass, A. M., Sass, H., Coolen, M. J. L., Cypionka, H. & Overmann, J. Microbial

Communities in the Chemocline of a Hypersaline Deep-Sea Basin (Urania Basin, Mediterranean Sea). *Appl. Environ. Microbiol.* **67**, 5392–5402 (2001).

16. Welch, D. B. M. & Huse, S. M. Microbial Diversity in the Deep Sea and the Underexplored 'Rare Biosphere'. *Handb. Mol. Microb. Ecol. II Metagenomics Differ. Habitats*
17. De Vitis, V. *et al.* Marine Microorganisms as Source of Stereoselective Esterases and Ketoreductases: Kinetic Resolution of a Prostaglandin Intermediate. *Mar. Biotechnol.* **17**, 144–152 (2015).
18. Romano, A., Romano, D., Molinari, F., Gandolfi, R. & Costantino, F. A new chemoenzymatic synthesis of d-cloprostenol. *Tetrahedron Asymmetry* **16**, 3279–3282 (2005).
19. Koszelewski, D., Tauber, K., Faber, K. & Kroutil, W.  $\omega$ -Transaminases for the synthesis of non-racemic  $\alpha$ -chiral primary amines. *Trends Biotechnol.* **28**, 324–332 (2010).
20. Cassimjee, K. E.  $\omega$ -Transaminase in Biocatalysis Methods, Reactions and Engineering. (KTH Royal Institute of Technology, Stockholm, 2012).
21. Hammes, G. G. & Haslam, J. L. A kinetic investigation of the interaction of erythro-beta-hydroxyaspartic acid with aspartate aminotransferase. *Biochemistry* **8**, 1591–8. (1969).
22. Silverman, R. B. *The Organic Chemistry of Enzyme-Catalyzed Reactions*. (Elsevier Science, 2000).
23. Ghislieri, D. & Turner, N. J. Biocatalytic approaches to the synthesis of enantiomerically pure chiral amines. *Top. Catal.* **57**, 284–300 (2014).
24. Kohls, H., Steffen-Munsberg, F. & Höhne, M. Recent achievements in developing the biocatalytic toolbox for chiral amine synthesis. *Curr. Opin. Chem. Biol.* **19**, 180–192 (2014).
25. Fuchs, M., Farnberger, J. E. & Kroutil, W. The Industrial Age of Biocatalytic Transamination. *European J. Org. Chem.* **2015**, 6965–6982 (2015).
26. Höhne, M., Schätzle, S., Jochens, H., Robins, K. & Bornscheuer, U. T. Rational assignment of key motifs for function guides in silico enzyme identification. *Nat. Chem. Biol.* **6**, 807–813 (2010).
27. Guo, F. & Berglund, P. Transaminase Biocatalysis: Optimization and Application. *Green Chem.* **19**, 333–360 (2016).
28. Aziz, R. K. *et al.* The RAST Server: Rapid Annotations using Subsystems Technology. *BMC Genomics* **9**, 75 (2008).
29. Ferraboschi, P. *et al.* Baker's yeast catalyzed preparation of a new enantiomerically pure synthon of (S)-pramipexole and its enantiomer (dexpramipexole). *Tetrahedron Asymmetry* **25**, 1239–1245 (2014).

# RECOMBINANT ENZYMES

Before checking the biocatalytic potential of marine recombinant enzyme, some commonly used enzymes were tested on pramipexole intermediates.

## BACKGROUND

### KETO-REDUCTASE

This enzyme superfamily was already presented in previous chapters. Here, a focus on some strategies for cofactor regeneration are described.

#### *RECYCLING COFACTOR SYSTEM*

Most biocatalytic reactions involving reductions of ketones operated by DH require stoichiometric quantities of reducing equivalents which are provided in the form of NADH or NADPH. The high cost of these cofactors, however, strongly limits their use; for these reasons, in recent decades the interest in the development of *in situ* cofactor regeneration systems has increased considerably.

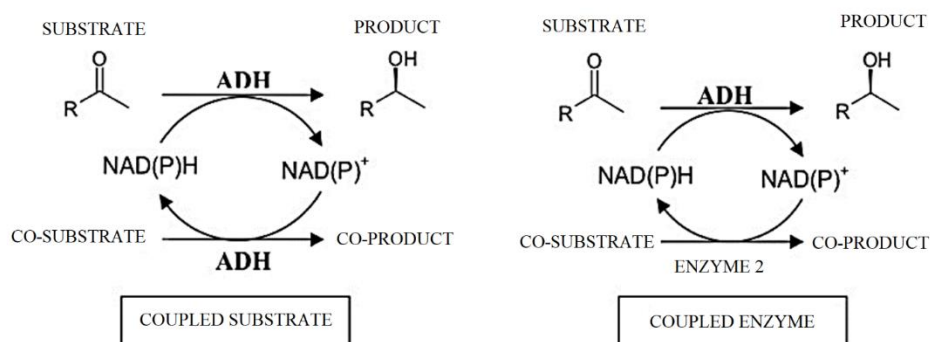


**Figure 4.1.** Scheme of the reduction reaction of a carbonyl group by the substrate-coupled method (left) and the enzyme-coupled method (right).

Enzymatic regeneration is a widely-diffused method, which involves two different methods of cofactor recycling: coupled enzyme method and coupled substrate method (figure 4.1). With the coupled enzyme method two distinct enzymes catalyze two different processes: the conversion of the main substrate and the cofactor recycling.

Different classes of enzymes are used as auxiliary catalysts in recycling of cofactors:

- Oxidation of formate to CO<sub>2</sub> catalyzed by formate dehydrogenase (FDH). The main advantage of this reaction is that both the auxiliary substrate and the product are not harmful to the enzyme and easy to remove from the reaction environment. FHD is a commercial enzyme, stable and therefore easily immobilized, if protected by self-oxidation.

- Glucose dehydrogenase (GDH) or glucose-6-phosphate dehydrogenase (G6PDH) are enzymes that oxidise glucose, allowing effective regeneration of both NADH and NADPH. The balance of this reaction is totally directed towards the formation of gluconolactone due to its spontaneous hydrolysis to gluconic acid. Active system, stable but very expensive.
- Oxidation of alcohols with aldehyde dehydrogenase (ADH). The low cost of ADH and the volatility of ethanol and acetaldehyde make this method attractive for large-scale use. Due to low redox potential, only reactive carbonyl derivatives such as aldehydes or cyclic ketones can be reduced. With other substrates, the balance must be forced by using an excess of ethanol or by removing the aldehyde. This latter result can be obtained by oxidizing the aldehyde to acetate with an aldehyde dehydrogenase, resulting in regeneration of a second low cofactor equivalent.
- Direct reduction of  $\text{NAD}^+$  with hydrogenase; hydrogenases are bidirectional enzymes that catalyze the production and oxidation of molecular hydrogen. The regeneration of the NADPH directed by using this enzyme is probably the most elegant solution, as there is no by-product formation.

An alternative method that does not require the implication of a second cofactor enzyme recirculation is referred to as a "substrate-coupled method" and is based on the addition of an auxiliary substrate reaction that provides the reducing power necessary for the primary reaction of reduction. The auxiliary substrate most widely added to the biotransformations is glucose as well as 2-propanol which in the process of producing chiral alcohols is oxidized to acetone as a coproduct of the reaction<sup>1,2</sup>. In this sense, the possibility of carrying biocatalysis reactions with enzymes that need cofactors is a huge advantage if you are working with whole cells. Indeed, these processes with respect to processes with isolated enzymes do not require cofactor recirculation systems and offer the ability to selectively synthesise the target molecules using large, abundant and low cost raw materials. However, these systems, though advantageous, require expensive and time consuming equipment. In some cases, the development of uncontrolled metabolic processes during cell growth, with the production of toxic products for cells, sometimes makes it difficult to separate products from the rest of cell culture<sup>3</sup>.

## ESTERASE AND LIPASE

Esterases and lipases are generally employed in stereospecific hydrolysis, transesterification, ester synthesis and other organic reactions.

The hydrolases (EC 3 -...) form a group of enzymes capable of catalysing the hydrolysis of a covalent bond between a carbon atom and a heteroatom by water intervention. Their natural function is purely

"digestive". Precisely because of the need to hydrolyse a wide variety of nutrients, this family includes several enzymatic groups often associated with a wide substrate specificity<sup>4</sup>.

Carboxyesterases (EC 3.1.1-) belong to this group of enzymes, and catalyse hydrolysis and the formation of ester bonds; they are classified in two enzymatic classes: lipases (EC 3.1.1.3) and properly esterases (EC 3.1.1.1), which differ in some catalytic properties<sup>5</sup>:

- Lipases preferably catalyse hydrolysis of non-soluble water esters such as long chain fatty acid triglycerides, while esterases hydrolyse low molecular weight and water soluble esters.
- Esterases follow Michaelis-Menten kinetics<sup>6</sup>, while lipases are active on the organic water-substrate interface and therefore they need a minimum substrate concentration for enzymatic activity: this phenomenon is known as "interface activation" and, thanks to structural studies, has been correlated with the presence of a hydrophobic domain that renders the active site inaccessible to the substrate; only in the presence of a minimal concentration of a hydrophobic molecule (the substrate itself or an organic solvent) the "lid" moves to show a conformational change able to access the substrate at the active lipase site<sup>7,8</sup>.
- Finally, while lipases generally show high enantioselectivity, especially to secondary alcohols, and organic solvent stability, esterases have greater variability in these two characteristics and are generally poorly active in organic solvents.

## $\omega$ -TRANSAMINASE

The topic of  $\omega$ -ATA was already introduced in previous chapters. A focus on two of these enzymes widely studied and applied in biocatalytic conversion is presented here.

The  $\omega$ -ATA from *Chromobacterium violaceum* DSM30191 which was described for the first time by Kaulmann *et al.*<sup>9</sup> shows 38% sequence identity to the *V. fluvialis* JS17 enzyme and resembles the latter in its preference for aromatic amine substrates. In fact, studies on the CV2025  $\omega$ -ATA from *C. violaceum* showed a very broad substrate specificity especially with respect to amine acceptors. The production of chiral aryl aminodiols from prochiral ketodiols looks promising and at present we are exploring possibilities to optimise ketodiol conversion by the native enzyme.

On the other hand, *Halomonas elongata* enzyme (HEWT) was recently characterised by Cerioli *et al.*<sup>10</sup> with interesting results. The  $\omega$ -ATA from this moderate halophile bacterium tolerated 20% (v/v) co-solvents over 22 h, the best solvents were MeOH (47%) and DMSO (27%). Acceptance of isopropylamine as amino donor is an advantage in asymmetric synthesis and a cost-effective benefit for industrial applications. With its high enantioselectivity, large substrate spectra and stability in

organic solvents, HEWT is a promising enzyme for biotechnological applications in the production of chiral amines.

## PROJECT AIM

In order to understand the possible biocatalytic applications on pramipexole intermediates, a new approach was investigated. Some more common and terrestrial recombinant enzymes were screened for the achievement of optically pure pramipexole precursor.

A recombinant non-marine ketoreductase from *Pichia glucozyma* (KRED1-Pglu)<sup>11-13</sup> used for the enantioselective reduction of various cyclic ketones was applied on pramipexole ketone intermediate by using co-factor recycling system.

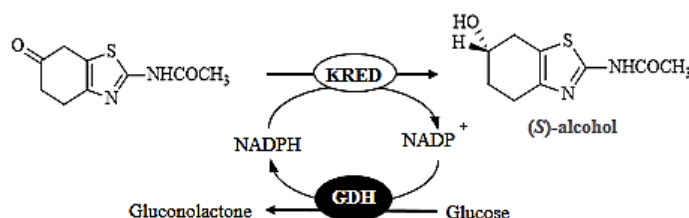
Another enzymatic activity was investigated in order to achieve optically pure intermediates for the preparation of both pramipexole enantiomers. Five of the most common commercial lipases and one new recombinant esterase from *Bacillus coagulans*<sup>14</sup> were tested on pramipexole ester intermediates.

Lastly, *Chromobacterium violaceum* and *Halomonas elongata*  $\omega$ -transaminases were screened for biocatalytic conversion of pramipexole intermediates.

## RESULTS

### KETO-REDUCTASE

Starting from the very promising results obtained with the novel recombinant keto-reductase from the non-common terrestrial yeast *Pichia glucozyma* (KRED1-Pglu) on a wide range of aromatic ketones, the idea was to check this reductase activity on the keto-intermediate of pramipexole. The employment of this recombinant enzyme has allowed the achievement of the alcohol intermediate with opposite stereochemical outcome in comparison with *S. cerevisiae* whole cells (scheme 4.1 and table 4.1).



**Scheme 4.1.** Recycling of cofactor employing KRED1-Pglu and a glucose dehydrogenase (GDH)<sup>15</sup>.

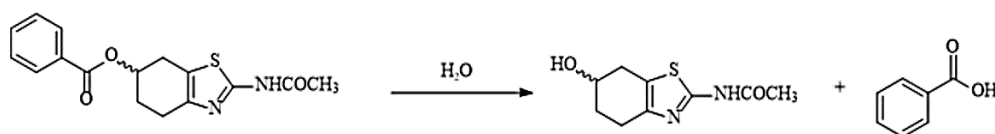
Time (h)	Conversion (%)	<i>e.e.</i> (%)	Configuration
----------	----------------	-----------------	---------------

4	75	86	S
---	----	----	---

**Table 4.1.** KRED1-Pglu-catalyzed bioconversion of pramipexole keto intermediate by using a cofactor recycling system.

## ESTERASE AND LIPASE

Based on former studies not already published on a new recombinant esterase from *Bacillus coagulans* (BCE), a benzoyl ester was synthesized in order to verify the enantioselective hydrolysis by BCE. Moreover, a commercial esterase active on benzoyl esters was assayed: pig liver esterase PLE (scheme 4.2 and table 4.2).

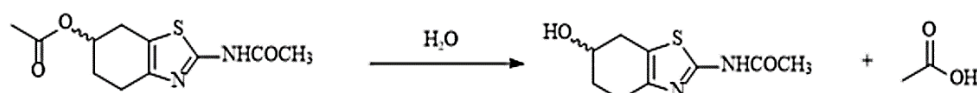


**Scheme 4.2.** Bioconversion of the benzoyl ester intermediate into alcohol intermediate and benzoic acid.

ESTERASE 24h	Conversion (%)	<i>e.e.</i> (%)	Configuration
BCE	12	100	R
PLE	-	-	-

**Table 4.2.** BCE- and PLE-catalyzed conversion.

For what concerns lipase activity, 5 commercial lipases as *Pseudomonas fluorescens* lipase (PFL), *Candida antarctica* lipase A and B (CAL A, CAL B), lipase from porcine pancreas (PPL) and from *Candida cylindracea* (CCL) were screened toward the acetyl ester intermediate of pramipexole (scheme 4.3 and table 4.3). The use of commercial lipases showed a high activity on this substrate but low molar conversion percentages, although the high *e.e.* with R-isomer preference like BCE.



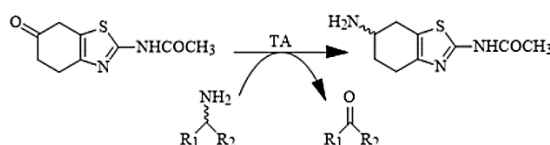
**Scheme 4.3.** Bioconversion of acetyl ester intermediate into alcohol intermediate and acetic acid.

LIPASE 20h	Conversion (%)	<i>e.e.</i> (%)	Configuration
CAL A-CLEA*	5	80	R
CAL B	49	71	R
PFL	5	100	R
PPL	7	100	R
CCL	9	20	R

**Table 4.3.** Biotransformation molar conversion and enantiomeric excesses. \*CLEA stands for cross-linked enzyme aggregates (CLEA Technologies).

## $\omega$ -TRANSAMINASE

The application of *H. elongata* (HEWT) and *C. violaceum* (CV2025)  $\omega$ -ATAs was exploited in bioconversion of pramipexole keto intermediate with (*S*)-1-phenylethylamine ((*S*)-1-PEA) and L-alanine as amine-donor (scheme 4.4). With both recombinant enzymes, no conversion of substrate has been seen.



**Scheme 4.4.** Transaminase catalysis on pramipexole intermediate.

## MATERIALS AND METHODS

### MATERIALS

All reagents and solvents were obtained from Sigma–Aldrich–Fluka and used without further purification or drying. TLC was performed with Merck silica gel 60 F254 pre-coated plates. Silica gel column chromatography was performed on silica gel 60 (40–63 mm particle size). Pramipexole keto intermediate (2-acetyl-6-oxo-4,5,6,7-tetrahydrobenzothiazole) was prepared following a procedure previously described<sup>16</sup>.

Commercial enzymes were employed following the patent WO 2006012277 A2<sup>17</sup> and the work by Ferraboschi *et al*<sup>18–20</sup>. Lipase from porcine pancreas (PPL, 23.9 U/mg), *Candida cylindracea* lipase (CCL, 3.86 U/mg), *Pseudomonas fluorescens* (PFL, 40.2 U/mg), Esterase from porcine liver (PLE,  $\geq 15$  U/mg) and *Candida antarctica* lipase B (CAL B, 5 U/mg) were purchased by Sigma-Aldrich. *Candida antarctica* lipase A CLEA (CAL A CLEA, 1.56 U/mg) was obtained from CLEA Technologies.

### CHARACTERISATION

Nuclear magnetic resonance (NMR) spectra were recorded at 300 K on a Bruker-Avance 500 MHz spectrometer operating at 500.13 and 125.76 MHz for <sup>1</sup>H and <sup>13</sup>C acquisitions, respectively. Chemical shifts ( $\delta$ ) of the <sup>1</sup>H NMR and <sup>13</sup>C NMR spectra are reported in ppm using the signal for residual solvent proton resonance as the internal standard (<sup>1</sup>H NMR: CDCl<sub>3</sub> 7.26, DMSO-d<sub>6</sub> 2.49, CD<sub>3</sub>OD 3.31 ppm; <sup>13</sup>C NMR: CDCl<sub>3</sub> 77.0 (central line), DMSO-d<sub>6</sub> 39.50 (central line), CD<sub>3</sub>OD 49.00 (central line) ppm). HPLC analyses were performed by using a Jasco Pu-980 equipped with a UV/Vis detector

Jasco UV-975. Chiral HPLC columns used: Chiralpak IA (4.6V250 mm, 5 mm, Daicel), Optical rotatory power determinations were performed by a Perkin–Elmer (mod. 241) polarimeter in a 1 dm cell at 20 °C, setting the wavelength at 589 nm or at 546 nm.

## KETO-REDUCTASE

KRED-Pglu was kindly provided by Professor Francesco Molinari's research group (University of Milan, DEFENS department, Milano, Italy). Recombinant GDH from *Bacillus megaterium* was kindly provided by Prof Daniela Monti (Istituto di Chimica del Riconoscimento Molecolare, C.N.R., Milano, Italy).

### *BIOTRANSFORMATIONS*

Molar conversion and enantioselectivity were determined using an enzyme-coupled system with glucose-glucose dehydrogenase (GDH) from *Bacillus megaterium*<sup>15</sup> for cofactor recycling.

Reductions were carried out in 5-mL screw-capped test tubes with a reaction volume of 1 mL with KRED1-Pglu (20 mU/ mL), GDH (1 U/mL), NADP<sup>+</sup> (0.1 mM), substrate (1 g/L), glucose (4×mmol of substrate) suspended in 50 mMTris-HCl buffer pH 8.0. The biotransformation was kept under stirring at 30 °C for 24 h.

Although the pH suitable for pramipexole ketone intermediate bioconversion is around pH 5-6, KRED1-Pglu is able to catalyse alcohol production with high rate avoiding substrate degradation.

For extraction, EtOAc was added in each sample collected at various time for monitoring conversion and the resulting mixture was shaken and centrifuged; the organic phases were collected, dried under N<sub>2</sub> and analysed by HPLC.

## ESTERASE AND LIPASE

BCE was kindly provided by Prof. Francesco Molinari's research group (University of Milan, DEFENS department, Milano, Italy).

### *ESTER SYNTHESIS*

For what concerns the acetyl ester, the procedure described by Ferraboschi *et al.*<sup>16</sup> was followed. For the preparation of pramipexole benzoyl ester intermediate, 6-hydroxy derivative was treated with benzoyl chloride in pyridine.

## BIOTRANSFORMATIONS

Benzoyl ester hydrolysis was carried out in 2 mL Eppendorf tubes with a reaction volume of 1 mL with BCE (20 mU/ mL), substrate (0.1 g/L) suspended in 50mMTris-HCl buffer pH 8.0, NaCl 100 mM. The biotransformation was kept under stirring at 30 °C for 24h.

DMSO as co-solvent was not employed in order to avoiding keto substrate degradation.

Acetyl ester hydrolysis, instead, was performed in 10-mL screw-capped test tubes with a reaction volume of 3 mL with the proper amount of commercial lipases<sup>17,19,18,20</sup>, H<sub>2</sub>O (5×mmol of substrate), substrate (20 mM) suspended in acetonitrile (ACN). The biotransformation was kept under stirring at 30 °C for 24h.

For extraction, EtOAc was added in each sample collected at various time for monitoring conversion and the resulting mixture was shaken and centrifuged; the organic phases were collected, dried under N<sub>2</sub> and analysed by HPLC.

## ω-TRANSAMINASE

During this experimental work, we had the opportunity to test aminotransferase potential of *Chromobacterium violaceum* and *Halomonas elongate* ω-ATAs on keto intermediate of pramipexole synthesis.

Both enzymes were kindly provided by Prof. Francesca Paradisi's research group.

## BIOTRANSFORMATIONS

The enzymatic reactions were carried out at 37 °C in 100 mM potassium phosphate buffer pH 8.0, 0.1 mM PLP using a purified enzyme solution (0.25 U/mL). The reaction mixture contained 10 mM (S)-1-PEA or 10 mM L-alanine and 10 mM pramipexole keto intermediate as amine-acceptor in a reaction volume of 200 μL.

For HPLC analysis, samples were collected at different time, diluted 1:50 with HCl 0.2% solution for quenching the reaction and injected.

## PURIFICATION AND CHEMICAL CHARACTERISATION

### *2-Acetylamino-6-hydroxy-4,5,6,7-tetrahydrobenzothiazole*

The reaction progress and *ee* were determined by using HPLC using a Chiralpak IA column (*n*-hexane/*i*PrOH 8:2 as eluent, flow rate: 0.7 mL min<sup>-1</sup>, 254 nm), *t<sub>r</sub>* (R)-**2** i 10.9 min, *t<sub>r</sub>* (S)-**2** i 14.8 min.<sup>16</sup>

Yellowish solid.  $R_f=0.25$  ( $\text{CH}_2\text{Cl}_2/\text{MeOH}$ , 95:5).  $ee=64\%$ .  $^1\text{H NMR}$  (300 MHz,  $\text{CD}_3\text{OD}$ ):  $\delta=1.91$  (dddd,  $J=14.2$ , 8.6, 7.7, 5.9 Hz, 1 H), 2.04 (dddd,  $J=14.2$ , 6.2, 5.9, 2.9 Hz, 1 H), 2.26 (s,  $\text{CH}_3$ , 3 H), 2.61–2.71 (m, 2 h), 2.79 (dddd,  $J=16.5$ , 5.9, 5.9, 1.8 Hz, 1 H), 2.99 (ddd,  $J=15.7$ , 4.7, 1.8 Hz, 1 H), 4.15 ppm (dddd,  $J=8.6$ , 6.9, 4.7, 2.9 Hz, 1 H);  $^{13}\text{C NMR}$  (300 MHz,  $\text{CD}_3\text{OD}$ ):  $\delta=21.2$ , 23.2, 30.5, 30.7, 66.2, 120.9, 143.2, 156.4, 169.1 ppm; elemental analysis calcd (%) for  $\text{C}_9\text{H}_{12}\text{O}_2\text{N}_2\text{S}$  (212.06): C 50.92, H 5.70, N 13.20; found: C 50.96, H 5.89 N 12.85.

### *2-Acetylamino-6-hydroxy-4,5,6,7-tetrahydrobenzothiazole, 6-benzoate*

HPLC analysis: Chiralpak IA, hexane/2-propanol 8:2 as eluent, flow rate 0.7 mL/min. Rt (*R*)-isomer 14.32 min; (*S*)-isomer 16.25 min.  $^1\text{H NMR}$  ( $\text{CDCl}_3$ ):  $\delta$  8.02 (2H, d,  $J = 8.0$  Hz, o-Ph H), 7.58 (1H, t,  $J = 8.0$  Hz, p-Ph H), 7.46 (2H, dd,  $J = 8.0$ , 8.0 Hz, m-Ph H), 5.58 (1H, dddd,  $J = 7.6$ , 5.5, 4.8, 2.5 Hz, 6-H), 3.20 (1H, ddd,  $J = 16.5$ , 4.8, 1.2 Hz, 7a-H), 3.02 (1H, dd,  $J = 16.5$ , 5.5 Hz, 7b-H), 2.93 (1H, ddd,  $J = 16.8$ , 8.4, 5.9 Hz, 4a-H), 2.86 (1H, dddd,  $J = 16.8$ , 6.2, 5.8, 1.4 Hz, 4b-H), 2.30 (3H, s,  $\text{CH}_3$ ), 2.30 (1H, dddd,  $J = 13.5$ , 7.6, 5.9, 5.8 Hz, 5a-H), 2.00 (1H, dddd,  $J = 13.5$ , 8.4, 6.2, 2.5 Hz, 5b-H).

## REFERENCES

- Hollmann, F., Arends, I. W. C. E. & Holtmann, D. Enzymatic reductions for the chemist. *Green Chem.* **13**, 2285–2314 (2011).
- Somogyi, L. P. The flavour and fragrance industry: Serving a global market. *Chem Ind.* **4**, 170–173 (1996).
- Graßmann, J. Terpenoids as Plant Antioxidants. *Vitam. Horm.* **72**, 505–535 (2005).
- Bornscheuer, U.T., Kazlauskas, R.J. *Hydrolases in Organic Synthesis*. (Weinheim: Wiley-VCH, 1999).
- Bornscheuer, U. T. Microbial carboxyl esterases: classification, properties and application in biocatalysis. *FEMS Microbiol Rev.* **26**, 73–81. (2002).
- Michaelis, L. & Menten, M. L. Die Kinetik der Invertinwirkung. *Biochem Z* **49**, 333–369 (1913).
- Holmquist, M. Alpha/Beta-hydrolase fold enzymes: structures, functions and mechanisms. *Curr Protein Pept Sci* **1**, 209–35 (2000).
- Schrag, J. D., Li, Y., Wu, S. & Cygler, M. Ser-His-Glu triad forms the catalytic site of the lipase from *Geotrichum candidum*. *Nature* **351**, 761–764 (1991).
- Kaulmann, U., Smithies, K., Smith, M. E. B., Hailes, H. C. & Ward, J. M. Substrate spectrum of  $\omega$ -transaminase from *Chromobacterium violaceum* DSM30191 and its potential for biocatalysis. *Enzyme Microb. Technol.* **41**, 628–637 (2007).
- Ceroli, L., Planchestainer, M., Cassidy, J., Tessaro, D. & Paradisi, F. Characterization of a novel amine transaminase from *Halomonas elongata*. *J. Mol. Catal. B Enzym.* **120**, 141–150 (2015).
- Contente, M. L. *et al.* Enzymatic reduction of acetophenone derivatives with a benzil reductase from *Pichia glucozyma* (KRED1-Pglu): electronic and steric effects on activity and enantioselectivity. *Org. Biomol. Chem.* **14**, 3404–3408 (2016).
- Contente, M. L. *et al.* Preparation of enantiomerically enriched aromatic  $\beta$ -hydroxynitriles and halohydrins by ketone reduction with recombinant ketoreductase KRED1-Pglu. *Tetrahedron* **72**, 3974–3979 (2016).
- Contente, M. L. *et al.* Stereoselective reduction of aromatic ketones by a new ketoreductase from *Pichia glucozyma*. *Appl. Microbiol. Biotechnol.* **100**, 193–201 (2016).

14. Romano, D. *et al.* Enhanced enantioselectivity of *Bacillus coagulans* in the hydrolysis of 1,2-O-isopropylidene glycerol esters by thermal knock-out of undesired enzymes. *Tetrahedron Asymmetry* **16**, 841–845 (2005).
15. Bechtold, M. *et al.* Biotechnological Development of a Practical Synthesis of Ethyl (S)-2-Ethoxy-3-(p-methoxyphenyl)propanoate (EEHP): Over 100-Fold Productivity Increase from Yeast Whole Cells to Recombinant Isolated Enzymes. *Org. Process Res. Dev.* **16**, 269–276 (2012).
16. Ferraboschi, P. *et al.* Baker's yeast catalyzed preparation of a new enantiomerically pure synthon of (S)-pramipexole and its enantiomer (dexpramipexole). *Tetrahedron Asymmetry* **25**, 1239–1245 (2014).
17. Valivety, R. H., Michels, P. C., Pantaleone, D. P. & Khmelnsky, Y. L. Biocatalytic process for preparing enantiomerically enriched pramipexole. (2005).
18. Ciceri, S., Ciuffreda, P., Grisenti, P. & Ferraboschi, P. Synthesis of the antitumoral nucleoside capecitabine through a chemo-enzymatic approach. *Tetrahedron Lett.* **56**, 5909–5913 (2015).
19. Ferraboschi, P., Mieri, M. D. & Ragonesi, L. Lipase-catalyzed preparation of corticosteroid 17 $\alpha$ -esters endowed with antiandrogenic activity. *Tetrahedron Lett.* **49**, 4610–4612 (2008).
20. Ferraboschi, P., Mieri, M. D. & Galimberti, F. Chemo-enzymatic approach to the synthesis of the antithrombotic clopidogrel. *Tetrahedron Asymmetry* **21**, 2136–2141 (2010).

## VPTA - *Virgibacillus pantothenicus* $\omega$ -transaminase

## BACKGROUND

### $\omega$ -TRANSAMINASE

Although the transaminase potential is under a magnifying glass since decades, their applicability in biotechnological fields for the preparation of chiral amino compounds is not entirely exploited yet. Combining ATAs with other enzymatic or chemical routes has been demonstrated to be a smart method for practical applications, particularly in regard to shortening the reaction routes, avoiding protecting steps, reducing chemical waste and achieving a high atom-efficiency<sup>1-3</sup>.

This makes these enzymes useful for synthesis of chiral amines, which are of high importance as building blocks for production of optically pure amino synthons in pharmaceutical like sitagliptin<sup>4</sup>, ethambutol<sup>5</sup>, imagabalin<sup>6</sup>, norephedrine and pseudoephedrine<sup>7</sup>, food, agrochemical and cosmetic additives<sup>8</sup>.

Synthesis by ATAs suffers from the unfavourable reaction equilibrium, especially in the asymmetric synthesis of amines from an amino acid as amino donor<sup>9</sup>. To maximize the productivity of ATAs, shifting the equilibrium to the side of product is extremely important<sup>10,11</sup>. Equilibrium displacement has been done by removal of the products or large excess of amino donor<sup>12,13</sup>.

Nevertheless, maintaining the quaternary and tertiary structures under non-physiological conditions (high concentrations of substrate and product, organic solvent, mechanical force, etc.) for a long period of time (10–100 h working time and an even longer storage time) is a huge task for all biocatalysts. The current trend in this research field is directing to the identification and designing of

new  $\omega$ -transaminases with defined substrate specificity and capable of adapting to the uncommon catalytic conditions of industrial processes.

## SOLUBILITY ISSUE

Protein overexpression systems, such as the *E. coli* T7 system, have been widely used for protein purification. However, due to improper folding of the overexpressed proteins, they often aggregate to form inclusion bodies, greatly reducing the protein yield. Different methods have been used to solve this problem<sup>14</sup>, such as optimization of bioprocess parameters or using dedicated screening tools for finding conditions for soluble expression<sup>15</sup>, expression at reduced temperature<sup>16</sup>, solubility-enhancing fusion tags<sup>17,18</sup>, co-expression of chaperones<sup>19</sup>, consideration of codon usage<sup>20</sup> and refolding of proteins after dissolving inclusion bodies in denaturing reagents<sup>21–23</sup> (fig. 5.1).

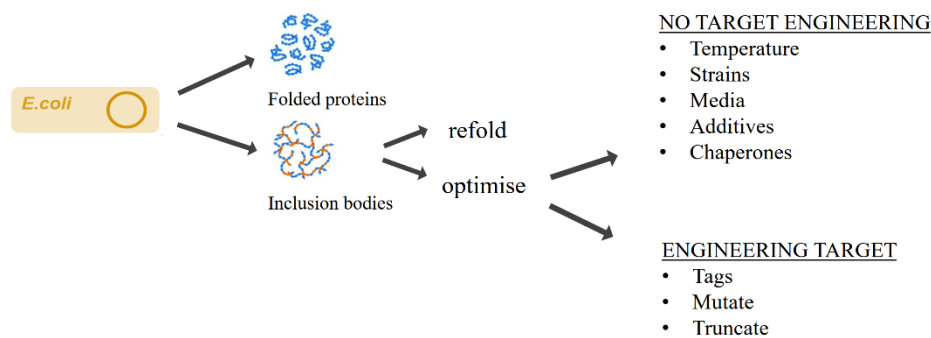


**Fig. 5.1.** All these methods were taken into account and the results illustrated below.

Solubility on overexpression of some proteins has been found to be altered by certain mutations<sup>24</sup>. Individual mutations differ in the extent to which they influence the solubility on overexpression. For example, the W131A and V165K mutants of human HIV type 1 integrase are only marginally more soluble, whereas the F185K is significantly more soluble relative to the wild-type under the same conditions of overexpression<sup>25</sup>.

Systematic replacement of hydrophobic residues has also been attempted, but only some of these mutations resulted in improved solubility<sup>25–27</sup>. Mutations involving substitution of less polar residues with more polar ones, identified by multiple sequence alignment of the insoluble protein with related soluble proteins<sup>27</sup> or predicted solvent accessibilities<sup>28</sup> have also been attempted, but only some mutations have manifested in improved solubility. Many of these types of mutations are identified by random mutagenesis procedures<sup>29,30</sup>. Asano *et al.*<sup>31</sup>, have created highly active and *in vivo* soluble mutants of MeHNL1 (hydroxynitrile lyase from *Manihot esculenta*, cassava plant) in *E. coli* by directed evolution, where several mutants of this enzyme were generated including His103 and also Lys-Pro mutants.

There are other examples of correlation between one single point mutation and folding changing. Particularly, regarding human transaminases, some specific mutations such as P11L (major allele) and G47R (minor allele) on alanine:glyoxylate aminotransferase (AGT) was proved to have a role in misfolding and pathogenic aggregation leading to Primary Hyperoxaluria Type I. These mutations seem to be involved in dimerization and stabilization of enzyme complex<sup>32,33</sup>.

## MUTAGENESIS

In recombinant applications, high levels of soluble expressed protein are usually required and often this entails an alteration of the physiological requirements for the enzyme natural folding leading to the formation of inclusions bodies. Therefore, thinking about a solubility improvement of enzyme sequences could be more than appreciable but not universally possible through a rational strategy. Moreover, utilization of proteins outside of their usual biological context, for example in industrial applications, often requires improvement of biophysical properties such as stability<sup>34,35</sup>. In the Introduction the mutagenesis strategies aimed at solving this issue were already presented.

Another approach based on multiple sequence alignments (MSAs) consists in statistical amino acid frequencies analysis<sup>36,37</sup>. Data-driven mutagenesis design is based on the simple assumption that the frequency of a given residue in an MSA of homologous proteins correlates with that amino acid's contribution to protein stability<sup>38-40</sup>. A *de novo* designed protein possessing the most frequent residue at each position should accordingly show maximum stability. Given the difficulty of predicting how individual residues contribute to overall stability<sup>41</sup>, this approach to protein stabilization is often preferable to classical rational design or is adopted as a complement of it, particularly as it does not depend on the availability of structural information.

## PROJECT AIM

The present work describes the attaining of soluble expression of a novel  $\omega$ -transaminase from a newly isolated halotolerant marine bacteria *Virgibacillus pantothenticus*(VPTA). This marine bacterium is part of the micro-biodiversity of Deep Hypersaline Anoxic Basins on the Mediterranean Ridge, a new and uncommon source of biocatalysts. Despite of several standard methodologies applied, the marine wild-type enzyme VPTA was total insoluble in *E. coli* host and it was satisfactorily solubilized by one single-point mutation, allowing the characterization of the new  $\omega$ -transaminase. Combining statistical amino acid frequencies analysis with a rational approach based on 3-D model, a target residue likely involved in structural stabilization and dimerization was selected. This finding has significant implications for  $\omega$ -transaminase structure-stability-solubility understanding and

represents one of the first works about semi-rational approach aimed at improving recombinant  $\omega$ -ATAs solubility allowing the characterization of this new halotolerant  $\omega$ -ATA. The enzyme shows an interesting salt and solvent tolerance in accordance to its origin and it results particularly active toward interesting building blocks.

## RESULTS AND DISCUSSIONS

### WILD-TYPE VPTA AND SOLUBILISATION STRATEGIES

The protein sequences of the *Vibrio fluvialis*, *Chromobacterium violaceum* and *Halomans elongata*  $\omega$ -ATAs were used to search for homologous proteins with the BLAST search option of Rast server at default settings. *H. elongata*  $\omega$ -ATA alignment showed the best results coming up with a sequence identity of 38% and similarity of 55%; with *V. fluvialis* and *C. violaceum* enzymes the similarity percentage was 36%. Rast annotation<sup>42</sup> describes this candidate as “omega-amino acid-pyruvate aminotransferase [EC 2.6.1.18]”, a member of the pyridoxal phosphate (PLP)-dependent aspartate aminotransferase superfamily (fold I)<sup>43</sup>. The selected gene is 1350 bp expressing a 448 residues wild-type protein. From the sequence alignment it was possible to identify the three residues considered to be responsible for the transaminase catalytic activity (figure 5.2):

- D244Aspartic acid: salt bridge/H-bond to N1 of pyridoxal 5'-phosphate;
- K273 Lysine: Schiff base with pyridoxal 5'-phosphate;
- R402 Arginine: salt bridge/H-bond with  $\alpha$ -carboxylate group of substrate.

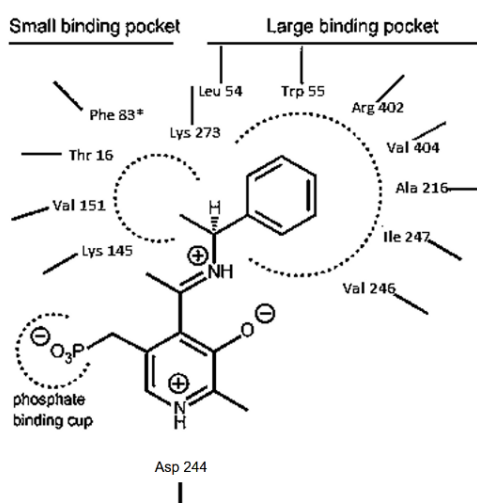


**Fig. 5.2.** Representation of small and large binding pockets of VPTA. Main residues involved in PLP and substrate interactions are showed<sup>44</sup>.

The nucleotide sequence was cloned in a classical *E. coli* BL21 DE3 expression system through Champion™ pET100/pET101 Directional TOPO™ Expression Kit with His-tagged tail in N-terminal and C-terminal respectively. Standard expressions in the *E. coli* strains BL21 DE3, BL21 DE3 star, Rosetta, Codon plus RIPL and also a co-expression with pGKJE8 plasmid (Takara Clontech) coding for most common chaperones resulted in inclusion bodies accumulation with no soluble protein production (figure 5.3). Better results were not achieved with protein refolding and cell-free expression (figure 5.3). The halophilic archaea host *Haloferax volcanii* was also exploited for the expression of the marine transaminase (figure 5.3) without any improvement<sup>45</sup>.

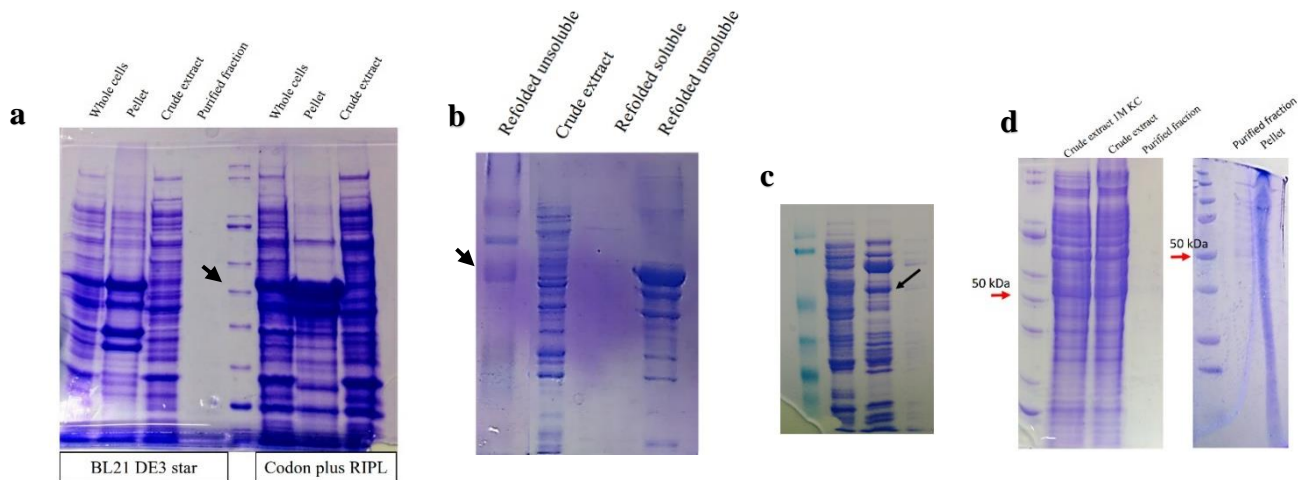


**Fig 5.3.** Wild-type VPTA has a molecular weight of 53 kDa; Marker 50 kDa band is underlined by arrows. Enzyme expression studies exploiting different strategies. Cold shock method with BL21 DE3 and Codon Plus RIPL *E. coli* strains (a); denaturation with urea and refolding (b); cell-free (c) and *Haloferax volcanii* expression (d).

Generally, the total expression level was always high in all the conditions, although to a different extent. Unfortunately, in all cases, the enzyme was obtained in insoluble form. Although soluble protein seems to be present in cell-free expression method and in *H. volcanii* expression, the kinetic assay by Schatzle *et al.*<sup>46</sup> showed no transaminase activity on these soluble fractions.

## MUTAGENESIS

Starting from ConSurf<sup>47</sup> analysis in which 500 homologous sequences were compared getting a statistical frequency (table 5.1) and a level of conservation (figure 5.4) for each position, some residues less conserved than the catalytic one were taken into account.

POSITION	AA with the HIGHEST FREQUENCY	% FREQUENCY
1	M	100
2	N	38
3	S	37
4	L	88
5	Q	29
6	E	35
7	L	59
8	D	88
9	A/R	23
10	A	38
11	H	88
12	H	41
13	L	52
14	H	88
15	P	97
<b>16</b>	<b>F</b>	<b>45</b>
17	T	49
18	D	31
19	L	14
20	K	34

**Table 5.1.** ConSurf results in terms of statistical amino acid frequency for each position. In the table, only the first 20 positions are shown as an example.

## ConSurf Results

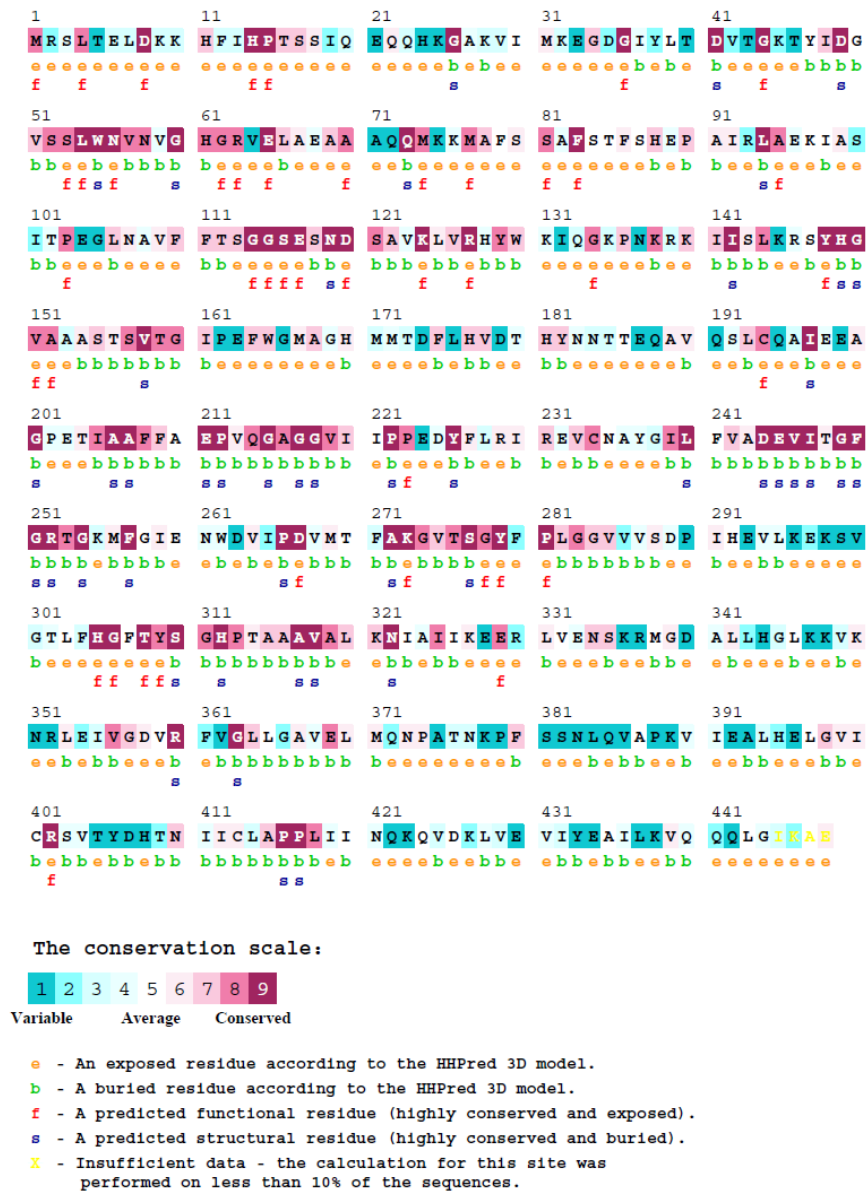


**Fig. 5.4.** Conservation scale by ConSurf on VPTA amino acid sequence. The position 16 shows a quite high conservation.

After target residues localization in tertiary structure model, threonine in position 16 was selected. Position 16 has a good level of conservation but the residue with the highest frequency in that position is phenylalanine (T16F).

The protein model was built using the SWISS-MODEL Homology Modeling tool<sup>48</sup>, superimposing the VTPA protein sequence on the resolved structure of the homologous amino transaminase from *Vibrio fluvialis* (PDB: 4E3Q). The result elaboration and the structural evaluation was achieved using the molecular visualization system PyMOL (open source license). Sequence analysis and alignment was performed with CunSurf, a software for multiple blast provided by BioSoft.

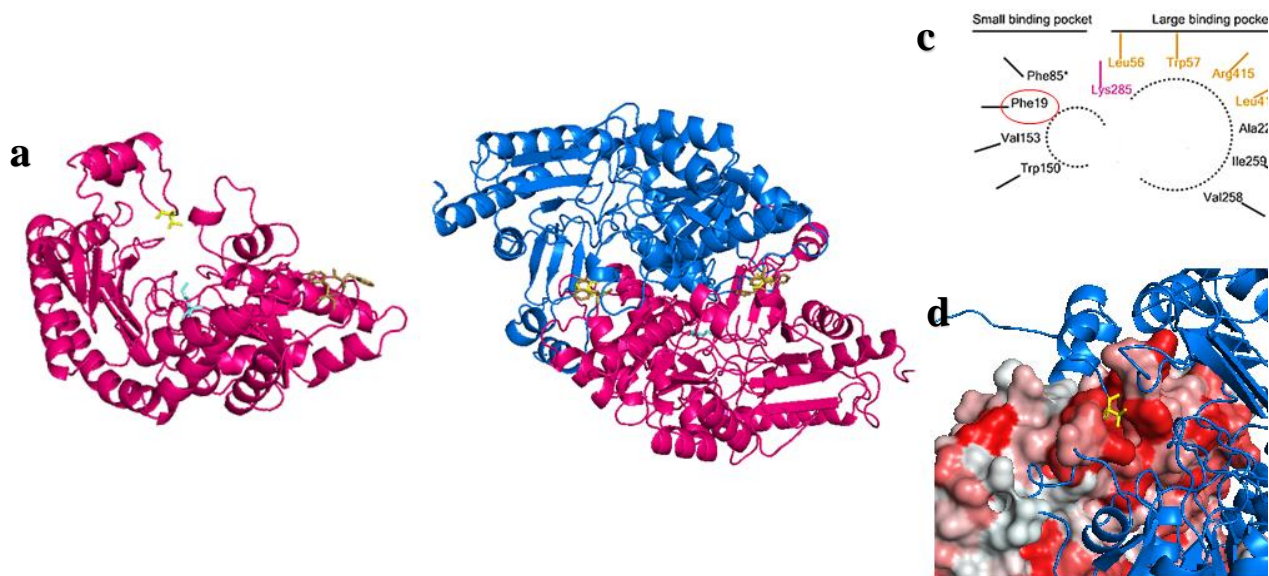


**Fig. 5.5.** VPTA model with threonine in yellow. This residue is localised on a small loop at N-terminal in a distinct motif above the catalytic K in light blue (**a**); the homodimerisation (**b**) involves hydrophobic amino acids (red) from both monomers in what is called hydrophobic pocket (**d**). In binding pockets of *V. fluvialis* ATA many hydrophobic residues are present (**c**) likely with a role in dimer formation.

The mutation choice reflects the current positions in regard to this residue involved in the active site with no particular predisposition to central catalytic role<sup>6,40,44,49</sup>, despite of proximity to substrate binding pocket and moderately high level of conservation of the positions (ConSurf analysis figure 5.4). The amino acids involved with high probability in the structural stabilization of the functional homodimer are less conserved than the catalytic ones at least, but they are preserved by evolution anyway. This could shed light on the structural role of this residue in the  $\omega$ -ATAs homodimerization and stabilization.

## VPTA T16F

The expression of the N-terminal his-tagged transaminase was performed and compared in different conditions and best results were achieved with ZYM-5052 auto-induction medium at 150 rpm, at 30 °C for 24 h. Purification was performed by immobilized metal affinity chromatography (IMAC). The enzyme was obtained in the pure form, expressed at higher concentration in auto-induction medium with a specific activity 2.4 U/mg and a volumetric yield 4 mg/L (figure 5.6).

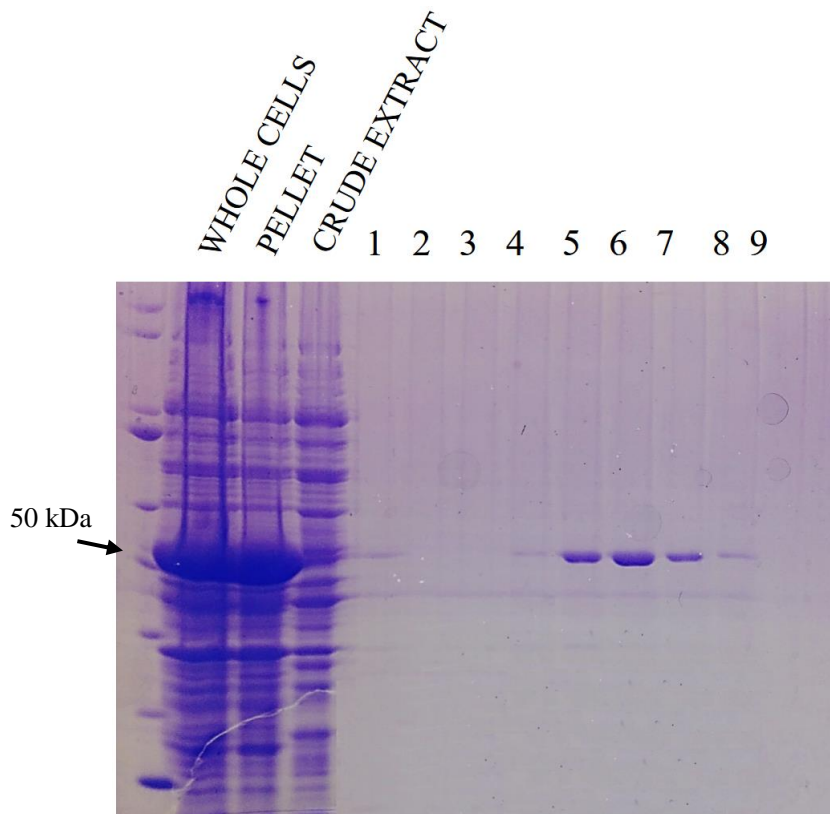


**Fig. 5.6.** VPTA T16F SDS-PAGE purifications fractions from auto-induction expression. The purified fractions present the molecular weight attended (53 kDa).

## EFFECT OF pH AND TEMPERATURE

VPTA preparation was suspended in a universal buffer solution at the desired pH and stored at 4 °C for 24 h. After incubation, the residual activity was determined with the spectrophotometric enzyme assay in standard condition<sup>46</sup> (figure 5.7). Only at pH 8 the enzyme is stable and active.

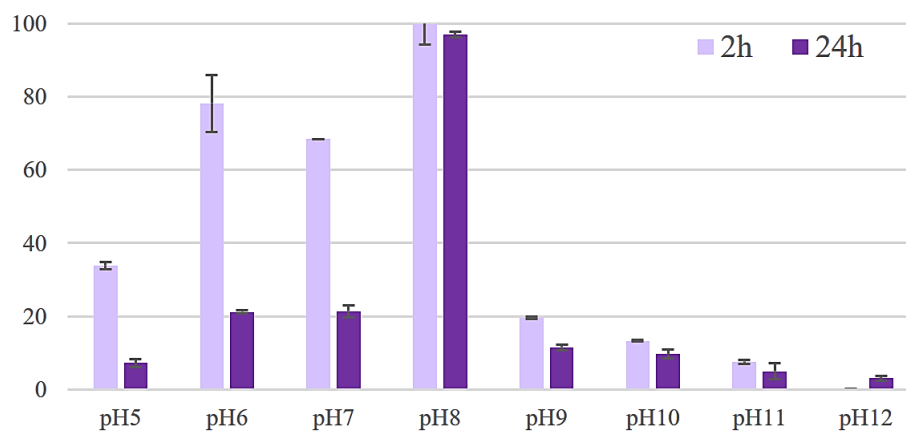


**Fig. 5.7.** Stability test at different pH: data are reported as relative percentages in comparison with the control in standard conditions. Every reaction was performed in three replicates and the results are reported as the average of the data obtained.

Thermal stability was tested after incubation of the enzyme at variable temperatures. After 20 h the enzyme maintains 80% of initial activity up to 45 °C.

The activity was determined with the spectrophotometric enzyme assay performed at the indicated temperature. The highest activity was reached between 25 °C and 45 °C.

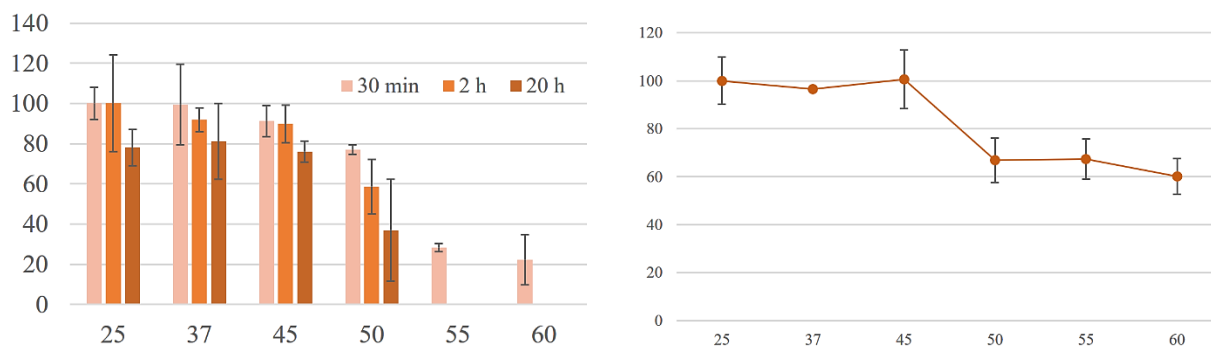
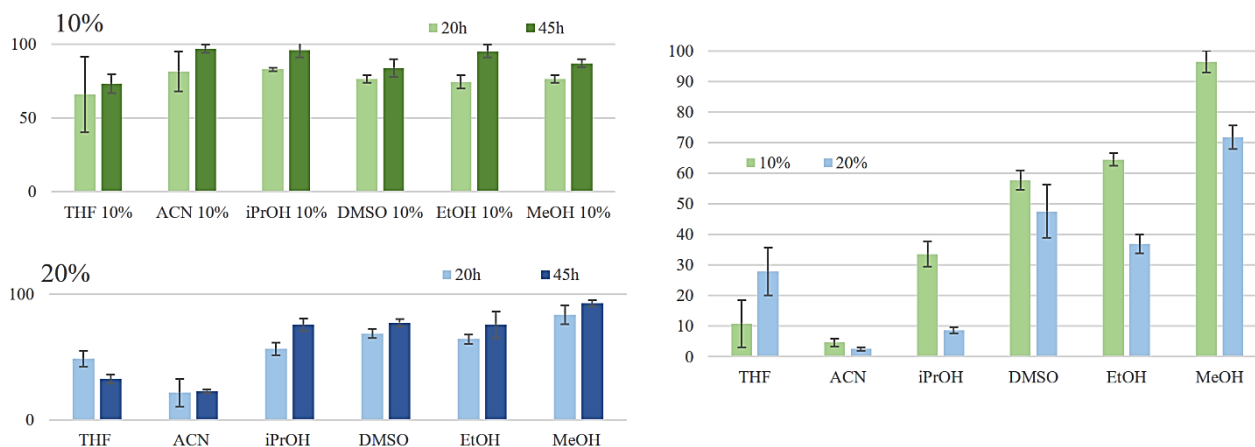


**Fig. 5.8.** The X axis shows the set of temperature selected while on Y axis the residual activity in percentage is reported. Left panel: stability test of VPTA in the range 25-60 °C. Right panel: activity test of VPTA in the range 25-60 °C. Each reaction was performed in triplicate. Results are reported as the average of the data obtained.

As described for the first time by Ikai *et al.*<sup>50</sup>, this high mesophilic profile could be confirmed by the VPTA high aliphatic index of 94.44 (ProtParam tool, accessible from the ExpASy website [www.expasy.ch](http://www.expasy.ch)).

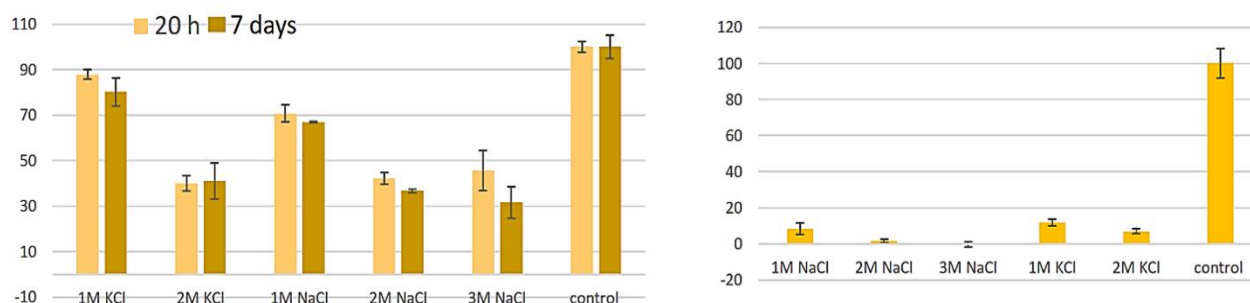
## EFFECT OF CO-SOLVENTS AND SALTS

The use of co-solvents is very useful if the bioconversion deals with a very low soluble substrate, for this reason the effect of different co-solvents on VPTA activity and stability was investigated. The stability analysis was carried out incubating the enzyme with 10% and 20% of a selection of common water-miscible organic solvent for 45 h (figure 5.9). In all cases, a decrease in enzyme activity was observed, even if VPTA shows a higher stability than HEWT under the same condition. With regard to the activity in presence of co-solvents, the best results were obtained with MeOH 10%. Hence, this enzyme is suitable for enantioselective amination of ketones and aldehydes where the presence of a co-solvent is necessary.



**Fig. 5.9.** The X axis shows the set of solvents selected while on Y axis the residual activity in percentage is reported. Left panel: stability test of VPTA with 10 and 20% solvents after 45 h. Right panel: activity test of VPTA with 10 and 20% solvents. Each reaction was performed in triplicate. Results are reported as the average of the data obtained.

The effect of different salt (NaCl and KCl) concentrations on enzyme stability and activity was also investigated. Under activity test conditions in the presence of salts, enzyme activity is very low, when compared to the enzyme at pH 8.0 in 50 mM phosphate buffer (figure 5.10). On the other hand, incubation of the enzyme in the presence of salts for seven days resulted in a satisfactory residual activity only when 1 M KCl was used.

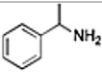
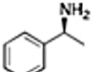
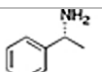
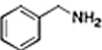
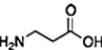
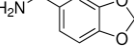
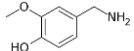
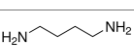


**Fig. 5.10.** The X axis shows the set of salts selected while on Y axis the residual activity in percentage is reported. On the left stability test: incubation was carried out at the indicated salt concentration for 45 h at 4 °C. On the right activity test in presence of salts: the residual activity of the enzymatic solution was determined by the standard spectrophotometric assay carried out in presence of the salt concentration indicated and expressed in function of the activity under standard conditions. Every reaction was performed in three replicates and the results are reported as the average of the data obtained.

## AMINO DONORS

A number of amino donors was investigated in order to understand the catalytical potential of VPTA and consequently its possible applications (table 5.2). VPTA does not display an activity for classical amino donors (*i.e.*, L-alanine isomolar with amino acceptor higher than that of HEWT, CV2025 and

*V. fluvialis*  $\omega$ -ATA. However, VPTA shows to be highly (*S*)-selective showing no detectable activity on (*R*)-(-)-1-phenylethylamine. The final conversion was determined after 24 h of reaction time.

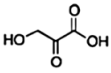
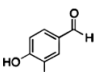
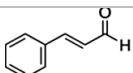
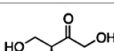
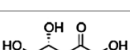
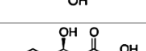
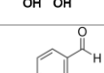
AMINO DONOR	STRUCTURE	FINAL CONVERSION (%)
rac-1-phenylethylamine		43
<i>S</i> -(-)-1-phenylethylamine		71
<i>R</i> -(-)-1-phenylethylamine		/
Isopropylamine*		/
benzylamine		47
$\beta$ -alanine*		/
L-alanine*		8
D-alanine*		/
cinnamyl-amine		74
3,4-(methylenedioxy)benzylamine		70
vanillylamine		90
putrescine*		/
cadaverine*		/
4-phenylbenzylamine		16

**Table 5.2.** VPTA specificity on different amino donors are reported. The enzymatic reactions with VPTA were carried out as reported in Materials and Methods. Every reaction was performed in three replicates and the results are reported as the average of the data obtained. Concentration of amino donors was kept constant at 10 mM, as amino acceptor 10 mM pyruvate was normally employed, except for the substrate with \*, where pyruvate was substituted with 10 mM benzaldehyde. The substrate was added in methanol solution to guarantee the correct concentration of the substrate in reaction mixture (final concentration 10% MeOH). Final conversions with VPTA were determined by HPLC analysis as reported in materials and methods.

## AMINO ACCEPTORS

VPTA shows no interesting activity on standard amino acceptors in comparison with HEWT, CV2025 and *V. fluvialis*  $\omega$ -ATA. Some promising conversions resulted for substrates such as phenylacetaldehyde, cinnamaldehyde, biphenyl-4-carboxaldehyde and 3-phenylpropionaldehyde (table 5.3). These bulky aldehydes are well accepted by the enzyme. The lack of activity with D-fructose and L-ribulose could be caused by a steric clash hampering the accommodation of the substrate in the catalytic pocket. The final conversion was determined after 24 h of reaction time.

AMINE ACCEPTOR	STRUCTURE	FINAL CONVERSION (%)
----------------	-----------	----------------------

pyruvic acid*		71
$\beta$ -hydroxypyruvic acid*		/
glyoxylic acid*		/
benzaldehyde		49
phenylacetaldehyde		90
2-phenylpropionaldehyde		53
vanillin		/
cinnamaldehyde		93
cyclohexanone*		/
1,3-dihydroxyacetone*		/
L-erythrose*		/
L-ribulose*		/
D-fructose*		/
4-nitrobenzaldehyde		50
3-nitrobenzaldehyde		86
2-nitrobenzaldehyde		68
biphenyl-4-carboxaldehyde		81
3-phenylpropionaldehyde		91

**Table 5.3.** VPTA specificity with different amino acceptors are reported. The enzymatic reactions with VPTA were carried out as reported in materials and methods. Every reaction was performed in three replicates and results reported as the average value. Concentration of amino acceptors was kept constant at 10 mM, as amino donor 1 M L-alanine was normally employed, except for the substrate with \*, where L-alanine was substituted with 50 mM (*S*)-PEA. The substrate was added in 10% methanol solution to guarantee the correct concentration of the substrate in reaction mixture. Final conversion with VPTA were determined by HPLC analysis as reported in materials and methods.

## ENZYME KINETICS

The maximum velocity ( $V_{\max}$ ) was  $0.19 \mu\text{M/s}$  and the Michaelis–Menten constants ( $K_m$ ) were  $1.9 \text{ mM}$  and  $10.7 \text{ mM}$  for (*S*)-(-)-1-phenylethylamine and pyruvate, respectively. The turnover number was also determined as  $k_{\text{cat}} 0.099 \text{ s}^{-1}$  (figure 5.13).

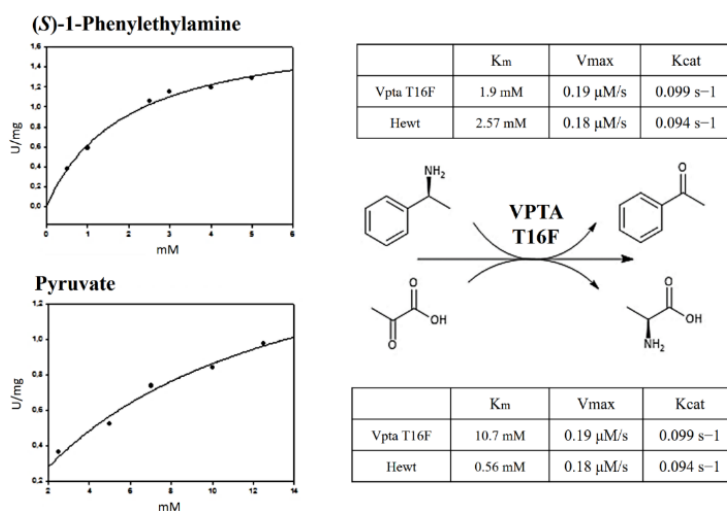


**Fig. 5.13.** Comparison between HEWT and VPTA kinetic parameters.

## MATERIALS AND METHODS

Unless stated otherwise, all chemicals and media components were purchased from Sigma-Aldrich (Steinheim, Germany), New England Biolabs (Ipswich, MA, USA) or Merck (Darmstadt, Germany), Fisher BioReagents (Loughborough, United Kingdom). Primers and sequencing were furnished by Eurofins MWG Operon (Ebersberg, Germany). Plasmid pG-KJE8 harboring Chaperonins was from Takara Clontech (Saint-Germain-en-Laye, France). Champion pET100 Directional TOPO Expression Kit and QuikChange Lightning Site-Directed Mutagenesis Kit were provided respectively by Invitrogen (Loughborough, United Kingdom) and Agilent Technologies (Santa Clara, CA, USA).

## MARINE MICROORGANISM, GENE IDENTIFICATION AND CLONING

*Virgibacillus pantothenicus* marine bacterial strain (EMBL database accession numbers HG799644) belongs to the European project Biodeep collection isolated from water-brine interface of the deep hypersaline anoxic basin *Discovery* ( $35^{\circ} 17' \text{ N}$ ,  $21^{\circ} 41' \text{ E}$ ), on the Mediterranean Ridge<sup>51</sup>. Due to the high halotolerant features<sup>52</sup>, *Virgibacillus pantothenicus* genome was selected for sequencing, the

data were deposited in The Seed database and genes were annotated by RAST software<sup>42</sup> (Rapid Annotation using Subsystems Technology).

*Virgibacillus pantothenicus* was grown in CYSP medium (casitone 15 g/L, yeast extract 5 g/L, soitone 3 g/L, peptone 2 g/L, MgSO<sub>4</sub>\*7H<sub>2</sub>O 15 mg/L, FeCl<sub>3</sub>\*6H<sub>2</sub>O 116 mg/L, MnCl<sub>2</sub>\*4H<sub>2</sub>O 20 mg/L, NaCl 30 g/L) at 30° C<sup>53</sup>. After 24 h the cells in stationary phase were harvested and genomic DNA was extracted with GenElute Bacterial Genomic DNA Kit (Sigma-Aldrich).

VPTA gene was identified by homology blasting *Chromobacterium violaceum*, *Vibrio fluvialis* and *Halomonas elongata* transaminase amino acidic sequences on *V. pantothenicus* genome at default settings of RAST software. All the three enzyme sequences match with the gene annotated as omega-amino acid-pyruvate aminotransferase. The gene was cloned in pET100, pET101 plasmid employing Champion pET Directional TOPO Expression Kit.

## EXPRESSION OF WILD-TYPE VPTA

Expression of the recombinant VPTA protein was performed using BL21 DE3, BL21 DE3 star, BL21(DE3), Rosetta, Codon Plus RIPL *E. coli* strains and pET100, pET101 expression vectors (His tag respectively in N-terminal and C-terminal). A following transformation with pG-KJE8 plasmid allowed the co-expression of VPTA with the chaperonins dnaK, dnaJ, grpE, groES, groEL following the protocol provided by Takata Clontech. Expression cultures were prepared growing a single colony of *E. coli* cells carrying the recombinant plasmid for 24h at 18, 25, 30, 37 °C, on a rotatory shaker at 200 rpm, in flasks containing LB/TB/ZYM-5052 auto-induction medium<sup>54</sup> with 100 µg/mL ampicillin. For LB and TB medium the IPTG added was 0.5 mM at 0.6 OD of cell growth, with 24 hours of expression time, unless stated otherwise. Experiments were carried out in 1 L baffled Erlenmeyer flasks containing 300 mL of liquid medium.

## MUTAGENESIS ON VPTA

The VPTA gene harbored in a pET100 plasmid was mutated employing the QuikChange Lightning Site-Directed Mutagenesis Kit provided by Agilent Technologies. The oligonucleotide primer was designed using the QuikChange Primer Design tool (Agilent Technologies). The T16F mutant was achieved using the following primer: 5'-atgttggtgctctt<sup>g</sup>atc<sup>g</sup>atgagaatggatggatgaaatgcttctatccaac-3' (mutated codon is underlined).

## EXPRESSION OF VPTA T16F

Expression of the recombinant VPTA protein was performed using BL21 DE3 *E. coli* strain with pET100 as expression vectors. Preliminary trials showed that this host yielded the higher VPTA

expression as compared to Codon plus RIPL cells. The best expression results were achieved in the following conditions: expression cultures were prepared growing a single colony carrying the recombinant plasmid in 1L flasks containing 300 mL of auto-induction broth with 100 µg/mL ampicillin at 30 ° C, with 180 rpm of stirring, for 24h. Cells were harvested by centrifugation.

## PURIFICATION

Pellets of 300 mL cultures were suspended in about 12 mL (2 mL per g pellet) of washing buffer (50 mM Tris-HCl pH8, 100 mM NaCl, 0.1 mM PLP, 30 mM imidazole) and lysed by sonication as described before<sup>55</sup>. The lysate was clarified by centrifugation at 13,000 × g for 1 h at 4°C, filtered through a 0.45 µm filter (Millipore, Bedford, MA, USA). Using an ÄKTA Start System (GE Healthcare, Little Chalfont, UK), crude extract was loaded at a flow rate of 1 ml/min into a 1mL HisTrap HP column pre-charged with NiSO<sub>4</sub> (0.1 M). The column was washed at a flow rate of 1mL/min with at least 10 column volumes of washing buffer and the enzyme was eluted with elution buffer (50 mM Tris-HCl pH8, 100 mM NaCl, 0.1 mM PLP, 300 mM imidazole), after an intermediate step with the 15% of elution buffer to remove non-specifically bound proteins. The fractions containing the enzyme were desalted via overnight dialysis against 50 mM phosphate buffer pH 8, containing 0.1 mM PLP. The purified enzyme was quantified by Epoch Take3 and stored at 4°C. The spectrophotometric enzymatic assays described by Deszsn *et al.*<sup>40</sup> was employed for testing the enzymatic activity. The acronym VPTA was adopted to recognize *Virgibacillus pantothenicus* omega-transaminase. Fractions of 0.5 ml were collected, analyzed by SDS-PAGE using a 12% polyacrylamide gel. For separation into soluble and insoluble fractions, samples were centrifuged at 13,000 × g for 1 h at 4°C, and the pellet was suspended in the same volume of 50 mM Tris-HCl buffer pH8.

## SDS-PAGE ANALYSIS

The concentration of the purified protein was determined spectrophotometrically by UV absorption at 280nm. The extinction coefficient 40.130 M<sup>-1</sup> cm<sup>-1</sup>, at 280nm, measured in water, was estimated by ExPASy ProtParam tool, accessible from the ExPASy website ([www.expasy.ch](http://www.expasy.ch)). SDS-PAGE was carried out employing a 12% polyacrylamide gels, stained with Coomassie Brilliant Blue R250 and a broad range protein marker was used for determination of relative molecular weight.

## SPECTROPHOTOMETRIC ENZYMATIC ASSAY

A kinetic assay derived from Schatzle *et al.*<sup>46</sup> was used as standard enzymatic assay. The reactions were carried out at 25 °C employing a reaction mixture containing 1 mL phosphate buffer (50 mM, pH 8), 2.5 mM (S)-(-)-1-phenylethylamine, 2.5 mM pyruvate, 0.25% DMSO, 0.1 mM PLP and a

proper amount of enzyme. These parameters were modified in order to investigate the behavior of the enzyme in different reaction conditions. The activity was estimated following the production of acetophenone during the first three minutes of reaction at 245 nm using a Bioteck Epoch Microplate Spectrophotometer. In the study of the effect of the pH on enzyme activity and stability, instead of the phosphate buffer, a universal buffer was employed. This system contains 25 mM citric acid, 25 mM  $\text{KH}_2\text{PO}_4$ , 25 mM Tris, 12.5 mM  $\text{Na}_2\text{B}_4\text{O}_7$ , and 25 mM  $\text{KCl}$ <sup>56</sup>.

VPTA stability at different temperatures was checked with a standard activity assay after enzyme incubation at 25, 37, 45, 50, 55, 60 °C for 20h. For what concerns activity studies, the spectrophotometric enzymatic activity test was carried on at these temperatures.

The effect of co-solvents on VPTA stability was studied storing the enzyme in the presence of either 10 or 20% (v/v) of co-solvent at 4 °C for 45 h. Before and after incubation the residual activity was determined by the standard spectrophotometric enzymatic assay. The effect of co-solvents on VPTA activity was checked in presence of the corresponding amount of co-solvents in the reaction mixture.

As done with solvents, stability was tested in presence of different concentrations of NaCl and KCl, the residual activity after 7 days was measured by the standard spectrophotometric assay. For activity analysis, the kinetic assay was carried on in the presence of salts. Residual activity was measured in both cases by the standard spectrophotometric assay.

## ENZYMATIC REACTION

The enzymatic reactions with different amino-donor and acceptors were carried out at 37 °C in 100 mM phosphate buffer pH 8. In amino-donor screening, the reaction mixture contained 10 mM enantiopure amino donor (20 mM if racemic), 10 mM pyruvate or benzaldehyde as amino acceptor (see table 5.2) and 0.1 mg/mL of VPTA in a reaction volume of 200  $\mu\text{L}$  (10% MeOH as co-solvent). Differently, amino-acceptors screening was carried out with 10 mM enantiopure amino-acceptor (20 mM if racemic), 1 M L-alanine or 50 mM (S)-PEA as amino-donor (see table 5.3) and 0.1 mg/mL of VPTA in a reaction volume of 200  $\mu\text{L}$  (10% MeOH as co-solvent). As a control, the reactions were set up as previously described but without the addition of VPTA. One enzymatic unit is defined as the amount of enzyme that converts 1  $\mu\text{mol}$  of (S)-(-)-1-phenylethylamine in 1 min in standard conditions. For storage conditions, VPTA was stable at 4 °C for ten days without evident loss of activity. Data were obtained by averaging the measurements on three independent samples.

## ANALYTICAL METHODS

### *SPECTROPHOTOMETRIC ANALYSIS*

The kinetic catalytic constants  $V_{\max}$  and  $K_m$  were measured at pH 8.0 and 25 °C using Bioteck Epoch Microplate Spectrophotometer as described above in the presence of 0.25% DMSO, 0.1 mM PLP and an appropriate amount of enzyme (0.1 mg/mL). Reactions were carried out at 2.5 mM pyruvate and various concentrations (0.5–5 mM) of (*S*)-(-)-1-phenylethylamine, at 2.5 mM (*S*)-(-)-1-phenylethylamine and various concentrations (2.5–12.5 mM) of pyruvate (figure 5.13). Concentrations higher than 5 mM of (*S*)-(-)-1-phenylethylamine gave significant interference with the UV detection signal and for this reason it was kept below saturation conditions. The initial-velocity data were fitted to the Michaelis–Menten equation using SigmaPlot software (Version 11.0).

### *HPLC ANALYSIS*

The final conversion of the different amino acceptor were determined employing a Thermo Scientific HPLC instrument equipped with Accucore C18, LC column, Particle size 2.6 microm, diameter 4.6 mm, length 150 mm. The substrates were detected at 210, 245, 280 nm using the following mobile phase A: formic acid (0.1% in water), B: ACN; the gradient elution method is 15% B (10 min), increasing to 80% B (over 8 min), decreasing 15% B (over 2 min) at 25 °C with a flow rate of 1 mL/min. The depletion of aromatic amines, aldehydes and the formation of acetophenone were evaluated by calibration curve. The samples were injected after a dilution of 1:50 with HCl 0.2% in the quenching step. The retention times in minutes are: acetophenone (8 min), benzaldehyde (6.3 min), benzylamine (4.1), cinnamaldehyde (16 min), 1-phenylethylamine (5 min), phenylacetaldehyde (14 min), 2-phenylpropionaldehyde (14.5 min), vanillin (1.8 min), 4-nitrobenzaldehyde (14 min), 3-nitrobenzaldehyde (14 min), 2-nitrobenzaldehyde (15 min), biphenyl-4-carboxaldehyde (18.7 min), 3-phenylpropionaldehyde (16 min), cinnamyl-amine (9 min), 3,4-(methylenedioxy)benzylamine (1.54 min), vanillylamine (5 min), 4-phenylbenzylamine (18.7 min). All samples were quenched with HCl 0.2% and then centrifuged before the HPLC analysis.

## REFERENCES

1. Simon, R. C., Richter, N., Busto, E. & Kroutil, W. Recent developments of cascade reactions involving  $\omega$ -transaminases. *ACS Catal.* **4**, 129–143 (2014).
2. Sattler, J. H. *et al.* Introducing an in situ capping strategy in systems biocatalysis to access 6-aminohexanoic acid. *Angew. Chemie - Int. Ed.* **53**, 14153–14157 (2014).
3. Villegas-Torres, M. F. *et al.* Multi-step biocatalytic strategies for chiral amino alcohol synthesis. *Enzyme Microb. Technol.* **81**, 23–30 (2015).
4. Savile, C. K. *et al.* Biocatalytic Asymmetric Synthesis of Chiral Amines from Ketones Applied to Sitagliptin Manufacture. *Science (80- )*. **329**, 305–309 (2010).

5. Malik, M. S., Park, E.-S. & Shin, J.-S.  $\omega$ -Transaminase-catalyzed kinetic resolution of chiral amines using l-threonine as an amino acceptor precursor. *Green Chem.* **14**, 2137 (2012).
6. Midelfort, K. S. *et al.* Redesigning and characterizing the substrate specificity and activity of *Vibrio fluvialis* aminotransferase for the synthesis of imagabalin. *Protein Eng. Des. Sel.* **26**, 25–33 (2013).
7. Sehl, T. *et al.* Efficient 2-step biocatalytic strategies for the synthesis of all nor(pseudo)ephedrine isomers. *Green Chem.* **16**, 3341–3348 (2014).
8. Contente, M. L., Dall'Oglio, F., Tamborini, L., Molinari, F. & Paradisi, F. Highly efficient oxidation of amines to aldehydes via flow-based biocatalysis. *ChemCatChem* (2017). doi:10.1002/cctc.201701147 IF:4.803
9. Mathew, S., Nadarajan, S. P., Chung, T., Park, H. H. & Yun, H. Biochemical characterization of thermostable  $\omega$ -transaminase from *Sphaerobacter thermophilus* and its application for producing aromatic  $\beta$ - and  $\gamma$ -amino acids. *Enzyme Microb. Technol.* **87–88**, 52–60 (2016).
10. Tufvesson, P. *et al.* Process considerations for the asymmetric synthesis of chiral amines using transaminases. *Biotechnol. Bioeng.* **108**, 1479–1493 (2011).
11. Abu, R. & Woodley, J. M. Application of Enzyme Coupling Reactions to Shift Thermodynamically Limited Biocatalytic Reactions. *ChemCatChem* **7**, 3094–3105 (2015).
12. Koszelewski, D., Tauber, K., Faber, K. & Kroutil, W.  $\omega$ -Transaminases for the synthesis of non-racemic  $\alpha$ -chiral primary amines. *Trends Biotechnol.* **28**, 324–332 (2010).
13. Green, A. P., Turner, N. J. & O'Reilly, E. Chiral amine synthesis using  $\omega$ -transaminases: An amine donor that displaces equilibria and enables high-throughput screening. *Angew. Chemie - Int. Ed.* **53**, 10714–10717 (2014).
14. Sørensen, H. P. & Mortensen, K. K. Soluble expression of recombinant proteins in the cytoplasm of *Escherichia coli*. *Microb. Cell Fact.* **4**, 1 (2005).
15. Schultz, T., Martinez, L. & de Marco, A. The evaluation of the factors that cause aggregation during recombinant expression in *E. coli* is simplified by the employment of an aggregation-sensitive reporter. *Microb. Cell Fact.* **5**, 28 (2006).
16. Schein, C. H. & Noteborn, M. H. M. Formation of Soluble Recombinant Proteins in *Escherichia Coli* is Favored by Lower Growth Temperature. *Nat. Biotechnol.* **6**, 291–294 (1988).
17. Waugh, D. S. Making the most of affinity tags. *Trends Biotechnol.* **23**, 316–320 (2005).
18. Esposito, D. & Chatterjee, D. K. Enhancement of soluble protein expression through the use of fusion tags. *Curr. Opin. Biotechnol.* **17**, 353–358 (2006).
19. Kolaj, O., Spada, S., Robin, S. & Wall, J. G. Use of folding modulators to improve heterologous protein production in *Escherichia coli*. *Microb. Cell Fact.* **8**, 9 (2009).
20. Rosano, G. L. & Ceccarelli, E. A. Rare codon content affects the solubility of recombinant proteins in a codon bias-adjusted *Escherichia coli* strain. *Microb. Cell Fact.* **8**, 41 (2009).
21. Guise, A. D., West, S. M. & Chaudhuri, J. B. Protein folding in vivo and renaturation of recombinant proteins from inclusion bodies. *Mol Biotechnol.* **6**, 53–64 (1996).
22. Mukhopadhyay, A. Inclusion bodies and purification of proteins in biologically active forms. *Adv Biochem Eng Biotechnol.* **56**, 61–109 (1997).
23. Kapust, R. B. & Waugh, D. S. *Escherichia coli* maltose-binding protein is uncommonly effective at promoting the solubility of polypeptides to which it is fused. *Protein Sci.* **8**, 1668–1674 (1999).

24. Idicula-thomas, S. & Balaji, P. V. Understanding the relationship between the primary structure of proteins and its propensity to be soluble on overexpression in *Escherichia coli*. *Protein Sci* **14**, 582–592 (2005).
25. Jenkins, T. M. *et al.* Catalytic domain of human immunodeficiency virus type 1 integrase: identification of a soluble mutant by systematic replacement of hydrophobic residues. *Proc Natl Acad Sci U S A* **92**, 6057–6061 (1995).
26. Murby, M. *et al.* Hydrophobicity Engineering to Increase Solubility and Stability of a Recombinant Protein from Respiratory Syncytial Virus. *Eur. J. Biochem.* **230**, 38–44 (1995).
27. Malissard, M. & Berger, E. G. Improving solubility of catalytic domain of human beta-1,4-galactosyltransferase 1 through rationally designed amino acid replacements. *Eur. J. Biochem.* **268**, 4352–8 (2001).
28. Dale, G. E., Broger, C., Langen, H., D'Arcy, A. & Stüber, D. Improving protein solubility through rationally designed amino acid replacements: solubilization of the trimethoprim-resistant type S1 dihydrofolate reductase. *Protein Eng.* (1994).
29. Lin, Z., Thorsen, T. & Arnold, F. H. Functional expression of horseradish peroxidase in *E. coli* by directed evolution. *Biotechnol. Prog.* **15**, 467–71 (1999).
30. Perry, M. Z. Improving protein solubility via directed evolution. (Queen's University Kingston, Ontario, Canada, 2009).
31. Dadashpour, M., Fukuta, Y. & Asano, Y. Comparative expression of wild-type and highly soluble mutant His103Leu of hydroxynitrile lyase from *Manihot esculenta* in prokaryotic and eukaryotic expression systems. *Protein Expr. Purif.* **77**, 92–97 (2011).
32. Lumb, M. J. & Danpure, C. J. Functional synergism between the most common polymorphism in human alanine:glyoxylate aminotransferase and four of the most common disease-causing mutations. *J. Biol. Chem.* **275**, 36415–36422 (2000).
33. Montioli, R. *et al.* Misfolding caused by the pathogenic mutation G47R on the minor allele of alanine:glyoxylate aminotransferase and chaperoning activity of pyridoxine. *Biochim. Biophys. Acta - Proteins Proteomics* **1854**, 1280–1289 (2015).
34. Schmid, A. *et al.* Industrial biocatalysis today and tomorrow. *Nature* **409**, 258–268 (2001).
35. Fasan, R., Chen, M. M., Crook, N. C. & Arnold, F. H. Engineered alkane-hydroxylating cytochrome P450BM3 exhibiting natively like catalytic properties. *Angew. Chemie - Int. Ed.* **46**, 8414–8418 (2007).
36. Polizzi, K. M., Bommarius, A. S., Broering, J. M. & Chaparro-Riggers, J. F. Stability of biocatalysts. *Curr. Opin. Chem. Biol.* **11**, 220–225 (2007).
37. Lehmann, M. & Wyss, M. Engineering proteins for thermostability: The use of sequence alignments versus rational design and directed evolution. *Curr. Opin. Biotechnol.* **12**, 371–375 (2001).
38. Steipe, B., Schiller, B., Plückthun, A. & Steinbacher, S. Sequence Statistics Reliably Predict Stabilizing Mutations in a Protein Domain. *J. Mol. Biol.* **240**, 188–192 (1994).
39. Jäckel, C., Bloom, J. D., Kast, P., Arnold, F. H. & Hilvert, D. Consensus protein design without phylogenetic bias. *J. Mol. Biol.* **399**, 541–546 (2010).
40. Deszcz, D. *et al.* Single active-site mutants are sufficient to enhance serine:pyruvate  $\alpha$ -transaminase activity in an  $\omega$ -transaminase. *FEBS J.* **282**, 2512–2526 (2015).
41. Wintrode, P. L. & Arnold, F. H. Temperature adaptation of enzymes: lessons from laboratory evolution. *Adv Protein Chem.* **55**, 161–225. (2000).

42. Aziz, R. K. *et al.* The RAST Server: Rapid Annotations using Subsystems Technology. *BMC Genomics* **9**, 75 (2008).
43. Rudat, J., Brucher, B. R. & Syldatk, C. Transaminases for the synthesis of enantiopure beta-amino acids. *AMB Express* **2**, 11 (2012).
44. Genz, M. *et al.* Engineering the Amine Transaminase from *Vibrio fluvialis* towards Branched-Chain Substrates. *ChemCatChem* **8**, 3199–3202 (2016).
45. Strillinger, E., Gr??tzinger, S. W., Allers, T., Eppinger, J. & Weuster-Botz, D. Production of halophilic proteins using *Haloferax volcanii* H1895 in a stirred-tank bioreactor. *Appl. Microbiol. Biotechnol.* **100**, 1183–1195 (2016).
46. Schätzle, S., Höhne, M., Redestad, E., Robins, K. & Bornscheuer, U. T. Rapid and sensitive kinetic assay for characterization of  $\omega$ -transaminases. *Anal. Chem.* **81**, 8244–8248 (2009).
47. ConSurf. Available at: <http://consurf.tau.ac.il/2016/>.
48. Swiss-Model Homology modeling tool. Available at: <https://swissmodel.expasy.org/>.
49. Abrahamsson, E. Master thesis in Biochemistry Changing or improving the enantioselectivity of omega-transaminase ... Changing or improving the enantioselectivity of  $\omega$  -transaminase towards ( R ) -amines , utilizing a semi-rational design approach Erik Abrahamsson Master. (2014).
50. Ikai, A. Thermostability and aliphatic index of globular proteins. *J. Biochem.* **1898**, 1895–1898 (1980).
51. Daffonchio, D. *et al.* The Enigma of Prokaryotic Life in Deep Hypersaline Anoxic Basins. **4**, 121–123 (2005).
52. De Vitis, V. *et al.* Marine Microorganisms as Source of Stereoselective Esterases and Ketoreductases: Kinetic Resolution of a Prostaglandin Intermediate. *Mar. Biotechnol.* **17**, 144–152 (2015).
53. Romano, D. *et al.* Enhanced enantioselectivity of *Bacillus coagulans* in the hydrolysis of 1,2-O-isopropylidene glycerol esters by thermal knock-out of undesired enzymes. *Tetrahedron Asymmetry* **16**, 841–845 (2005).
54. Studier, F. W. Protein production by auto-induction in high-density shaking cultures. *Protein Expr. Purif.* **41**, 207–234 (2005).
55. Cerioli, L., Planchestainer, M., Cassidy, J., Tessaro, D. & Paradisi, F. Characterization of a novel amine transaminase from *Halomonas elongata*. *J. Mol. Catal. B Enzym.* **120**, 141–150 (2015).
56. Davies, M. T. A universal buffer solution for use in ultra-violet spectrophotometry. *Analyst* **84**, (1959).

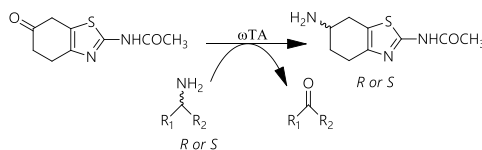
## CONCLUSIONS

## WHOLE CELL SCREENING – MARINE YEASTS

The stereoselective reduction of structurally different ketones using halotolerant marine yeasts (*Meyerozyma guilliermondii* and *Rhodotorula mucilaginosa*) was studied using cells grown and bio-converted in seawater. The preparation of valuable chemicals through water-saving (bio)processes based on the direct exploitation of seawater is a significant step towards sustainable biocatalysis. By choosing a suitable strain, high yields and stereoselectivity could be achieved in most cases. Notably, high chemoselectivity and enantioselectivity were observed using *R. mucilaginosa* in the reduction of aromatic  $\beta$ -ketonitriles, which allowed the recovery of the optically pure corresponding alcohols; notably, reduction with whole cells of yeasts generally give a mixture of undesired products, as observed with *M. guilliermondii*. Although the examples reported here are still limited to the laboratory scale, these results show that freshwater can be replaced by seawater in a whole bio-catalysis process using marine yeasts. It can be foreseen that halophilic and/or halotolerant marine yeasts (and more generally halophilic and/or halotolerant microorganisms) could be a plentiful source of enzymes to accomplish bio-catalysis in seawater.

## WHOLE CELL SCREENING – MARINE BACTERIA

Starting from the new synthetic pathway developed by Ferraboschi *et al.*, the possibility of employing an omega-transaminase enzyme to convert the ketone directly into optically pure amine intermediate was taken into account.



Therefore, thirty-three marine bacteria species were screened to identify a transaminase activity on model substrates like pyruvate and racemic methyl benzylamine to produce acetophenone. The acetophenone detected in some biotransformations confirms the presence of transaminase activity. The best performance was achieved with *Virgibacillus pantothenticus* that was selected for genome sequencing.

## RECOMBINANT ENZYME

About ketoreductase activity, recombinant enzymes were also employed. A newly isolated ketoreductase from the uncommon yeast *Pichia glucozyma* was able to produce the pramipexole *S*-alcohol intermediate with 86% *e.e.* in four hours.

Other enzymatic activities were investigated in order to achieve optical pure intermediate for the preparation of both pramipexole enantiomers. Some of the most common commercial lipases and a new recombinant esterase from *Bacillus coagulans* were tested on pramipexole ester intermediates without achieving optically pure compounds.

## VPTA

In recombinant applications, high levels of soluble expressed protein are usually required and often this entails an alteration of the physiological requirements for the enzyme natural folding leading to the formation of inclusions bodies. Therefore, thinking about a solubility improvement of enzyme sequences could be more than appreciable but not universally possible through a rational strategy.

The present work illustrates the attaining of soluble expression of a novel omega transaminase from a newly isolated halo-tolerant marine bacteria *Virgibacillus pantothenicus*. This marine bacterium is part of the micro-biodiversity of Deep Hypersaline Anoxic Basins on the Mediterranean Ridge, a new and uncommon source of biocatalysts.

Despite of several standard methodologies applied, the marine wild-type enzyme was total insoluble in *E. coli* host and it was satisfactorily solubilized by one single-point mutation, allowing the characterization of the new omega transaminase. The enzyme shows an interesting salt and solvent tolerance, in accordance to its origin and it results particularly active on some interesting building blocks molecules.

The constant demand of chiral amines by the Food, Pharmaceutical and Fine Chemical industries has made  $\omega$ -transaminases ( $\omega$ -ATAs) some of the most interesting biocatalysts of the last decades. The research current trend is directing to the identification and designing of new  $\omega$ -ATAs with defined substrate specificity and capable of high stress-tolerance, in order to complement or replace the traditional synthetic methods. To date,  $\omega$ -ATAs biocatalytic potential is not entirely exploited yet, despite of remarkable progresses achieved either by random and rational approaches.

This latter strategy was followed to select a target residue likely involved in structural stabilization. Comparison of primary sequences and three-dimensional models has shed light on a possible structural involvement of this amino acid in the  $\omega$ -ATAs homo-dimerization and stabilization.

This finding has significant implications for omega transaminase structure-stability-solubility understanding and represents one of the first works about a rational approach aimed at improving recombinant  $\omega$ -ATAs solubility. Further studies will be addressed to VPTA crystallization and tertiary structure investigation in order to understand the real effect of T16F mutation on the protein soluble folding.

## LIST OF PUBLICATIONS & CONFERENCE PROCEEDINGS

## CONFERENCES

- Riunione dei Biochimici dell'Area Milanese, Palazzo Feltrinelli in Gargnano(BS), 12<sup>th</sup>-14<sup>th</sup> April 2015 (poster presentation);
- Biotrans Conference 2015, Vienna (Austria), 20<sup>th</sup>-30<sup>th</sup> July 2015 (poster presentation);
- Workshop "INDUSTRIAL ENZYMES", Pavia (PV), 22<sup>nd</sup>-23<sup>rd</sup> September 2015;
- Riunione dei Biochimici dell'Area Milanese, Palazzo Feltrinelli in Gargnano(BS), 20<sup>th</sup>-22<sup>nd</sup> March 2016 (poster presentation);
- Frontiere nelle Biotecnologie Enzimatiche, The Protein Factory, Università degli Studi dell'Insubria –Varese, 18<sup>th</sup> May 2016;
- 28° Riunione nazionale "A. Castellani" dei Dottorandi di Ricerca in Discipline Biochimiche, Brallo di Pregola, 6<sup>th</sup>-10<sup>th</sup> June 2016 (oral and poster presentaions);
- Gordon Research Conference Biocatalysis, University of New England (USA), 10<sup>th</sup>-15<sup>th</sup> July 2016 (poster presentation);
- XIVth Annual UK Workshop on Archaea, University of Bristol, 5<sup>th</sup>-6<sup>th</sup> January 2017
- Riunione dei Biochimici dell'Area Milanese, Palazzo Feltrinelli in Gargnano(BS), 25<sup>th</sup>-27<sup>th</sup> June 2017 (oral presentaion);
- Biotrans 2017, Budapest (Hungary), 9<sup>th</sup>-13<sup>th</sup> July 2017 (poster presentation).

## COURSES

- Corso di formazione in modalità e-learning sul tema della Prevenzione e Sicurezza sul Lavoro organizzato da UNIMI;
- Corso sulla "Comunicazione della Ricerca Scientifica", 5-6 maggio, 16-17giugno 2015, Milano;
- Corso sulla Sicurezza "Prevenzione dei rischi biologico e chimico nel laboratorio biologico e nel laboratorio di analisi", 20 marzo 2015, Segrate.

## PUBLICATIONS

- Serra, I., Guidi, B., Burgaud, G., Contente, M.L., Ferraboschi, P., Pinto, A., Compagno, C., Molinari, F., Romano, D. Seawater-Based Biocatalytic Strategy: Stereoselective Reductions of Ketones with Marine Yeasts (2016) *ChemCatChem*, 8 (20), pp. 3254-3260.
- Contente, M.L., Guidi, B., Serra, I., De Vitis, V., Romano, D., Pinto, A., Lenna, R., de Souza Oliveira, R.P., Molinari, F. Development of a high-yielding bioprocess for 11- $\alpha$  hydroxylation of canrenone under conditions of oxygen-enriched air supply (2016) *Steroids*, 116, pp. 1-4.
- Contente, M.L., Serra, I., Palazzolo, L., Parravicini, C., Gianazza, E., Eberini, I., Pinto, A., Guidi, B., Molinari, F., Romano, D. Enzymatic reduction of acetophenone derivatives with a benzil reductase from *Pichia glucozyma* (KRED1-Pglu): electronic and steric effects on activity and enantioselectivity (2016) *Organic and Biomolecular Chemistry*, 14 (13), pp. 3404-3408.
- De Vitis, V., Guidi, B., Contente, M.L., Granato, T., Conti, P., Molinari, F., Crotti, E., Mapelli, F., Borin, S., Daffonchio, D., Romano, D. Marine Microorganisms as Source of Stereoselective Esterases and Ketoreductases: Kinetic Resolution of a Prostaglandin Intermediate (2015) *Marine Biotechnology*, 17 (2), pp. 144-152.